HIGH-FIELD MAGNETIC PHASE TRANSITIONS

M. W. VAN TOL

HIGH-FIELD MAGNETIC PHASE TRANSITIONS

PROEFSCHRIFT

TER VERKRIJGING VAN DE GRAAD VAN DOCTOR IN DE WISKUNDE EN NATUURWETENSCHAPPEN AAN DE RIJKSUNIVERSITEIT VAN LEIDEN, OP GEZAG VAN DE RECTOR MAGNIFICUS DR. A. E. COHEN, HOOGLERAAR IN DE FACULTEIT DER LETTEREN, VOLGENS BESLUIT VAN HET COLLEGE VAN DEKANEN TE VERDEDIGEN OP WOENSDAG 29 NOVEMBER TE KLOKKE 14.15 UUR

DOOR

MAURITS WILLEM VAN TOL
GEBOREN TE EINDHOVEN IN 1945

1972
DRUKKERIJ J. H. PASMANS, 'S-GRAVENHAGE

Promotor: PROF. DR. N.J. POULIS

STELLINGEN

I

De conclusie van Wittekoek, dat de door hem waargenomen "canting" van de koperspins in kopersulfaat-pentahydraat verdwijnt wanneer het uitwendige magnetische veld evenwijdig is aan de $g_\perp$ richting, wordt niet gerechtvaardigd door de door hem gegeven metingen.

S. Wittekoek en N.J. Poulis, Physica 32 (1966) 2051.

II

Gezien de anisotropie van de g-tensor in koper-tetramine-sulfaat-monohydraat is het weinig zinvol de magnetisatiemetingen aan deze stof, verkregen met een uitwendig veld langs de a, b en c as, te middelen alvorens ze met de berekende krommen voor een antiferromagnetische lineaire keten te vergelijken.

S. Saito, J.Phys.Soc.Japan, 26 (1969) 1388.
T. Haseda en H. Kobayashi, J.Phys.Soc.Japan 19 (1964) 1260.

III

Het verdient aanbeveling met behulp van spingolftheorie de fase-overgangstemperatuur van zwak gekoppelde antiferromagnetische lineaire ketensystemen in aanwezigheid van een uitwendig magnetisch veld te berekenen.

J. Des Cloizeaux en J.J.Pearson, Phys.Rev. 128 (1962) 2131.

IV

Het is zinvol te onderzoeken of ook in "zuivere" een-dimensionale antiferromagneten, zoals bijvoorbeeld koper-tetramine-sulfaat-monohydraat, een fase-overgang voorkomt van het in dit proefschrift beschreven type.

Dit proefschrift, hoofdstuk V.

V

De manier waarop Adair zijn metingen aan het Scott-effect presenteert leert meer over de afmetingen van de gebruikte apparatuur dan over de fysische achtergrond van het effect.

T.W.Adair III, Phys.Rev. 6 (1972) 487.

VI

De meting van het fonteineffect in supergeleiders via een asymmetrie in de kritische stroom van een supergeleidend puntcontact, zoals die door Clark en Freake werd uitgevoerd, is mede daarom onbevredigend omdat is nagelaten de asymmetrie als functie van een aangelegd magneetveld te onderzoeken.

J.Clark en S.M. Freake, Phys.Rev.Lett. 29 (1972) 588.

VII

Het is mogelijk een supergeleidende magneet van het split-coil type te construeren die een veld van 50 kOe levert met een homogeniteit beter dan 1 Oe over 2 cm. De diameter van een dergelijke spoel behoeft niet groter te zijn dan 7 maal de breedte van de spleet.

VIII

Het aantal electronenbanen dat Csorba berekent teneinde de modulatie-overdrachtsfunctie van een electrostatische electronenlens te bepalen is onnodig groot.

I.P.Csorba, R.C.A. Review 33 (1972) 393.

IX

In de beschrijving van hun warmte-pulsexperiment verwaarlozen Guo en Maris de verstrooiing der fononen aan het oppervlak van hun preparaat. Hun conclusie dat er een grote transmissie van transversale fononen vanuit silicium naar vloeibaar helium zou bestaan is dan ook onjuist.

C-J.Guo en H.J.Maris, Phys.Rev.Lett. 29 (1972) 855.

X

Het is mogelijk in een ENDOR experiment, waarbij gebruik wordt gemaakt van een spin-echo methode, de tijdsconstante te meten waarmee het electron dipool-dipoolsysteem en het kern-Zeemansysteem in een verdund paramagnetisch zout met elkaar in evenwicht komen.

XI

De leesbaarheid van de geschreven taal is gediend met een spelling die in tijd en plaats niet varieert. Daar een tekst slechts eenmaal geschreven en doorgaans vele malen gelezen wordt, dienen de eventuele nadelen van een "niet-vereenvaudigde" spelling op de koop toe genomen te worden.

De brochure van de NS "Waar gaat 't heen" gaat geheel voorbij aan het gebruik van de fiets als verplaatsings- en recreatiemiddel. Gezien in het licht van de recente beperkingen in het fietsenvervoer per trein doet dit ernstige twijfel rijzen aan de milieu-bewustheid van de Nederlandse Spoorwegen.

"Waar gaat 't heen", uitgave NS 1972.

Leiden, 29 november 1972 M.W. van Tol

Aan Cobie en Fleur

ERRATA

Equation (12) of chapter IV should read (for the entropy):

$$S/R = \frac{1}{\pi} \int_0^{\pi} [\ \ln (2 \cos h\, p) - p \tan h\, p\ ]\, d\omega$$

Equation (22) of chapter IV should read:

$$p(\omega) = \frac{1}{2kT} [\{g\beta H - J'(1 + E^2) \cos \omega\}^2 + (2J'E \sin \omega)^2]^{1/2}$$

TABLE OF CONTENTS

CHAPTER I
INTRODUCTION AND SURVEY

It is well known that interactions between magnetic moments in a lattice may give rise to transitions from an unordered, paramagnetic state to a magnetically ordered state, of which the ferromagnetic, antiferromagnetic and ferrimagnetic ones are the best known examples. Such an ordered state is always characterized by the existence of long-range order, which means that two magnetic moments, even in the limit when they are infinitely far apart, exhibit a non-zero correlation.

Thermodynamically a phase transition can be described as a cooperative effect, always accompanied by a singularity in the Gibbs free energy F. According to the concept of Ehrenfest [1], the nature of this singularity determines the order of the transition in the following way. A n-th order transition is defined by a discontinuity in the n-th order derivatives of F with respect to the temperature T and the generalized forces, *i.e.* the external magnetic field H. So at a second-order phase transition - the kind that usually occurs in magnetic systems - thermodynamic quantities like the specific heat capacity and the susceptibility will exhibit an anomaly at the transition temperature. From the further development of the theory of second-order phase transitions the important contributions by Landau [2] should not be left unmentioned.

A substance that shows a phase transition must of course meet certain necessary conditions, the most important of which is that each magnetic moment is coupled to all other moments in an infinite number of ways. Lattices that do not meet this condition give rise to the formation of clusters or, in some cases, to linear chains of magnetic moments. In this context a cluster is defined as a finite number of magnetic moments coupled by an interaction which is large compared to the interactions between different clusters. A linear chain consists of an infinite number of magnetic moments arranged in a one-dimensional lattice. At non-zero temperatures no long-range order is possible in such chains, unless the magnetic forces are of infinite range instead of being restricted to the nearest neighbours, as shown by Baker [3].

However, apart from the cluster or chain-forming interaction, other (weaker) interactions may exist which couple the clusters or linear chains together in an (at least two-dimensional) ordered system. It is evident that the occurrence of a phase transition depends ultimately on the strength of these interactions in relation to the structure of the ions, clusters or chains and their configuration in the lattice.

This can be seen from the following argument. A phase transition, if present, will occur at a temperature of the order of the interaction energy divided by the Boltzmann constant. At this temperature at least two energy levels per magnetic moment (cluster, chain) must be populated in order to provide enough entropy removable at (or near) the transition temperature. When in the absence of the "ordering" interaction the ground state is degenerate, this condition is immediately fulfilled. On the other hand, a separation between the lowest two energy levels which is much larger than the interaction energy, will never lead to any phase transition. Somewhere between these two extremes a critical value exists for the ratio between the "ordering" interaction and the energy-level separation, which of course depends on the configuration of the interacting units, the type of interaction *etc.*

A clear illustration of this effect is provided by lattices of magnetic ions with integer spin values and singlet ground state. The first excited energy level of such an ion is determined by the crystal-field splitting. Then a critical value exists for the ratio between the exchange interaction and this splitting, below which no phase transition occurs. After its first indication by Trammel [4], refined calculations of the critical ratio are given by Cooper [5], Wang and Cooper [6].

Of course, an external magnetic field may change the relative positions of the energy levels and consequently influence the transition temperature. As is well known, a phase transition may even disappear entirely if the field is strong enough. An interesting situation occurs when the external magnetic field compensates the crystal-field splitting or some cluster-forming interaction in systems with a singlet ground state. In the presence of such a field, one of the excited

energy levels may cross the lowest level, so that the ground state in that field is again degenerate. An interaction that was too weak to arrange long-range order in zero field may well be able to cause a phase transition in the presence of the external magnetic field. As far as the description of this type of transitions is concerned, a simple theory can be set up representing each ion, cluster or chain by an effective spin, the magnitude of which is determined by the field-induced multiplicity of the ground state. Phase transitions of this special type form the subject-matter of the present work.

The number of substances in which such a high-field phase transition can be detected is limited by the experimental equipment, especially be the maximum field that can be produced. This maximum immediately imposes an upper limit to the zero-field energy-level splitting of the substances to be studied. In practice this limit is, expressed in temperature units, about 10 K for ions with a g value of 2. On the other hand, the energy-level splitting in zero field or the main interaction has to be large compared to the "ordering" interaction. So the minimum temperature which can be reached - it must be lower than the transition temperature - imposes indirectly a lower limit to the main interaction in the compounds to be studied. The realization of an experimental apparatus that allows detection of phase transitions in magnetic fields up to 75 kOe at temperatures down to 50 mK is described in Chapter II.

The three classes of substances that might exhibit a high-field phase transition will be discussed shortly.

1. Magnetic ions with integer spin and singlet ground state

The crystal-field splitting necessary for a singlet ground state requires a local symmetry at the ion site lower than cubic. In case of a spin $S = 1$ ion, such as V^{3+} or Ni^{2+}, the spin hamiltonian for an isolated ion then becomes

$$\mathcal{H} = D(S_z^2 - \tfrac{2}{3}) + E(S_x^2 - S_y^2) - g\beta\, \vec{H}\cdot\vec{S} \qquad (1)$$

Here $g\beta$ is the magnetic moment of the ion while the coefficients D and E represent the crystal field. The corresponding energy levels are

given in Fig. 1 as a function of the external field H for directions of H parallel to the principal axes of the crystal-field tensor. A deviation of H from these special directions removes the level crossing, but when it is not too large, a minimum in the separation of the energy levels will remain. It is clear that in the vicinity of the level crossing even a small inter-ion interaction can lead to a phase transition. A theoretical investigation of this case has been given by Tsuneto and Murao [7] within the framework of the molecular field approximation.

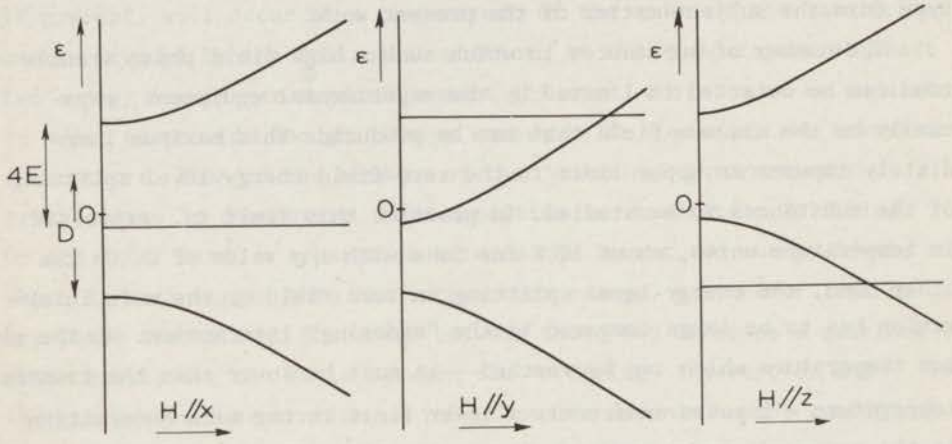

Fig. 1. Energy-level diagrams for an $S = 1$ ion in a crystal field. The magnetic field is directed along the principal axes of the crystal-field tensor.

From experimental point of view, the number of substances in which a transition can be expected is small by reasons explained above. Up to now only the nickel salts $NiSO_4 \cdot 6H_2O$, $NiSO_4 \cdot 7H_2O$ and $K_2Ni(SO_4)_2 \cdot 6H_2O$ are known to have a crystal-field splitting within the limits imposed by the experimental equipment. Our failure to detect a phase transition in these compounds may be due to their sensitivity to slight misorientations of the magnetic field, or to a too low transition temperature. Recently Myers, Polgar and Friedberg [8] reported experiments on the specific heat and magnetization of $NiSnCl_6 \cdot 6H_2O$. They suggest the existence of short-range order effects at $T = 0.35$ K when an external field of 5 kOe is present along the trigonal axis. It might well be possible that in this compound a phase transition of the type discussed above occurs at a lower temperature.

2. Clusters of magnetic ions

A second class of substances which might exhibit a high-field phase transition is formed by lattices containing clusters of magnetic ions, coupled together by some magnetic intra-cluster interaction which gives rise to a singlet ground state of the cluster in zero field. One of the excited levels may cross this ground state in the presence of a magnetic field, so that then a weak intercluster interaction is enough to produce a phase transition.

Since Kambe's [9] explanation of Welo's [10] susceptibility measurements a relatively large number of substances containing clusters of three trivalent chromium or iron ions is known, most of which are complex acetates. Another example of (relatively) isolated clusters is formed by the family of cupric salts of straight-chain fatty acids having the general formula $Cu_2(C_nH_{2n+1}CO_2)_4 \cdot xH_2O$ with x = 0 or 2 [11]. They contain strongly coupled pairs of cupric ions. However, the exchange interactions in all these substances exceed 100 K, so that magnetic fields of over 600 k0e would be necessary to make the lower two levels cross.

Up to now, the only compound of the cluster type that is found to fall within the experimental range is $Cu(NO_3)_2 \cdot 2\frac{1}{2}H_2O$, usually referred to as cupric nitrate "trihydrate". Several experimental studies by Friedberg *et al.* [12, 13, 14] indicate that this salt contains pairs of Cu^{2+} ions, coupled by an antiferromagnetic exchange interaction of J/k = - 5.2 K. If the interaction is assumed to be of the Heisenberg type, the hamiltonian for an isolated pair in the presence of an external field H would read

$$\mathcal{H} = - J\vec{S}_1 \cdot \vec{S}_2 - g\beta \vec{H} \cdot (\vec{S}_1 + \vec{S}_2) \qquad (2)$$

The corresponding energy levels consist of a singlet ground state and an excited triplet at 5.2 K. They are shown as a function of the external field H in Fig. 2. Owing to the Heisenberg character of the interaction and the different symmetry of the singlet and the triplet, the direction of the external field does not influence the energy-level crossing. Even when the interaction would be slightly anisotropic and must be represented by a tensor J, the energy levels still cross, independent on the field direction.

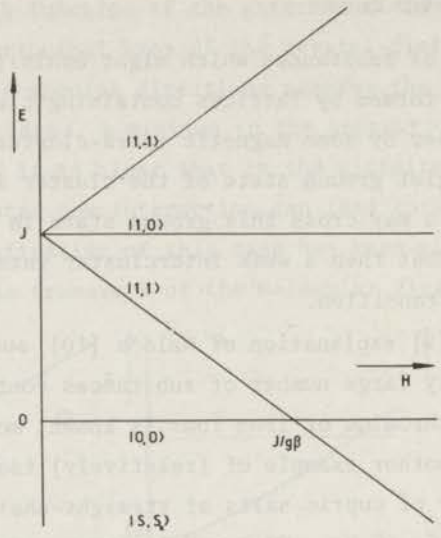

Fig. 2. Energy-level diagram for a pair of $S = \frac{1}{2}$ ions in an external field H. The quantum numbers of the total spin S and its z component S_z are indicated.

Again, in the vicinity of the crossing point even a weak interpair coupling is sufficient to cause a transition to a magnetically ordered phase. Since the experiments on cupric nitrate constitute a large part of the measurements described in this work, the theory dealing with different types of interpair interactions is discussed separately in Chapter IV. The experiments on cupric nitrate - started after a suggestion of Dr. Matsuura - are described in Chapter III. They prove unambiguously the existence of a high-field phase transition, occurring at 175 mK in an external field of 36 kOe.

3. Linear chains of magnetic ions

The third class to be considered is formed by crystals containing one-dimensional arrays of strongly coupled magnetic moments, with a weak interchain interaction. The antiferromagnetic linear chain (a.l.c.) of spins $S = \frac{1}{2}$ with Heisenberg coupling will be treated as an example. The hamiltonian of such an a.l.c. in an external field H is given by

$$\mathcal{H} = -J\sum_{i=1}^{N-1} \vec{S}_i \cdot \vec{S}_{i+1} - g\beta H \sum_{i=1}^{N} S_i^z \qquad (3)$$

where J represents the intrachain interaction and $\frac{1}{2}g\beta$ is the magnetic moment per ion.

Because the number of spins N approaches infinity for a real chain, the problem is much more complicated than in the preceding cases. This may be illustrated by Fig. 3, where the energy-level diagram has been

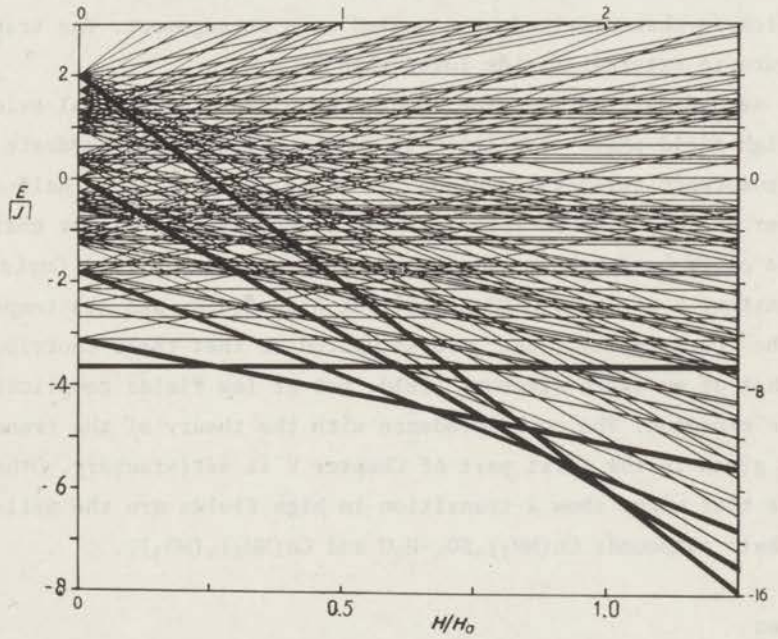

Fig. 3. Energy-level diagram for a ring of eight spins coupled by an isotropic antiferromagnetic exchange interaction (after Bonner and Fisher).

plotted for a ring of only eight spins with antiferromagnetic nearest-neighbour interaction*. It shows a rather uniform energy-level density, while the only degeneracies in the ground state are twofold and arise from the crossing of one level by a level for which the total spin $\Sigma_i S_i^z$ has increased by one unit. All crossings occur at fields lower

* The Figure has been copied from a paper by J.C. Bonner and M.E. Fisher (Proc. Phys. Soc. 80 (1962) 508).

than H_0, where $H_0 = 2|J/g\beta|$ is the equivalent of twice the intrachain interaction. Extrapolating these results to linear chains with N spins, one expects the energy levels to form a continuum in the limit $N \to \infty$, while the N crossings in the ground state still occur in the field interval $[-H_0, H_0]$.

In Chapter V a theory will be developed concerning antiferromagnetic linear chains with hamiltonian (3). It is shown that a weak, isotropic interchain interaction causes a transition to an ordered state which is characterized by a canted spin arrangement. The transition occurs in external fields lower than H_0.

The second part of the same chapter provides experimental evidence on the high-field phase transition in cupric sulphate pentahydrate and in the isomorphic selenate compound. In these substances one half of the number of Cu^{2+} ions is coupled in antiferromagnetic linear chains, while the other half behaves as a paramagnetic system with a Curie-Weiss constant θ of about 0.03 K [15]. At high fields and low temperatures the "paramagnetic ions" are saturated so that their contribution equals that of an extra external field, but at low fields complications are to be expected. The correspondence with the theory of the transitions as given in the first part of Chapter V is satisfactory. Other compounds that might show a transition in high fields are the well-known linear chain compounds $Cu(NH_3)_4SO_4 \cdot H_2O$ and $Cu(NH_3)_4(NO_3)_2$.

References

1. P. Ehrenfest, Comm. Leiden Suppl. 756 (1933).
2. L.D. Landau, Zhur. Eksp. i Teor. Fiz. 7 (1937) 627.
3. G. Baker Jr., Phys. Rev. 130 (1963) 1406.
4. G.T. Trammel, J. appl. Phys. 31 (1960) 362 S.
   Phys. Rev. 131 (1963) 932.
5. B.R. Cooper, Phys. Rev. 163 (1967) 444.
6. Y. Wang and B.R. Cooper, Phys. Rev. 172 (1968) 539. *ibid.* 185 (1969) 696.
7. T. Tsuneto and T. Murao, Physica 51 (1971) 186.
8. B.E. Myers, L.G. Polgar and S.A. Friedberg, to be published.
9. K. Kambe, J. Phys. Soc. Japan 5 (1950) 48.

10. L.A. Welo, Phil. Mag. 6 (1928) 481.

11. R.L. Martin and H. Waterman, J. Chem. Soc. (1957) 2545.

12. L. Berger, S.A. Friedberg and J.T. Schriempf, Phys. Rev. 132 (1963) 1057.

13. S.A. Friedberg and C.A. Raquet, J. Appl. Phys. 30 (1968) 1132.

14. B.E. Myers, L. Berger and S.A. Friedberg, J. appl. Phys. 40 (1969) 1149.

15. S. Wittekoek, T.O. Klaassen and N.J. Poulis, Physica 39 (1968) 293.

CHAPTER II
EXPERIMENTAL EQUIPMENT

Introduction

Before describing the different parts of the experimental equipment in detail, it is useful to pay attention to the arguments which finally led to the present construction. The detection of a high-field phase transition proceeds essentially in the same way as that of a transition in zero field, the only difference being the large external magnetic field in which the experiments have to be carried out. The very presence of this field seems to favour magnetic resonance as a detection method.

Since its first application by Poulis and Hardeman [1] on the antiferromagnet $CuCl_2 \cdot 2H_2O$, nuclear magnetic resonance (n.m.r.) has proved to be a powerful and accurate means to study phase transitions. In particular, it enables the determination of many important properties of the ordered state, such as the (sublattice) magnetization, the transition temperature as a function of the external field and the threshold-field phenomena. Therefore the experimental setup was especially designed for n.m.r. experiments, without excluding the possibility to study the expected phase transitions also by other methods, *e.g.* by specific-heat measurements. Of course, n.m.r. requires some special arrangements, the most important of which are the application of a magnetic field of extreme homogeneity and the use of single-crystal samples.

The work of Wittekoek [2, 3, 4] on the linear-chain compounds $CuSO_4 \cdot 5H_2O$ and $CuSeO_4 \cdot 5H_2O$ as well as the existing data on $Cu(NO_3)_2 \cdot 2\frac{1}{2}H_2O$ [5, 6] indicated that the interesting field range exceeded the capability of conventional magnets, so that the use of a superconducting device was inevitable. As some experience with the construction of such magnets for n.m.r. application was already available from experiments by Ancher, the only problem existed in raising their maximum field while maintaining the necessary homogeneity of about 1 Oe over the sample.

More difficulties were encountered in the realization of the low temperature at which the phase transitions were expected. As explained

in the previous chapter, the interaction which arranges the long-range order is assumed to be much weaker than the cluster or chain-forming interaction. A rough estimate of the transition temperature, obtained by dividing this weak interaction energy by the Boltzmann constant, restricts the interesting temperature range to the region well below 1 K. The simplest way to enter this region is the application of ^{3}He evaporation.

Unfortunately the most promising compounds, cupric sulphate and cupric nitrate, did not show any transition even at the lowest temperature obtainable with the ^{3}He cryostat used. In order to obtain lower temperatures, a choice had to be made between two possibilities: ^{3}He - ^{4}He dilution refrigeration or adiabatic demagnetization. Because of its relative simplicity and its ability of rapid temperature changes, the latter method was preferred.

Since adiabatic demagnetization requires a low fieldstrength at the position of the cooling salt, this salt has to be placed at some distance from the resonance magnet. The single crystal to be studied can be connected to it via a heat link. The field necessary to magnetize and demagnetize the cooling salt must be generated by a second superconducting coil, in order to avoid the extreme forces on the cryostat wall that would result from the use of a conventional magnet. Moreover, the application of two superconducting coils admits a simple and compact uniaxial construction, that can easily cope with the force arising from simultaneous operation of both magnets.

Of course, the specific demands imposed by n.m.r. in combination with the demagnetization method caused many complications in the design of the apparatus.

Demagnetization apparatus

The main difficulties, arising from the demands explained in the previous section are twofold:

i) The connection between sample and cooling salt must exhibit a very good thermal conductivity, while joule heating of the material at the sample position by the radio-frequency field inherent to n.m.r. should be minimal.

ii) Complete thermal isolation of the sample from the surrounding helium bath should be realized while maintaining a reasonable value for the filling factor of the resonance coil.

The first problem was solved by the application of a large number ($\sim$ 1000) of very thin (50 μ) copper wires. The wires were spread around the crystal and tightened by nylon threads. Apiezon N grease established the heat contact between crystal and wires. At the other end, the bundle of wires was silver soldered to a 6 mm diameter copper rod.

The second problem involves the filling factor of the resonance coil. Since this coil has to be placed outside the vacuum wall surrounding the whole demagnetization apparatus, a reasonable filling factor can only be obtained when the distance between sample and wall is small compared to the sample size.

The very careful fixation of the sample, required for such a small distance was obtained by an araldite-impregnated paper tube that enveloped the copper wires and fitted closely over the copper rod. The rod, together with paper tube and sample was screwed to the cooling salt, which consisted of a perspex cylinder filled with chromium-potassium alum. A brush of copper wires increased the heat contact between alum and copper rod. A thin-walled teflon tube at the top and four teflon screws at half height fixed the whole assembly firmly and thermally insulated in a perspex frame, which was precooled by two manganese-ammonium sulphate guard salts above and below the main cooling salt. The frame itself rests on a 25 mm grinded joint at the inside of the glass vacuum jacket, thermal insulation being provided by four poly-vinyl chloride columns.

This rigid construction, which is shown in detail in Fig. 1, allows rapid sample replacements with a minimum chance of involuntary heat contacts to the vacuum jacket. The materials for the cooling salt and the guard salts were selected according to their thermal properties. Adiabatically demagnetized from about 1 K and 20 kOe, chromium-potassium alum easily reaches a minimum temperature of 10 mK while it possesses a reasonably large heat capacity between 10 mK and 100 mK. Although the manganese-ammomium sulphate only cools down to about 50 mK, its large specific heat above 100 mK makes it an ideal material for guard-salt applications.

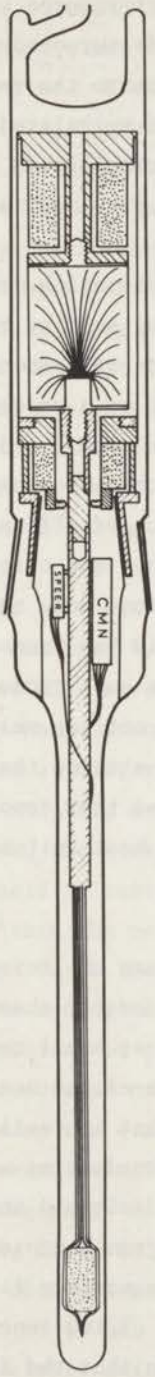

Fig. 1. Details of the demagnetizing apparatus.

A layer of aquadag on the glass vacuum jacket reduced the heating by room-temperature radiation. Black paper shields surrounded the lower part of the inner cryostat, while the pumping line to the vacuum jacket was equipped with a radiation trap. The use of spiralized niobium wire minimized the heat inleak through the electrical leads necessary for heater and thermometer. The lower guard salt provided these leads with a thermal ground.

During the specific-heat and adiabatic-magnetization measurements, the sample was thermally isolated from the cooling salt by replacing a part of the copper rod in the heat link by a piece of epibond. A strip of tin foil with a cross section of 0.3 mm^2 acted as a superconducting heat switch and short-circuited the epibond piece. The field of the demagnetization magnet also operated the heat switch: after magnetization of the cooling salt at 1 K the contact gas was pumped off as usual and the fieldstrength was reduced to a value just above the critical field of the tin switch. After allowing the sample to cool down to the lowest temperature of about 40 mK the demagnetizing field was turned off completely, thereby bringing the tin switch into the superconducting state and thus isolating the sample thermally from the cooling salt. The overall heat inleak amounted to 10^{-7} W at 0.1 K, a value that dropped to zero at 0.3 K and finally became negative above that temperature owing to the increasing heat conductivity of the heat switch.

The magnets

From the foregoing discussion it is clear that the resonance magnet must produce at least 50 kOe at a homogeneity of better than 1 Oe over the sample, while the stray field has to be kept as small as possible. Since the latter requirement demands minimization of the overall dimensions of the magnet, the design should be such that it realizes a high homogeneous field with a minimum volume of superconducting wire. This is achieved by calculating the dimensions of the solenoid and the correction coils at both its ends by a computer program composed after the ideas of Garrett [7]. This procedure computes the maximum field to current ratio H/i of the magnet at a given value of the inner diameter and a given length of wire, under the restriction that the field at the

center of the solenoid is compensated up to the sixth order. The minimum value of the clear bore depends on the dimensions of the demagnetization apparatus, which in turn are determined by the compromise between the filling factor and the thermal isolation of the sample, as explained in the previous section.

Once the inside diameter has been fixed, the amount of wire is determined by the required fieldstrength. The type of wire is then selected according to various criteria concerning its behaviour in high magnetic fields, among which the current-carrying capability and the stability are the most important ones.

The final design yielded a solenoid with an inner diameter of 25 mm, an outer diameter of 72 mm and a length of 176 mm. The correction coils at both ends made the total diameter increase to 90 mm. The magnet was wound from a 5.2 km long single piece of niobium-titanium wire, stabilized by a cover of high-conductivity copper and formvar insulated (Supercon type T48B 010/016). The field to current ratio and the homogeneity were measured by n.m.r. on the ^{19}F nuclei present in a 2 mm probe that could be moved along the main axis of the solenoid. Fig. 2 shows the resonance frequency of these nuclei as a function of the probe position at different current values. Although the field pattern proves to be slightly dependent on the fieldstrength, probably due to frozen-in flux, the overall homogeneity is better than 3×10^{-5} over 20 mm. The field to current ratio equals its calculated value of 1.95 kOe/A within the measuring accuracy, while at 4.2 K the quench field amounted to 78 kOe at a current of 41 A, which is only 0.5% lower than the specified short-sample characteristic of the wire.

The dimensions of the demagnetization magnet were obtained from the same procedure as had been used for the resonance magnet, the only difference being the constraint that for this coil a large space was required in order to allow the use of a maximum amount of cooling salt. The field homogeneity is of less importance in this case. The inner diameter being fixed at 60 mm, only 2 km of T48B 008/013 wire was necessary to obtain a maximum field of 28 kOe with a homogeneity of 3% over a length of 85 mm. Both magnets were fed from stabilized current supplies especially designed for this experiment. The current from the

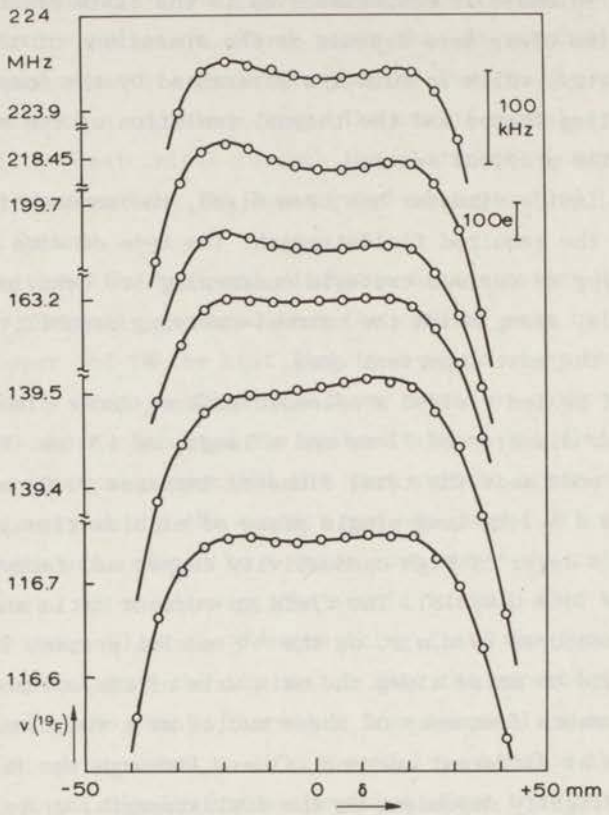

Fig. 2. Resonance frequencies of ^{19}F nuclei in a teflon probe, plotted *versus* the probe position on the axis of the n.m.r. magnet. Different curves correspond to different values of the energizing current.

main supply was stable to within 10^{-5} over a period of one hour, so that it was unnecessary to equip the resonance magnet with a persistent-mode switch. In the other supply a motor-driven potentiometer guaranteed a uniform demagnetization procedure.

The distance between the two solenoids is a compromise between the tolerable stray field of the resonance magnet at the position of the cooling salt and the length of the heat link to the sample. In the final construction the centers were 315 mm apart. At this distance, the force between the magnets was calculated to be $F = 0.9\ I_1\ I_2$ (N). This force, which reaches a value of 1800 N when both magnets are oper-

ated at full power, is easy to handle provided the directions of the currents are chosen such that it is attracting.

The 100 mm inside diameter cryostat which contained the two magnets was kept at 4.2 K. When filled with 8 l liquid helium the resonance magnet remained in the superconducting state for a period of 15 hours. A separate cryostat inside the two magnets contained the demagnetization apparatus. It could be pumped down to 1.0 K with the aid of an Edwards 9B3 booster pump and allowed 8 hours of experiments with a 1.5 l helium content.

N.M.R. equipment

From the various methods to detect nuclear magnetic resonance the marginal oscillator was used. The main advantage of an oscillator-detector system is its flexibility upon changes of the operating frequency, which is very useful when n.m.r. spectra are studied over a large frequency range. However, both the high magnetic field and the very low temperatures turned out to be sources of complications.

A field of 50 kOe requires an operating frequency of over 200 MHz to detect proton magnetic resonance signals. As it was desirable to perform n.m.r. experiments in fields down to at least 10 kOe with one and the same oscillator, a circuit had to be found that operated with a reasonable sensitivity from 50 MHz to over 200 MHz. The only circuit which is simple enough to operate reliably over such a wide frequency range is the one given by Robinson [8] in 1965. A few improvements finally led to the scheme given in Fig. 3, which operates essentially the same as the original Robinson circuit up to a frequency of 240 MHz.

The length of the cryostat determined the minimum length between resonance coil and tuning capacitor at 1.5 m. Since this length is of the same order of magnitude as the wavelength, the resonance circuit must be considered as a multimode cavity the tuning of which demanded a special artifice. A T-piece with a short-circuited cable at one end, inserted between the oscillator and the coaxial line to the resonance coil proved to be the solution. The tuning characteristics of the thus created cavity may be illustrated by the discussion of the Smith chart shown in Fig. 4. In this diagram the complex reflection coefficient

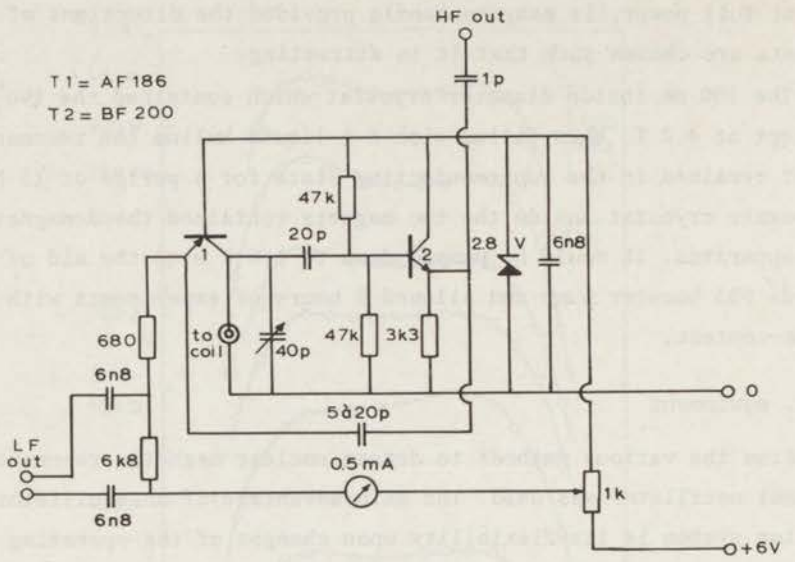

Fig. 3. Circuit of the modified Robinson oscillator used for n.m.r. detection.

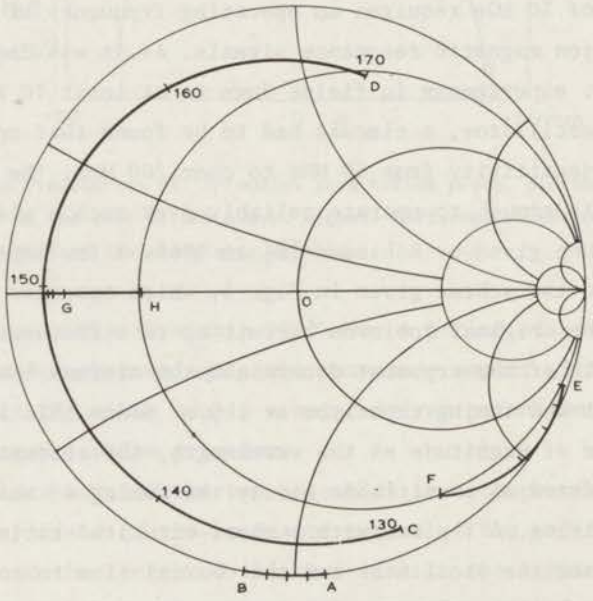

Fig. 4. Smith chart representing the reflection coefficients at different positions in the resonant cavity. For explanation see text.

$\rho = (Y_0 - Y) / (Y_0 + Y)$ at different points in the resonant circuit is indicated as a function of frequency for one particular mode. The curve AB represents the reflection coefficient ρ_L of the resonance coil. The coaxial line in the cryostat of length l transforms AB into CD by multiplication of ρ_L by a factor $\exp - 2 (\alpha + i\beta)l$, where β equals the wave number ω/c and α represents the damping (greatly exaggerated in the figure). At the T-piece, the short-circuited side cable acts as a parallel admittance and transforms CD into EF. The short line between T-piece and oscillator and the tuning capacitor remove the pure imaginary part of the admittance and bring the reflection coefficient onto the real axis in GH. In this way the range of 80 MHz to 200 MHz is covered by three modes, each of which is about 40 MHz wide.

The relatively poor heat contacts between sample, heat link and cooling salt together with the limited heat capacity of the last demanded operation of the oscillator at a constant and very low level. As can be seen from the foregoing discussion, the impedance of the resonance circuit changes with frequency. Therefore the amplitude of the r.f. voltage was stabilized externally by regulating the supply voltage of the oscillator by the amplified and detected r.f. signal. However, even with the aid of this mechanism stable operation at levels lower than 3 mV was not possible, which inhibited n.m.r. experiments at temperatures lower than 80 à 90 mK because of the heating up of the copper wires in the heat link. In the crystals discussed in this thesis no difficulties were encountered by heating up of the sample itself or by saturation of the studied nuclear transitions.

Fortunately, the large proton polarization at the lower temperatures allowed the application of a less sensitive detection method based on the use of a hybrid junction and which exhibits the same frequency-sweep capabilities as the marginal oscillator. A hybrid junction is a four-port network, comparable to the "magic tee" in microwave applications. In the ideal case, the output voltage at the fourth port equals half the input voltage at the first port, multiplied by the difference of the reflection coefficients ρ_2 and ρ_3 at the second and third ports. Thus, if the second and third ports are connected to two equal resonance coils via two equal coaxial transmission

lines, these reflection coefficients will be exactly equal and no output will result, independent of the frequency of the signal generator at the first port. One of the coils is mounted around the sample. Whenever nuclear magnetic resonance occurs, ρ_2 and ρ_3 no longer cancel each other and a signal appears at the fourth port. This signal is amplified, and finally phase-sensitive detection in a balanced mixer discriminates between absorption and dispersion. Although the sensitivity is essentially smaller by a factor $\sqrt{Q}$ than any method that applies a tuned circuit with quality factor Q, the hybrid junction is quite useful in high-field and low-temperature work. In combination with the described demagnetization apparatus it even allowed n.m.r. measurements at a temperature as low as 50 mK. Because the commercially available hybrid junctions never meet the ideal case mentioned before, some difficulties arise whenever the cable lengths at the second and third ports approach uneven multiples of $\lambda/4$, but these can be easily omitted.

The signal to noise ratio of both detection methods was improved in the usual way by application of field modulation and phase-sensitive detection. The resonance frequencies were measured by simultaneous plotting the output from the PAR 121 lock-in amplifier and a calibration signal obtained from a HP 5246L electronic frequency counter on a Philips PR 2210 chart recorder.

Thermometry

The sample temperature was measured by a carbon resistance thermometer of the Speer type. These resistors exhibit a high sensitivity in the temperature range below 1 K and are only slightly influenced by the presence of moderate magnetic fields [9]. Nevertheless the resistor was placed at some distance from the resonance magnet. An experiment using the proton resonance-line splitting in cupric nitrate just below the critical temperature proved that at 0.15 K the misreading in the temperature due to the stray field of the resonance magnet was negligible compared to the measuring accuracy. A separate heat link, also constructed of many very thin copper wires, connected sample and thermometer in order to avoid temperature differences originating in the heat flow in

the main link. An a.c. Wheatstone bridge and phase-sensitive detector operating at 31.5 Hz were used to measure the resistance.

Warming up of the thermometer by the measuring current was excluded by keeping its dissipation always below 10^{-11} W, while spurious r.f. currents due to the n.m.r. equipment were short circuited by a bypass capacitor of 47 pF. However, it also proved to be necessary to decouple all electrical leads to the cryostat in order to exclude heating up by r.f. fields produced by other experiments in the laboratory and broadcasting stations.

The resistor, a nominal 560 Ω, ¼ watt type, was calibrated against the susceptibility of cerous-magnesium nitrate (CMN) in the same apparatus. The extremely low Curie-Weiss value of this compound makes it

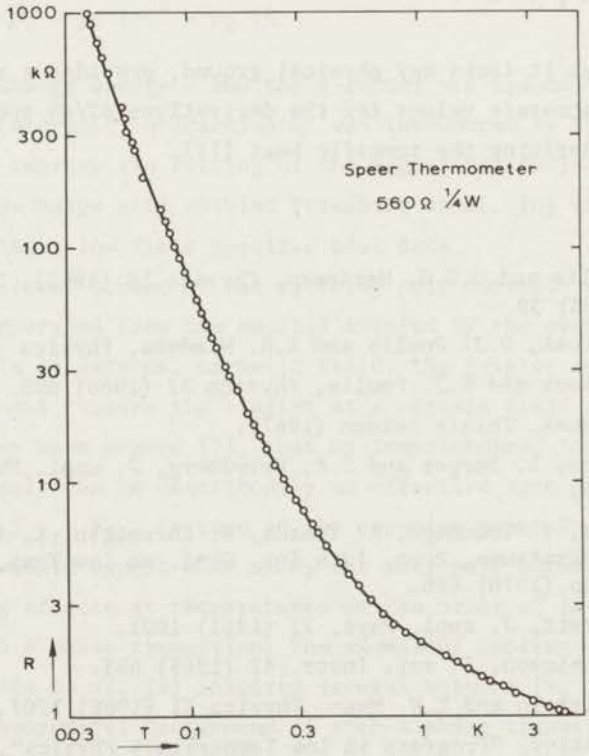

Fig. 5. Resistance of the Speer thermometer *versus* temperature. The drawn curve represents the polynomial mentioned in the text.

an ideal material for very low temperature thermometry [10]. The calibrations of the Speer resistor were made in separate runs before and after each measuring series. During these runs a miniature coil system, developed by Haasbroek [11], containing about 100 mg CMN was connected to the copper cooling rod.

A current of about 70 mA through the demagnetization magnet was necessary to compensate for the remanent field due to frozen-in flux. This current was determined by maximizing the susceptibility reading at the highest resistance value. The resistance *versus* temperature relation is shown in Fig. 5. A machine calculation fitted the coefficients C_k in the polynominal

$$\frac{1}{T} = \sum_{k=1}^{12} C_k \, (\log R)^{k-1}$$

which, although it lacks any physical ground, provides a suitable interpolation and accurate values for the derivatives dT/dR and d^2T/dR^2 necessary in deriving the specific heat [12].

References

1. N.J. Poulis and G.E.G. Hardeman, Physica 18 (1952), 201. *ibid.* 19 (1953) 39.
2. S. Wittekoek, N.J. Poulis and A.R. Miedema, Physica 30 (1964) 1051.
3. S. Wittekoek and N.J. Poulis, Physica 32 (1966) 693.
4. S. Wittekoek, Thesis Leiden (1967).
5. B.E. Myers, L. Berger and S.A. Friedberg, J. appl. Phys. 40 (1969) 1149.
6. T. Haseda, Y. Tokunaga, R. Yamada, R. Kuramitsu, K. Amaya and S. Sakatsume, Proc. 12th Int. Conf. on low Temp. Phys., Kyoto (1970) 685.
7. M.W. Garrett, J. appl. Phys. 22 (1951) 1091.
8. F.N.H. Robinson, J. sci. Instr. 42 (1965) 653.
9. A.S. Edelstein and K.W. Mess, Physica 31 (1965) 1707.
10. J.C. Wheatley, "Progress in Low Temperature Physics", vol. VI (1970) p. 132.
11. J.N. Haasbroek, private communication.
12. E. Lagendijk, Thesis Leiden (1972).

CHAPTER III
THE HIGH-FIELD PHASE TRANSITION IN $Cu(NO_3)_2 \cdot 2\frac{1}{2}H_2O$

Introduction

The Cu^{2+} ions in cupric nitrate "trihydrate" are coupled in binary clusters by an antiferromagnetic interaction. The first experimental evidence suggesting this fact was the measurement of the susceptibility by Berger, Friedberg and Schriempf in 1963 [1]. In the following years the pair model was established by various experiments on specific heat [2], proton magnetic resonance [3], paramagnetic relaxation [4] and magnetization isotherms [5]. All the afore mentioned properties could be explained satisfactory with the hamiltonian for an isolated pair:

$$\mathcal{H} = -J\,\vec{S}_1 \cdot \vec{S}_2 - g\beta\,(S_1^z + S_2^z)H \qquad (1)$$

in which the exchange energy J and the g factor are assumed to be isotropic. A weak interpair interaction J' was introduced by Myers *et al.* [5] in order to improve the fitting of the magnetization isotherms. A weak interpair exchange also enabled Friedberg *et al.* [6] to perfect the fitting of their low-field specific heat data.

The energy-level scheme of the isolated pair consists of a singlet ground state, separated from the excited triplet by the exchange energy $|J|/k$ = 5.2 K. In an external magnetic field, the triplet splits and the lower component crosses the singlet at a certain field H_0 as shown in Fig. 1. It has been argued [7], that at temperatures, low compared to $|J|/k$, each pair can be described by an effective spin $S' = \frac{1}{2}$ in an effective field H_{eff}. H_{eff} is zero at the crossing point H_0. If this were true, one should expect that at H_0 the interpair exchange J' would lead to ordering effects at temperatures of the order of $|J'|/k$ and possibly also to a phase transition. The anomalous cooling effects reported by Haseda *et al.* [8] inspired several authors [9, 10] to investigate the theoretical background of such a phase transition. Because it is disputable to prove the existence of a phase transition only by the concavity of an adiabatic magnetization curve, Dr. Matsuura suggested us to perform further n.m.r. experiments on cupric nitrate in the

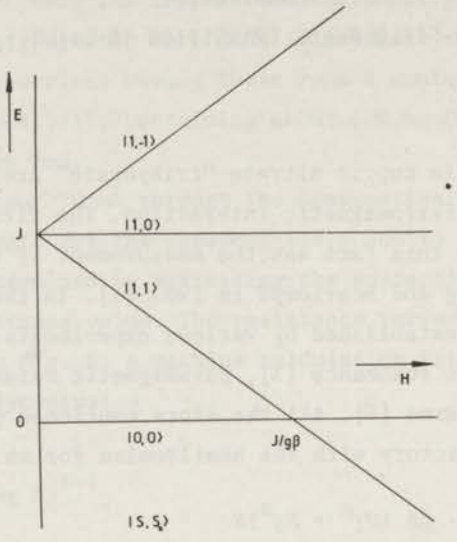

Fig. 1. Energy levels for an isolated pair of $S = \frac{1}{2}$ spins. The quantum numbers indicating the total spin S and its component S_z in the direction of the external field are given in brackets.

high-field range. The existence of short-range order was clearly demonstrated below 0.4 K [11]. Since no phase transition was found down to 0.27 K, an experimental arrangement was set up which should allow n.m.r. experiments at still lower temperatures in the interesting field range around H_0. A slight alteration of this experimental setup created the possibility to measure also the specific heat and the adiabatic cooling effects down to 50 mK. In this chapter the existence of a long-range ordered phase is proved between 29 kOe and 43 kOe and below 175 mK. However, a comparison of the results with the existing theories revealed some fundamental discrepancies. Therefore a more detailed discussion will be postponed to Chapter IV, in which also a more elaborate theory will be introduced.

Proton magnetic resonance

The crystallographic structure of $Cu(NO_3)_2 \cdot 2\frac{1}{2}H_2O$ has been determined by Garaj [12] and Morosin [13]. It belongs to the monoclinic space

group I2/a. The unit cell contains 8 formula units and has the dimensions a = 16.45 Å, b = 4.936 Å and c = 15.96 Å with β = 93.77°.

With the aid of proton magnetic resonance it is possible to measure the value of the magnetic field at the 40 proton positions. The magnetic field at the i-th proton position is the vector sum of the external field $\vec{H}$ and the internal field $\vec{h}^{(i)}$ due to the surrounding Cu^{2+} ions. This internal field can be expressed in the tensor equation

$$\vec{h}^{(i)} = \sum_k D^{(ik)} \cdot \langle \vec{\mu}_k \rangle \qquad (2)$$

where $\langle \vec{\mu}_k \rangle$ is the magnetic dipole moment of the k-th cupric ion, averaged over a period of the order of the inverse proton resonance frequency. If the copper-proton interaction is of a purely dipolar character the components of $D^{(ik)}$ are given by

$$D_{mn}^{(ik)} = \frac{3r_m^{(ik)} r_n^{(ik)} - \delta_{mn} r^{(ik)2}}{[r^{(ik)}]^5} \qquad (3)$$

Here δ_{mn} is the Kronecker symbol and $\vec{r}^{(ik)}$ represents the position vector of the i-th proton relative to the k-th copper ion. In high magnetic fields the time-averaged magnetic moment of the copper ions $\langle \mu_k \rangle$ can be obtained in a relatively simple manner from the lineshift Δ. This Δ is defined as the difference between the actual resonance frequency $\upsilon = \gamma/2\pi \cdot H_t$ and the free proton resonance frequency $\upsilon_0 = \gamma/2\pi \cdot H$. The factor γ represents the proton gyromagnetic ratio. The total magnetic field at a proton position is given by

$$H_t = |\vec{H} + \vec{h}| = H + h_{//} + \frac{h_\perp^2}{H + H_t + h_{//}} \qquad (4)$$

In this equation $\vec{H}$ is the external field, while the components of the internal field parallel and perpendicular to $\vec{H}$ are represented by $h_{//}$ and $h_\perp$, respectively.

Since in all experiments reported in this chapter the external field H exceeds the internal field $h^{(i)}$ by a factor of at least 50, the last term in equation (4) may be neglected in most calculations and the

lineshift Δ is almost entirely due to the parallel component of the internal field:

$$\Delta^{(i)} = \gamma/2\pi (H_t^{(i)} - H) = \gamma/2\pi \; h_{//}^{(i)} = \gamma/2\pi \sum_k \frac{\vec{H}}{H} \cdot D^{(ik)} \cdot \langle \vec{\mu}^k \rangle \qquad (5)$$

If all magnetic moments $\langle \vec{\mu}^k \rangle$ should be identical, equation (5) will reduce to:

$$\Delta^{(i)} = \frac{\gamma}{2\pi} \left[\sum_k \frac{\vec{H}}{H} \cdot D^{(ik)} \right] \cdot \langle \vec{\mu} \rangle = \frac{\gamma}{2\pi} \vec{G}^{(i)} \cdot \langle \vec{\mu} \rangle \qquad (6)$$

where $\vec{G}^{(i)}$ depends only on the direction of the magnetic field and the i-th proton position.

In order to simplify the discussion, the different states of a magnetic system in an external field will be defined as follows:

i) A system is in the paramagnetic state when all magnetic moments $\langle \vec{\mu}^k \rangle$ are identical and have the same direction as the external field.

ii) A system is in the ferromagnetic state when all magnetic moments are identical but have a direction which is generally different from that of the external field.

iii) A system is in the antiferromagnetic state when the magnetic moments can be distributed over two sublattices with magnetizations $\langle \vec{\mu}_1 \rangle$ and $\langle \vec{\mu}_2 \rangle$ which only differ in direction and are in general not collinear with the external field.

It is evident that more than one magnetic system can be present in the same crystal, while also states with more than two sublattices are possible.

In the paramagnetic state equation (6) for the lineshift simplifies to:

$$\Delta_p^{(i)} = \frac{\gamma}{2\pi} \left[\sum_k \frac{\vec{H}}{H} \cdot D^{(ik)} \cdot \frac{\vec{H}}{H} \right] \langle \mu \rangle = \frac{\gamma}{2\pi} G^{(i)} \langle \mu \rangle \qquad (7)$$

so that all lineshifts $\Delta^{(i)}$ differ only by a factor $G^{(i)}$ which is independent of fieldstrength and temperature. Because two of the three crystal-symmetry operations in the unit cell of cupric nitrate leave the factors $G(i)$ invariant, the number of proton resonance lines in

the paramagnetic state amounts to ten, apart from the splitting due to proton-proton interaction. It even reduces to five when the magnetic field is directed parallel or perpendicular to the twofold *(b)* axis.

Results

The rotating diagram given in Fig. 2 has been made at 1.3 K with a field of 26 kOe in the *bc* plane of the crystal. Ten resonance lines were recorded which coincide two by two when the field approaches the *b* and *c* axes. Since the actual plane in which the magnetic field rotated did not contain the crystallographic *b* axis exactly, the coincidence of the resonance lines did not occur at one and the same angle. The correspondence between the resonance lines and the proton positions in the

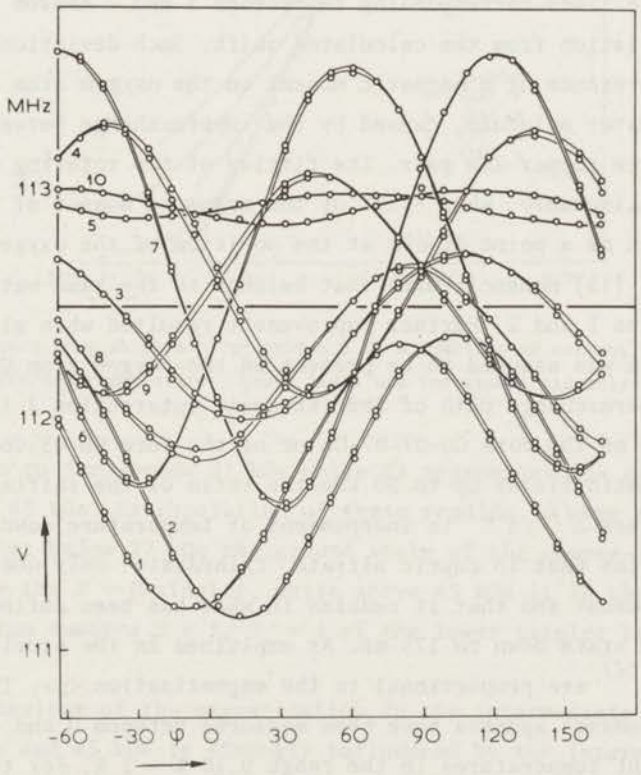

Fig. 2. Rotating diagram of $Cu(NO_3)_2 \cdot 2\frac{1}{2}H_2O$ at T = 1.3 K. The external field H = 26 kOe is rotating in a plane close to the *bc* plane of the crystal.

unit cell was obtained from the study of the dipole-dipole interaction between the two protons in each water molecule. This interaction causes a small splitting of the resonance lines in the rotational diagram, which unambiguously determines the water molecule from which each resonance line originates. In order to distinguish the two resonance lines from the same water molecule, the internal field due to the surrounding cupric ions must be taken into account. This internal field can be calculated from the crystal structure, provided the copper ions may be considered as point dipoles. A numerical calculation summing the dipolar contributions of all cupric ions within a sphere of 40 Å radius (about 1600) describes the measured rotating diagram fairly well for the protons 3, 4 and 5 (Morosin's [13] nomenclature). However, the resonance lines corresponding to protons 1 and 2 showed an extraordinary deviation from the calculated shift. Such deviations may indicate the presence of a magnetic moment on the oxygen atom of that particular water molecule, caused by the superexchange between the two members of the copper-ion pair. The fitting of the rotating diagram improved considerably, when -1.5% of the magnetic moment of the cupric ion was taken as a point dipole at the position of the oxygen atom (07 in Morosin's [13] nomenclature) that belongs to the same water molecule as the protons 1 and 2. Further improvement resulted when also +1.5% of the Cu^{2+} spin was assumed to be present on the oxygen atom 08. Therefore the superexchange path of the intrapair interaction J is expected to be either of the form Cu-07-07-Cu or of the form Cu-08-06-Cu.

In magnetic fields up to 50 kOe the ratio of the shifts of any two resonance lines $\Delta^{(i)}/\Delta^{(j)}$ is independent of temperature down to 175 mK. This implicates that in cupric nitrate "trihydrate" only one magnetic system is present and that it remains in what has been defined as the paramagnetic state down to 175 mK. As explained in the previous section, the shifts $\Delta^{(i)}$ are proportional to the magnetization $\langle\mu\rangle$. The proton magnetic resonance spectra have been measured between 0 and 50 kOe at five different temperatures in the range 0.18 K - 1 K. For the resonance line with the largest shift the results are shown in Fig. 3 as a function of the external field H. From these isotherms the pair structure of the copper ions can be recognized. With decreasing temperature the magneti-

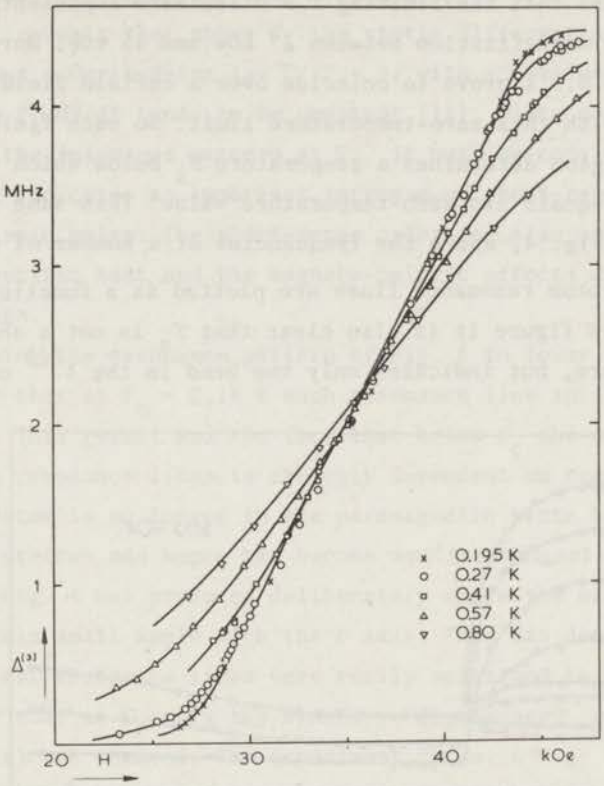

Fig. 3. Resonance-line shift $\Delta^{(3)}$ of proton 3 as a function of external magnetic field at different temperatures. Drawn lines are for visual aid only.

zation tends to zero below 27 kOe while it approaches its saturation value above 45 kOe. Extrapolation of these results to zero temperature indicates that below 27 kOe the ground state of the copper-spin pairs is formed by the $S = 0$ singlet, while above 45 kOe it is characterized by the quantum numbers $S = 1$, $S_z = 1$ of the lower triplet level (compare Fig. 1).

The behaviour of the magnetization in the intermediate fields between 27 kOe and 45 kOe is strongly influenced by the interpair interaction. If there was no interpair interaction at all, the zero-temperature isotherm should have the form of a step function at the crossing field H_0. However, from extrapolation of the measured magnetization iso-

therms it appears that the limiting $T = 0$ isotherm represents a linear increase of the magnetization between 27 kOe and 45 kOe. Moreover, the isotherms below 0.5 K prove to coincide over a certain field range around 36 kOe with this zero-temperature limit. So each field in the intermediate region determines a temperature T_s below which the magnetization $\langle \mu(T) \rangle$ equals its zero-temperature value. This same feature is illustrated in Fig. 4, where the frequencies of a number of well-distinguishable proton resonance lines are plotted as a function of temperature. From this figure it is also clear that T_s is not a sharply defined temperature, but indicates only the bend in the $\Delta^{(i)}$ *vs.* T curves.

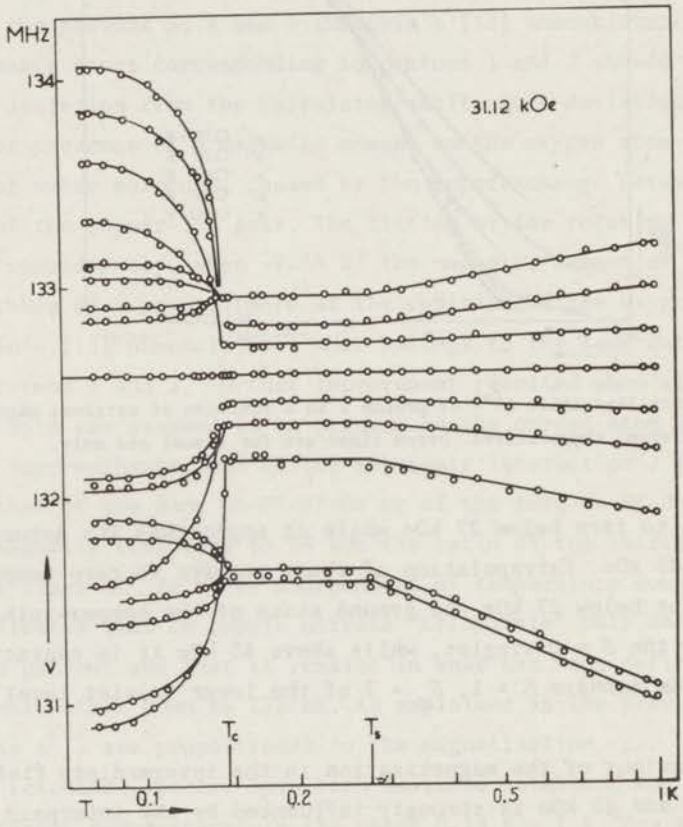

Fig. 4. Resonance-line shifts $\Delta^{(i)}$ for the best distinguishable lines of a function of temperature at an external magnetic field of 31.12 kOe. The direction of the magnetic field encloses a small angle with the crystallographic b axis.

A further experimental study of the temperature dependence of the shifts $\Delta^{(i)}$ reveals that above T_s the static differential susceptibility dM/dH follows a Curie-Weiss law $C/(T - \theta)$ with a θ-value of -0.2 K, while below T_s dM/dH tends to be constant [11]. Since no other change appears in the resonance pattern at T_s, it must be concluded that this temperature indicates an important increase of short-range order among the copper spin pairs. The short-range order can also be recognized from the specific heat and the magneto-caloric effects discussed in the next sections.

Following the resonance pattern of Fig. 4 to lower temperatures, it is clear that at T_c = 0.14 K each resonance line splits into two components. This result and the fact that below T_c the ratio $\Delta^{(i)}/\Delta^{(j)}$ for any two resonance lines is strongly dependent on temperature, prove that the system is no longer in the paramagnetic state but must consist of two sublattices and hence has become antiferromagnetic. The resonance diagram of Fig. 4 was produced deliberately while the magnetic field made a certain small angle with the b axis. This was done to ensure that at T_c all resonance lines were really split and to exclude the possibility that at T_c only the symmetry "degeneracy" (resulting from $\langle\vec{\mu}\rangle$ // b axis) was removed. The experiment shown in Fig. 4 was carried out before the series reported hereafter, in which the magnetic field was parallel to the crystallographic b axis to within 0.5 degree.

In the antiferromagnetic state the shifts of every two resonance lines which coincide in the paramagnetic state can be described by the phenomenological relation:

$$\Delta_{\pm}^{(i)} = \frac{\gamma}{2\pi} \{G_z^{(i)} \langle\mu_z(T)\rangle \pm G^{(i)'} \langle\mu'(T)\rangle\} \qquad (8)$$

In the Figures 5 and 6 the temperature dependence of the resonance pattern in the ordered state is shown for three values of the external magnetic field. These figures clearly illustrate that the first term of equation (8) $G_z^{(i)}\langle\mu_z\rangle$, almost equals the shift due to the magnetization parallel to the external field in the paramagnetic state. The splitting $\Delta_+^{(i)} - \Delta_-^{(i)}$, which equals twice the second term in relation (8), shows the characteristic temperature dependence of a spontaneous

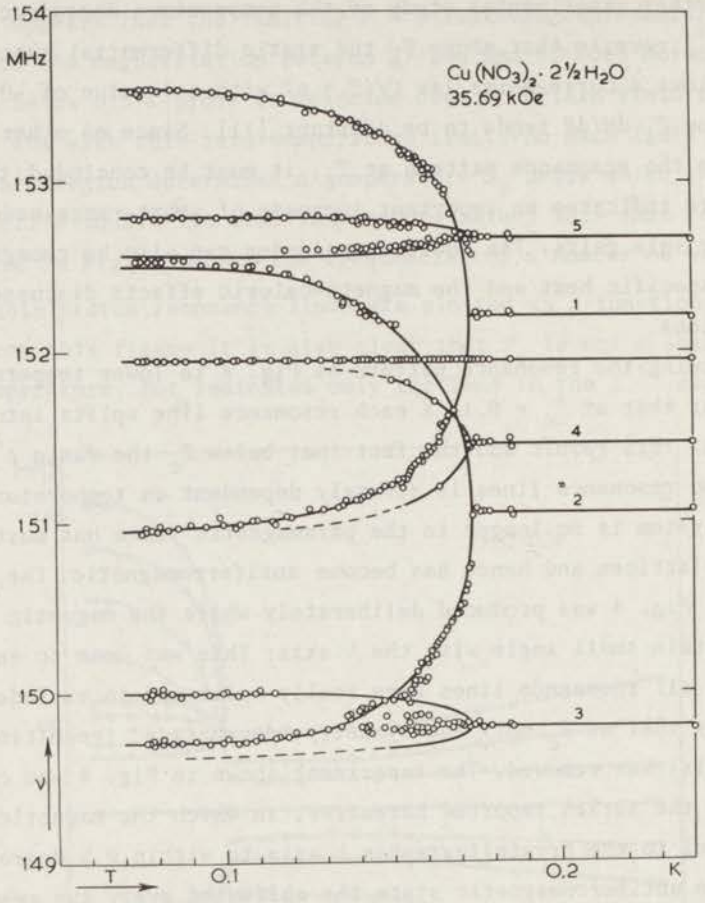

Fig. 5. Shifts $\Delta^{(i)}$ for all resonance lines as a function of temperature. The magnetic field amounts to 35.69 kOe and is parallel to the crystallographic b axis.

magnetization. Moreover, it is independent of the external magnetic field over the whole field range in which it occurs. (The only exception to this rule is formed by resonance line nr. 3, in which a slight field dependence of the splitting can be detected. The source of this deviation will be discussed at the end of this section.)

The two sublattice magnetizations $\langle\vec{\mu}_+\rangle$ and $\langle\vec{\mu}_-\rangle$ can always be expressed as the sum and difference of the components $\langle\mu_z\rangle$ and $\langle\mu'\rangle$ in the directions $\vec{u}_z$ and $\vec{u}'$ respectively:

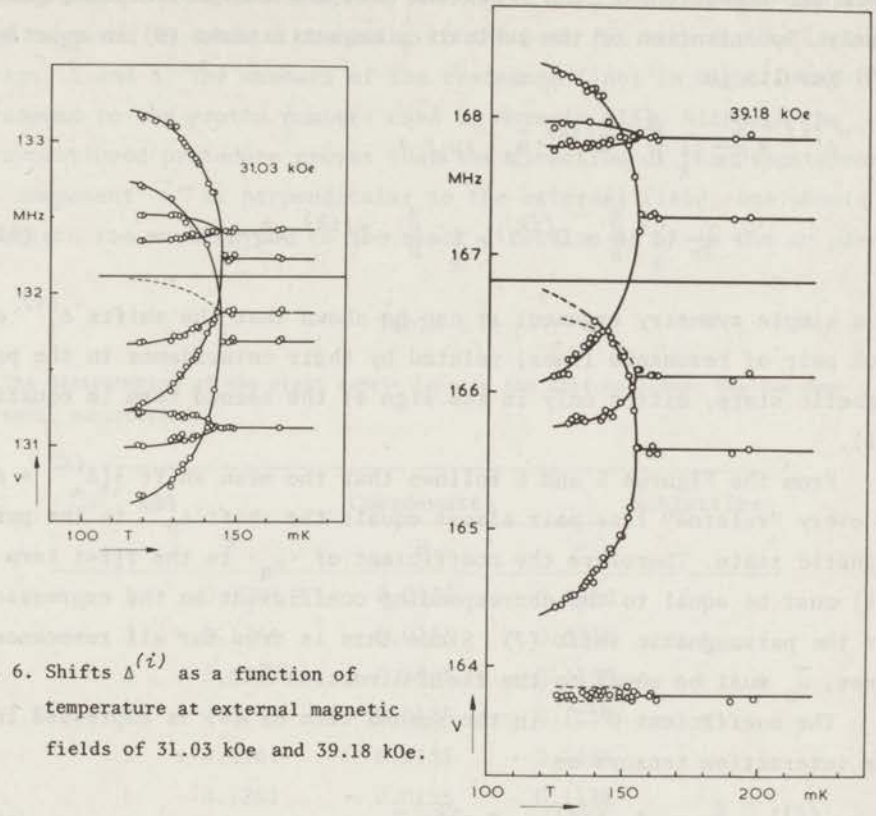

Fig. 6. Shifts $\Delta^{(i)}$ as a function of temperature at external magnetic fields of 31.03 kOe and 39.18 kOe.

$$\langle \vec{\mu}_{\pm} \rangle = \langle \mu_z \rangle \vec{u}_z \pm \langle \mu' \rangle \vec{u}' \qquad (9)$$

First will be proved from the experimental results that the direction $\vec{u}_z$ is parallel to the external field, while the direction $\vec{u}'$ is perpendicular to it. Secondly the magnitudes of the two components $\langle \mu_z \rangle$ and $\langle \mu' \rangle$ will be shown to have a remarkably different temperature dependence, as was to be expected from Figs. 5 and 6 and equation (8). In order to determine the directions $\vec{u}_z$ and $\vec{u}'$ from the resonance data, the experimental coefficients $G_z^{(i)}$ and $G^{(i)'}$ in equation (8) must be related to the interaction tensors $D^{(ik)}$ in equation (5). When the magnetic system consists of two sublattices, equation (5) reads

$$\Delta^{(i)} = \frac{\gamma}{2\pi} \{ \sum_k^+ \frac{\vec{H}}{H} \cdot D^{(ik)} \} \cdot \langle \vec{\mu}_+ \rangle + \frac{\gamma}{2\pi} \{ \sum_k^- \frac{\vec{H}}{H} \cdot D^{(ik)} \} \cdot \langle \vec{\mu}_- \rangle \qquad (10)$$

where the summations Σ^+ and Σ^- extend over the two sublattices, respectively. Substitution of the sublattice magnetizations (9) in equation (10) results in

$$\Delta^{(i)} = \frac{\gamma}{2\pi} \{\Sigma_k \frac{\vec{H}}{H} \cdot D^{(ik)} \cdot \vec{u}_z\} \langle \mu_z \rangle +$$

$$+ \frac{\gamma}{2\pi} \{\Sigma_k^+ \frac{\vec{H}}{H} \cdot D^{(ik)} - \Sigma_k^- \frac{\vec{H}}{H} \cdot D^{(ik)}\} \cdot \vec{u}' \langle \mu' \rangle \qquad (11)$$

By a simple symmetry argument it can be shown that the shifts $\Delta_{\pm}^{(i)}$ of each pair of resonance lines, related by their coincidence in the paramagnetic state, differ only in the sign of the second term in equation (11).

From the Figures 5 and 6 follows that the mean shift $\frac{1}{2}(\Delta_+^{(i)} + \Delta_-^{(i)})$ of every "related" line pair almost equals the shift $\Delta_p^{(i)}$ in the paramagnetic state. Therefore the coefficient of $\langle \mu_z \rangle$ in the first term of (11) must be equal to the corresponding coefficient in the expression for the paramagnetic shift (7). Since this is true for all resonance lines, $\vec{u}_z$ must be equal to the field direction $\vec{H}/H$.

The coefficient $G^{(i)'}$ in the second term of (8) is expressed in the interaction tensors as

$$G^{(i)'} = \frac{\vec{H}}{H} \cdot \{\Sigma_k^+ D^{(ik)} - \Sigma_k^- D^{ik}\} \cdot \vec{u}' \qquad (12)$$

The field direction being known, the direction of the spontaneous component can be found when the second factor in (12) has been determined. This factor cannot be obtained from the experimental data and must be calculated from the crystal structure. In these calculations it has been assumed that the copper-proton interaction is of a purely dipolar character. The dipole tensors of all ions within a sphere of 40 Å radius surrounding each proton were summed, so that the contribution of about 1600 cupric ions was taken into account. The distribution over the two sublattices was found by a trial and error method.

The only direction $\vec{u}'$, compatible with the measured splittings of all resonance lines shown in Fig. 5 and 6 is perpendicular to $\vec{u}_z$ and makes angles of 87 and 7 degrees with the crystallographic a and c axes,

respectively. The distribution of the cupric ions over the two sublattices is given in Table I according to the best fit with the splittings in Figs. 5 and 6. The numbers of the resonance lines in Figs. 5 and 6 correspond to the proton numbers used by Morosin [13]. Although the above-mentioned procedure proves that the direction of the "spontaneous spin component" $\vec{u}'$ is perpendicular to the external field, one should not attach too much weight to the exact direction of $\vec{u}'$ in the *ac* plane,

Table I

The distribution of the eight cupric ions in the unit cell over the two magnetic sublattices.

Cu^{2+}-ion	Coordinates			Sublattice
	x	y	z	
1	-0.1261	+ 0.0135	+ 0.3862	+
2	+ 0.1261	- 0.0135	+ 0.6138	+
3	+ 0.6261	+ 0.4865	+ 0.1138	+
4	+ 0.3739	+ 0.5135	- 0.1138	+
5	+ 0.1261	+ 0.0135	+ 0.1138	-
6	- 0.1261	- 0.0135	- 0.1138	-
7	+ 0.3739	+ 0.4865	+ 0.3862	-
8	+ 0.6261	+ 0.5135	+ 0.6138	-

since the cupric ions form rather covalent bonds with the surrounding oxygen atoms from water molecules and NO_3 groups. Especially the strong intrapair interaction between the cupric ions, which is of a super-exchange nature, will cause an appreciable amount of magnetic moment to be present on the oxygens in the super-exchange path. However, even the presence of 1.5% of the magnetic moment on 07 and 08 does not permit a direction for $\vec{u}'$ outside the *ac* plane. Bearing this in mind, the analysis given before indicates that the sublattice magnetizations are tilted in a direction of about the *c* axis and that the antiferromagnetic state in cupric nitrate is characterized by a spontaneous component of

the time-averaged magnetic moment of the cupric ions perpendicular to the external field.

It is not surprising that the magnitude of the external field will have some influence on the direction of $\vec{u}'$. Of all resonance lines, nr. 3 is the most sensitive to such an effect and, indeed, the Figures 5 and 6 show a slight variation of the splitting of this line with the external field.

Spontaneous magnetization

The spontaneous component $\langle\mu'\rangle$ of the magnetization in the antiferromagnetic state can be derived easily from the splitting $\Delta_+ - \Delta_-$ according to equation (8) of the preceding section. The measured values of the splittings of resonance lines 1 and 2 in an external field H = 35.7 kOe (Fig. 5) are shown on a reduced scale in Fig. 7. The drawn line in this figure represents the phenomenological equation

$$\langle\mu'(T)\rangle/\langle\mu'(0)\rangle = \Delta^{(i)}(T)/\Delta^{(i)}(0) = \sqrt{1 - (T/T_c)^{\beta}} \qquad (13)$$

where $\Delta^{(i)}(0)$ represents the splitting of the i-th resonance line at zero temperature. The exponent β and the constants $\Delta^{(i)}(0)$ have been chosen so as to minimize the r.m.s. deviation δ of the experimental data from the curve (13). The best fit is obtained with $\beta = 5.0 \pm 0.2$. From the values of $\Delta^{(i)}(0)$ together with the geometrical factors $G^{(i)'}$, calculated from equation (12) it is possible to derive the value of the spontaneous perpendicular component $\langle\mu'(0)\rangle$ at zero temperature. This procedure is submitted to the same objections as those mentioned at the determination of $\vec{u}'$, arising from the point-dipole assumption used in the calculation of the $G^{(i)'}$. However, a value of $\langle\mu'(0)\rangle$ = 0.35 Bohr magneton is in reasonable accordance with the measurements. Although the so-obtained maximum spontaneous component agrees rather well with the prediction (0.4 Bohr magneton) from the molecular-field approximation by Tachiki *et al.* [9], the temperature dependence of $\langle\mu'\rangle$ given in Fig. 7 certainly does not. This shows that the molecular-field theory is a too simple description of the ordered state.

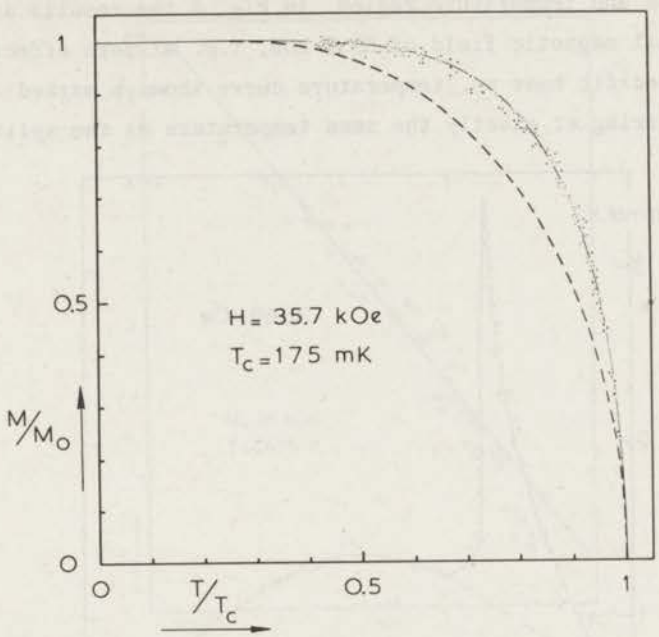

Fig. 7. Spontaneous magnetization *vs.* temperature. The drawn curve corresponds to equation (13) with $\beta = 5.0$. The dashed curve has been obtained from the molecular field theory according to Tachiki [9].

Specific heat capacity

In the previous sections it has been shown that in cupric nitrate "trihydrate" a phase transition from the paramagnetic state to the antiferromagnetic state exists between 27 kOe and 45 kOe. Since the copper spin pairs may be treated as effective spins $S' = \frac{1}{2}$ in an effective field H_{eff}, one should expect that the behaviour of this system around 36 kOe, *i.e.* that field where $H_{eff} = 0$, is comparable to a system of "normal" spins $S = \frac{1}{2}$ in an external magnetic field around zero. In particular, the transition to the antiferromagnetic state should also show up in the specific heat in the same way as it does in "normal" spin systems in zero field.

With the help of the heat switch and heater, described in Chapter II, the specific heat capacity of the same crystal was measured in the

relevant field and temperature region. In Fig. 8 the results are shown for an external magnetic field of 35.7 kOe, *i.e.* at zero effective field. The specific heat *vs.* temperature curve shows a marked λ-type anomaly, occurring at exactly the same temperature as the splitting of

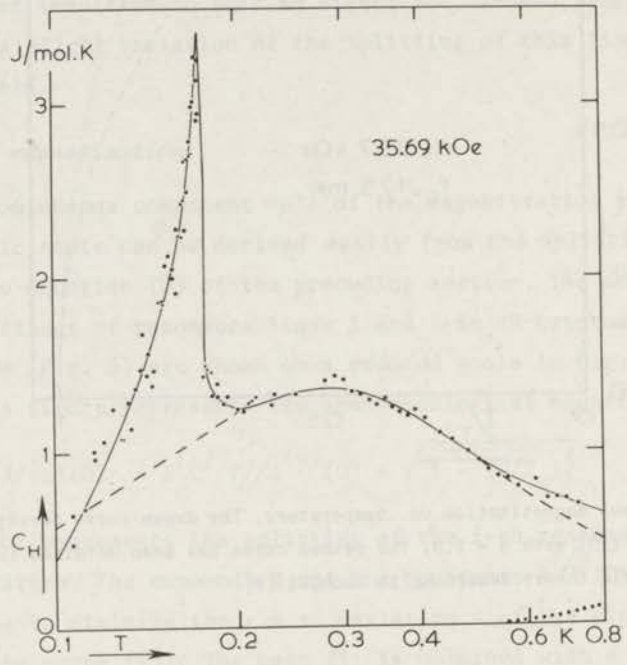

Fig. 8. Specific heat *vs.* temperature in an external magnetic field of 35.69 kOe. The dashed curve represents equation (18) with $f = 0$ and $K/k = -0.217$. The dotted curve is the contribution of the higher triplet levels to the specific heat.

the resonance lines discussed in the previous section. When considering Fig. 8, one should be aware of the fact that the specific heat C_H is expressed per grammolecule $Cu(NO_3)_2 \cdot 2\frac{1}{2}H_2O$, *i.e.* per half "gram-ion pair". In Fig. 9 the specific-heat data below the transition temperature are compared with the expression

$$C_H/\tfrac{1}{2}R = A \ln |1 - T/T_c| + B \qquad (14)$$

This type of relation fits the anomalies, found experimentally at phase transitions in many (anti)ferromagnetic substances in zero field [14,

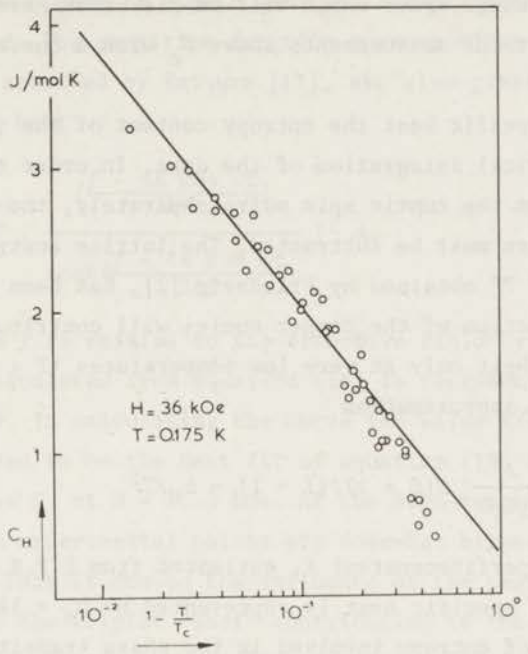

Fig. 9. Specific heat *vs.* $1 - T/T_c$ on a semi-logarithmic scale. The drawn line represents equation (14) with $A = -0.185$ and $B = +0.075$.

15]. Equation (14) is also a good approximation to Onsager's exact calculations for the simple quadratic Ising lattice [16] if the values $A = -0.49$ and $B = -0.29$ are chosen. The best fit of expression (14) to the results in Fig. 9 has been obtained using $A = -0.185$ and $B = +0.075$ and is given by the drawn line. Over the limited region $1\ \text{mK} < T_c - T < 10\ \text{mK}$ it is also possible to fit the data at the low-temperature side of the singularity with a power law of the form

$$C_H/R \sim (1 - T/T_c)^{-\alpha} \qquad (15)$$

The so determined critical exponent amounts to $\alpha = 0.25 \pm 0.05$.

Thus far, the specific heat curve and especially the λ-type anomaly resemble those found in "normal" (anti)ferromagnets in zero field. Above the transition temperature the specific heat falls steeply to a value of about 1.3 J/mol K. Owing to the occurrence of the unusually large

amount of short-range order which will be discussed hereafter, it is impossible to fit the measurements above T_c with a curve of the type (14) or (15).

From the specific heat the entropy content of the system can be derived by numerical integration of the data. In order to obtain the contribution from the cupric spin pairs separately, the contributions from other sources must be subtracted. The lattice contribution, $C/R = 1.3 \times 10^{-4}\ T^3$ obtained by Friedberg [2], has been neglected. The hyperfine interaction of the copper nuclei will contribute appreciably to the specific heat only at very low temperatures ($T < 0.1$ K). The high-temperature approximation

$$C_{hfs}/R = \frac{A^2}{9k^2T^2}\ S(S+1)I(I+1) = b_N/T^2 \qquad (16)$$

was used with hyperfineconstant A, estimated from E.P.R. data. Its contribution to the specific heat is represented by $b_N = 10^{-4}$ K^2.

The amount of entropy involved in the phase transition amounts to only 30% of the expected value $\frac{1}{2}R$ ln 2. This indicates that an appreciable amount of short-range order must be present above the critical temperature. Moreover, the specific heat *vs.* temperature curve shows a broad maximum around 0.28 K. It is well known that in an (anti)ferromagnetic linear-chain model the short-range order, which develops gradually with decreasing temperature, is accompanied by a similar broad maximum in the specific heat. Therefore the experimental data of Fig. 8 above T_c were fitted with the calculated values for the linear chain model. In these calculations from the many interactions possible in the linear chain, that one was chosen in which only the perpendicular (XY) components of the "effective spins" are exchange coupled. This particular choice was made because in the antiferromagnetic state the ordering is characterized by a spontaneous component of the magnetization perpendicular to the field direction. The hamiltonian for this model can be expressed in the effective spins S' as

$$\mathcal{H}_{int} = K \sum_{i}^{N/2} (S'_{xi}S'_{xi+1} + S'_{yi}S'_{yi+1}) + g\beta H_{eff} \sum_{i}^{N/2} S'_{zi} \qquad (17)$$

in which N is the number of cupric ions and K represents the interpair coupling constant. The partition function corresponding to this hamiltonian has been obtained by Katsura [17], who also gives the expression for the specific heat

$$C_H/R = \frac{1}{2\pi} \int_0^{\pi} \left[\frac{\left(\frac{f - 4K \cos \omega t}{2kT}\right)}{\cosh\left(\frac{f - 4K \cos \omega t}{2kT}\right)} \right]^2 d\omega \qquad (18)$$

In this equation f is related to the effective field by $f = g\beta H_{eff}$. The specific heat calculated from equation (18) is represented in Fig. 8 by the dashed curve. In calculating the curve the value K/k = - 0.217 K is used, which proved to be the best fit of equation (18) to the experimental data above T_c at H = 35.7 kOe. At the high-temperature side above 0.6 K, the experimental points are somewhat higher than the calculated values. This is due to the influence of the neglected higher energy levels of the triplet. Their contribution to the specific heat can in first approximation be considered as separate from the short-range order discussed above. The calculated values of this contribution are represented by the dotted line in Fig. 8 and account for the difference between curve (18) and the measurements in a satisfactory way. The total entropy involved in the phase transition and the short-range order together, as obtained by graphical integration below T_c and using equation (18) above T_c, amounts to 0.36 R. It equals the expected $\frac{1}{2}R$ ln 2 within the measuring accuracy.

In Fig. 10 the specific heat C_H at 29.7 kOe and 31.8 kOe is compared with the 35.7 kOe curve. It is clear, that with decreasing fields the peak shifts to lower temperatures, while the C_H *vs.* T curve above T_c also changes its shape. In Fig. 11 the same is done at 39.2 kOe and 41.7 kOe with the same result. From these figures it follows that an increase of the absolute value of the effective field H_{eff}, either in positive (H > 35.6 kOe) or in negative sense (H < 35.6 kOe), leads to the same results, *viz.* a shift of the peak to lower temperatures and a shift of the broad short-range order maximum to higher temperatures.

A very remarkable feature is, that the λ peak remains sharp and that its high-temperature side becomes only slightly less steep in ef-

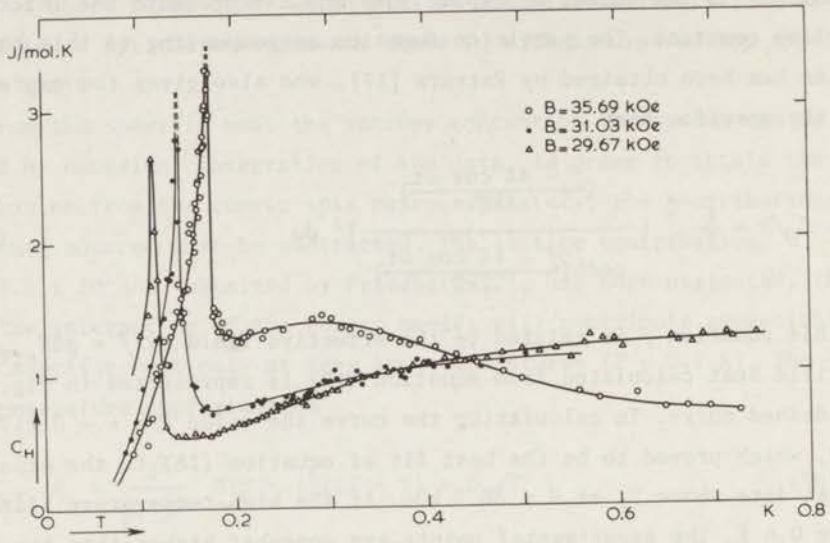

Fig. 10. Specific heat *vs.* temperature at magnetic field values below 35.7 kOe. For comparison also the 35.7 kOe data are shown.

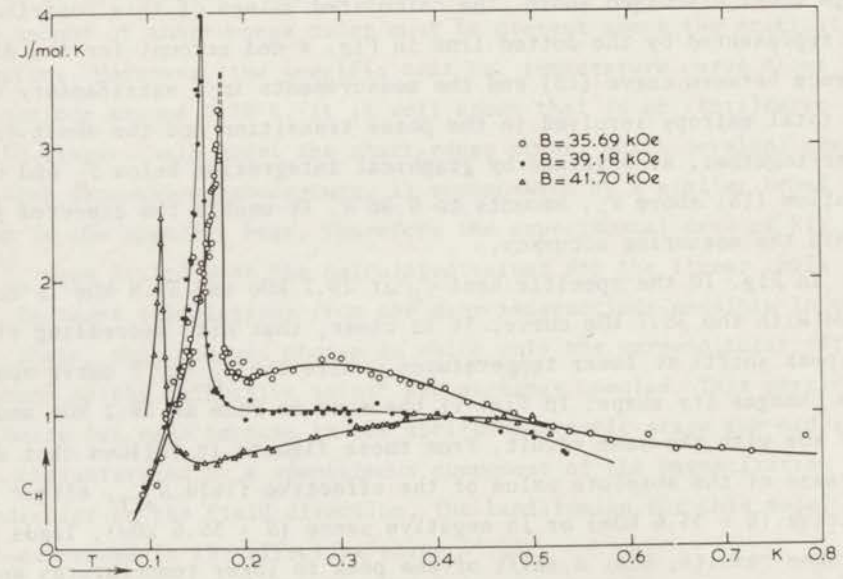

Fig. 11. Specific heat *vs.* temperature for magnetic field values above 35.7 kOe. For comparison also the 35.7 kOe data are shown.

fective fields as high as 6 kOe. This might be another indication that the ordering occurs only among the spin components perpendicular to the external magnetic field. When the temperature approaches T_c from above, the steep rise of the specific heat just above T_c is accompanied by a large increase of the width of the proton resonance lines. This effect is to be interpreted as the critical broadening described by Moriya [18]. Splitting of the resonance lines occurs only at and below the temperature where C_H attains its maximum value. A temperature region in which both the broadened "paramagnetic" line and the splitted "antiferromagnetic" lines appear was not observed.

When the specific heat C_H is measured at external fields outside the ordered region, the singularity disappears entirely, while the broad maximum shifts to still higher temperatures and the whole C_H *vs.* T curve attains more and more the Schottky-type shape. Again, this occurs both at the low-field side and at the high-field side, as is shown in Figs. 12 and 13, respectively.

An attempt to fit expression (18) to the experimental data at non zero effective fields succeeded for all curves between 25 kOe and 47 kOe. For each field, the constants f and K in formula (18) were

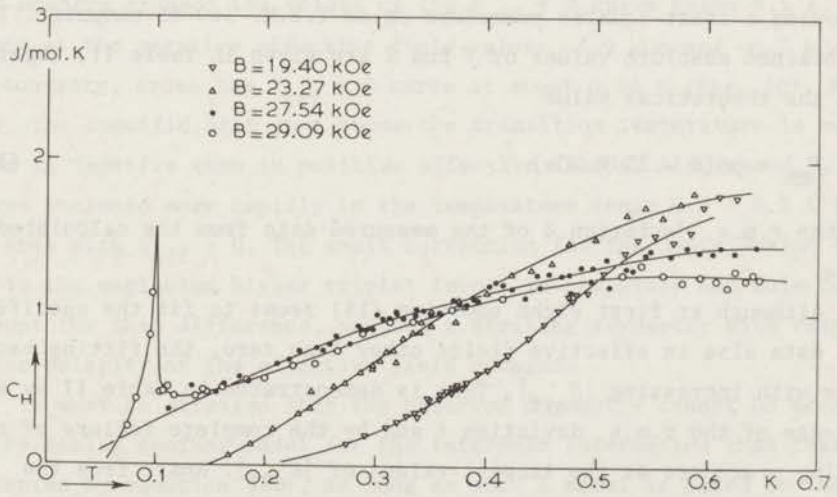

Fig. 12. Specific heat *vs.* temperature outside the ordered region. The magnetic field is smaller than 30 kOe.

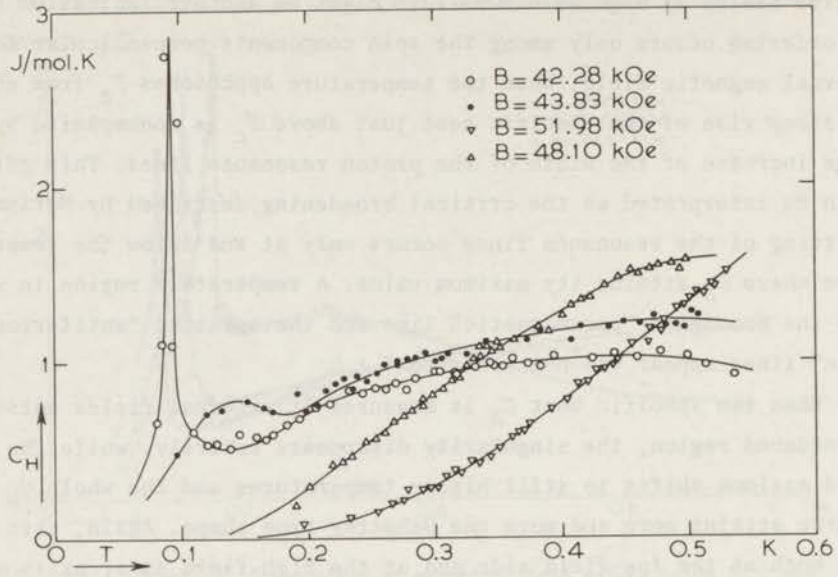

Fig. 13. Specific heat *vs.* temperature outside the ordered region. The magnetic field is larger than 42 kOe.

taken as parameters to get the best fit with the experimental results following a least-squares procedure on an I.B.M. 360-65 computer. The so obtained absolute values of f and K are given in Table II, together with the theoretical value

$$f_{th} = g\beta(H - 35.9 \text{ kOe}) \qquad (19)$$

and the r.m.s. deviation δ of the measured data from the calculated curve.

Although at first sight equation (18) seems to fit the specific heat data also in effective fields other than zero, the fitting becomes worse with increasing $|H_{eff}|$. This is demonstrated in Table II by an increase of the r.m.s. deviation δ and by the complete failure of the fitting procedure at the largest values of $|H_{eff}|$. Apart from the rather large scatter in the produced f and K values in Table II, it seems important to pay attention to the differences between the C_H *vs.* T curves in the Figures 10 and 11.

Table II

The critical temperature T_c at different values of the external magnetic field, together with the best fitting parameters of the linear chain model of equation (18).

H	T_c	f/k	K/k	δ	f_{th}/k
27.54	-	1.37	0.22	5.8	-1.34
29.09	98(±5)	0.55	0.45	9.4	-1.09
29.67	115	1.38	0.25	3.7	-1.00
31.03	142	0.71	0.39	4.1	-0.79
35.69	175	0.00	0.22	3.2	-0.05
39.18	156	0.38	0.18	4.5	+0.50
41.70	113	0.83	0.39	3.7	+0.90
42.28	94(±5)	0.60	0.19	6.2	+0.99
43.83	-	1.18	0.21	10.3	+1.24
kOe	mK	K	K	%	K

In effective fields of +3.3 kOe and +5.8 kOe (Fig. 11) the specific heat nowhere exceeds the values of the $H_{eff} = 0$ curve below 0.5 K. The curves at the negative effective field values -4.9 kOe and -6.2 kOe, on the contrary, cross the $H_{eff} = 0$ curve at about 0.45 K (Fig. 10). Moreover, the specific heat just above the transition temperature is much lower in negative than in positive effective fields. Also the $H_{eff} < 0$ curves increase more rapidly in the temperature range 0.2 - 0.5 K than the ones with $H_{eff} > 0$. The small correction for the contribution to C_H due to the neglected higher triplet levels is certainly not able to account for this difference, so that a striking asymmetry with respect to the polarity of the effective field remains.

It must be stressed that the observed asymmetry cannot be accounted for by taking another model for the interpair interaction than that represented by equation (17), as long as such a model is based on the linear variation of the effective field H_{eff} with the external field H, which in turn follows from the assumption that the energy levels of the

isolated spin pair are straight lines in the E-H diagram of Fig. 1. Together with a field-independent interaction constant K this leads to the symmetry of all thermodynamical quantities with respect to the polarity of the effective field.

Magneto-thermal effect

The magneto-thermal effect in cupric nitrate "trihydrate" was measured while the orientation of the crystal with respect to the external magnetic field was the same as in the n.m.r. and specific-heat experiments. The experimental procedure is simple: the sample is cooled down to the desired starting temperature in the desired starting field and the heat switch is opened. Then the temperature is recorded while the magnetic field is varied adiabatically at a speed of 50 Oe/s. Changing the speed to 20 Oe/s or 100 Oe/s did not alter the measurements in any respect. At 200 Oe/s a slight hysteresis was observed, due to the thermal response time of the crystal and the thermometer heat link. At 10 Oe/s the heat inleak caused an intolerable entropy variation during the measuring procedure. The heat leak to the sample amounted to 10^{-7} W at 0.1 K and became negative above 0.35 K, owing to the increasing heat conductivity of the tin switch. Because in the field range between 20 kOe and 50 kOe the specific heat is relatively large, these imperfections in the thermal isolation did not seriously affect the measurements. Each isentrope shown in Fig. 14 has been obtained by taking the mean values of two T *vs.* H curves, measured immediately after each other with increasing and decreasing field, respectively. The difference between these two curves never exceeded 5 mK, except at temperatures above 0.5 K. Measurements in magnetic fields below 20 kOe and above 50 kOe were not reproducible, probably because of the extremely small specific heat in these field ranges. The entropy value of each isentrope has been calculated from the specific-heat curve in 35.7 kOe shown in Fig. 8.

In Fig. 14 the phase-boundary curve $T_c(H)$ between the antiferromagnetic state and the paramagnetic state, as obtained from the preceding n.m.r. and specific-heat measurements, is represented by the dashed line. It is clear, that a large temperature decrease occurs

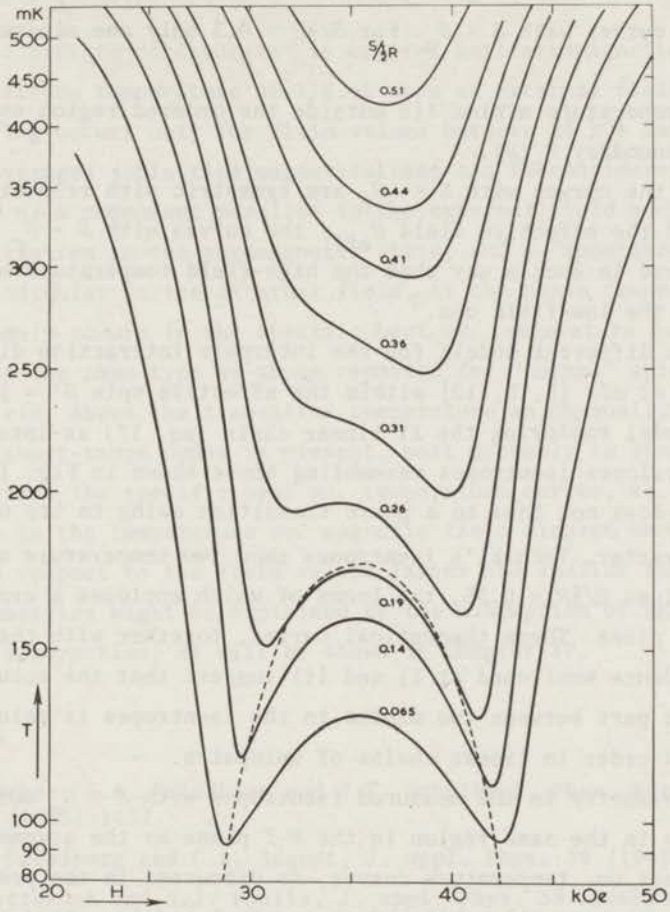

Fig. 14. Experimental isentropes in the H-T plane. The entropy value has been calculated from integration of the C_H *vs.* T curve in Fig. 8. The dashed curve represents the phase boundary $T_c(H)$ between the antiferromagnetic and the paramagnetic state.

when the magnetic field approaches the ordered region. This was to be expected, since the spin-pair system is "effectively demagnetized". Around the crossing field H_0 = 35.9 kOe the isentropes show the following features:

i) All curves corresponding to an entropy $S/\frac{1}{2}R$ smaller than 0.3 exhibit two minima. It is remarkable that these two minima appear in the

curves for which S is larger than the critical entropy $S_c/\frac{1}{2}R = 0.21$ as well as in curves with $S < S_c$. For $S/\frac{1}{2}R > 0.3$ only one minimum is present.

ii) All temperature minima lie outside the ordered region enclosed by the phase boundary $T_c(H)$.

iii) While the curves with $S << S_c$ are symmetric with respect to the polarity of the effective field H_{eff}, the curves with $S > S_c$ are clearly asymmetric in such a way that the high-field temperature minimum is lower than the low-field one.

Of the different models for the interpair interaction discussed by Tachiki *et al.* [8, 9, 19] within the effective spin $S' = \frac{1}{2}$ framework, only the model employing the XY linear chain (eq. 17) as interpair interaction, developes isentropes resembling those shown in Fig. 14. Although this model does not lead to a phase transition owing to its one-dimensional character, Tachiki's isentropes show two temperature minima for entropy values $S/\frac{1}{2}R < 0.35$, the locus of which encloses a certain region in the H-T plane. These theoretical curves, together with the experimental evidence mentioned at i) and ii) suggest that the occurrence of the concave part between two minima in the isentropes is mainly due to short-range order in linear chains of spinpairs.

The asymmetry in the measured isentropes with $S > S_c$ mentioned at iii) occurs in the same region in the H-T plane as the asymmetry in the specific heat *vs.* temperature curves, as discussed in the previous section. Up to now, all published theoretical models within the effective-spin $S' = \frac{1}{2}$ framework have been based on an isotropic intrapair interaction J in equation (1). Therefore they lead, no matter what model is used for the interpair interaction, to a behaviour of all thermodynamical quantities which is symmetric with respect to the polarity of the effective field. In Chapter IV the influence will be discussed of an anisotropic J on the various thermodynamical quantities; it will be shown that the asymmetries in the specific heat and magnetothermal effect measurements, discussed in the present chapter, can be explained satisfactorily. A first indication of the anisotropy of the intrapair interaction J was already found in measurements of the differential susceptibilities χ' and χ'' performed in this laboratory [20].

Conclusion

Cupric nitrate "trihydrate" is ordered antiferromagnetically below a transition temperature of 175 mK when an external field is present. This ordering occurs only for field values between 28 kOe and 44 kOe. The time-averaged sublattice magnetizations can be considered as the vector sum of a component parallel to the external field and equal to the magnetization in the paramagnetic state, and a "spontaneous" component perpendicular to the external field. At the phase transition a λ-type anomaly occurs in the specific heat *vs.* temperature curves which is of the same type as those reported for "normal" spin systems in zero field. Above the transition temperature an unusually large amount of short-range order is present, most probably in linear chains of spin pairs. The specific heat *vs.* temperature curves, as well as the isentropes in the temperature *vs.* magnetic field diagram show an asymmetry with respect to the field values larger and smaller than 35.9 kOe. These asymmetries might be explained by the assumption of an anisotropic intrapair interaction, as will be shown in Chapter IV.

References

1. L. Berger, S.A. Friedberg and J.T. Schriempf, Phys. Rev. 132 (1963) 1057.
2. S.A. Friedberg and C.A. Raquet, J. appl. Phys. 39 (1968) 1132.
3. S. Wittekoek and N.J. Poulis, J. appl. Phys. 39 (1968) 1017.
4. K. Amaya, Y. Tokunaga, R. Yamada, Y. Ajuri and T. Haseda, Phys. Lett. 28A (1969) 732.
5. B.E. Myers, L. Berger and S.A. Friedberg, J. appl. Phys. 40 (1969) 1149.
6. J.C. Bonner, S.A. Friedberg, H. Kobayashi and B.E. Myers, Proceedings of the Twelfth International Conference on Low Temperature Physics, Kyoto 1970, Ed. E. Kanda (Keigaku Publ. Co. Tokyo 1971) p. 691.
7. T. Murao and T. Tsuneto, Physica 51 (1971) 186.
8. T. Haseda, Y. Tokunaga, R. Yamada, Y. Kuramitsu, S. Sakatsume and K. Amaya, Proceedings of the Twelfth International Conference on Low Temperature Physics, Kyoto 1970. Ed. E. Kanda (Keigaku Publ. Co. Tokyo 1971) p. 685.
9. M. Tachiki and T. Yamada, J. Phys. Soc. Japan 28 (1970) 1413.

10. M. Tachiki, T. Yamada and S. Maekawa, J. Phys. Soc. Japan 29 (1970) 663.

11. M.W. van Tol, M. Matsuura and N.J. Poulis, Journal de Physique Colloque C1 suppl. 2-3, 32 (1971) C1-943.

12. J. Garaj, Acta Chem. Scand. 22 (1968) 1710.

13. B. Morosin, Acta Cryst. B26 (1970) 1203.

14. A.R. Miedema, R.F. Wielinga and W.J. Huiskamp, Physica 31 (1965) 1585.

15. R.F. Wielinga, H.W.J. Blöte, J.A. Roest and W.J. Huiskamp, Physica 34 (1967) 223.

16. L. Onsager, Phys. Rev. 65 (1944) 117.

17. S. Katsura, Phys. Rev. 127 (1962) 1508.

18. T. Moriya, Progr. Theor. Phys. 28 (1962) 371.

19. M. Tachiki and T. Yamada, Suppl. Progr. Theor. Phys. 46 (1970) 291.

20. M.W. van Tol, H.M.C. Eijkelhof and A.J. Van Duyneveldt, Physica 60 (1972) 223.

CHAPTER IV
THEORY OF THE HIGH-FIELD PHASE TRANSITION IN $Cu(NO_3)_2 \cdot 2\frac{1}{2}H_2O$

Introduction

From several experimental studies by Friedberg *et al.* [1, 2, 3] it is known, that in cupric nitrate "trihydrate" the cupric ions are coupled in pairs by an antiferromagnetic exchange interaction $J/k = -5.2$ K. Since there is no reason for the interaction to be highly anisotropic, the substance can be described by a model of mutually non-interacting spin pairs with hamiltonian

$$\mathcal{H} = -J\vec{S}_1 \cdot \vec{S}_2 - g\beta H(S_1^z + S_2^z) \qquad (1)$$

Here H is the applied magnetic field and β is the value of the Bohr magneton. The g tensor is taken isotropic. The energy-level scheme resulting from (1) consists of a $S = 1$ triplet, 5.2 K above the $S = 0$ singlet ground state and is shown in Fig. 1a as a function of the external field.

To obtain a better agreement with their measurements of the magnetization isotherms of cupric nitrate, Myers *et al.* [3] extended this simple model with a classical molecular field approximation in order to account for the interpair interaction. A few years later, the adiabatic magnetization experiments of Haseda *et al.* [4] stimulated Tachiki and Yamada [5] to develop a theory which introduced the interpair interaction into the hamiltonian. Considering only the lower two energy levels and using a molecular field model, they predicted a second order phase transition that should occur in magnetic fields near the crossing of the energy levels (*i.e.* at $g\beta H = |J|$).

In Fig. 1b the transition temperature T_c calculated thus is given as a function of external field.

We succeeded in detecting such a phase transition by n.m.r. experiments [6] the critical temperature being $T_c = 0.175$ K at $H = 36$ kOe. The measured values of T_c at different fields are represented in Fig. 1c.

Bonner *et al.* [7] were the first to propose a different model, in

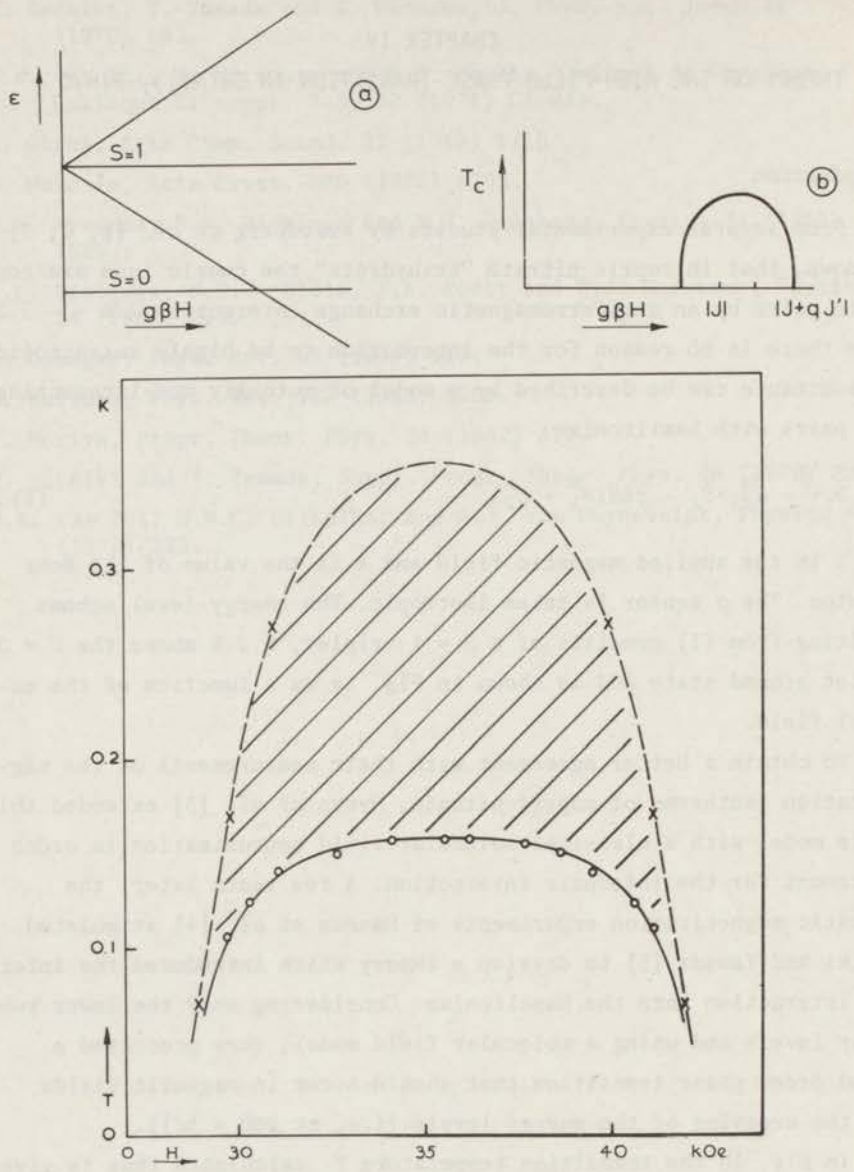

Fig. 1. The model with isotropic intrapair interaction J.

a) Energy-level scheme as a function of magnetic field.

b) Phase-boundary curve, calculated according to ref. 5.

c) Experimental transition temperature *versus* external magnetic field. Shaded area represents large short-range order, dashed curve connects minima in the (experimental) isentropes.

which the spin pairs are coupled in a linear chain. They considered two different possibilities for the interpair interaction: (A) the spin pairs are coupled as the rungs of a ladder, and (B) the spin pairs are arranged as the steps in a staircase. Both models are compatible with the crystal structure which recently has been determined very accurately by Morosin [8]. Bonner *et al.* solved the eigenvalue equation numerically for chains of 6 spin pairs. Their solution fits Friedberg's low-field heat-capacity data and susceptibility measurements as well as the magnetization isotherms of Myers *et al.* [3]. After this proposition Tachiki *et al.* [9] proved that the adiabatic magnetization effects could also be explained by the development of short-range order in a linear-chain model. Owing to their one-dimensionality, these models do not lead to any phase transition at all.

In the previous chapter the presence of a considerable amount of short-range order over a large temperature range directly above T_c has been proved (shaded area in Fig. 1c). It has also been shown that a linear-chain model fits the specific-heat measurements above T_c remarkably well. Hence it seems justified to assume that the interpair interaction consists of a dominant exchange J' in one dimension. The resulting linear chains of spin pairs are coupled by a much weaker interchain interaction, which establishes the long-range order below 0.175 K in the region of the crossing point at H = 36 kOe.

In Chapter III also a certain asymmetry was found to exist in the specific heat and the magneto-thermal effect, depending on the external magnetic field being larger or smaller than 36 kOe, *i.e.* with respect to the polarity of the effective field $H_{eff} = H - 36$ kOe.

These asymmetries cannot be accounted for by taking another type of interpair interaction, but must be explained by assuming the intrapair exchange J in equation (1) to be anisotropic. For, if J is isotropic, any model considering only the lower two energy levels leads to expressions for the adiabatic temperature change $(dT/dH)_S$ and the specific heat C_H which are even functions of the deviation H_{eff} of the magnetic field from its "crossing point value".

The anisotropy $\Delta J/J$ was expected to be smaller than 10%, since it is of the same order of magnitude as the anisotropy in the g factor

$\Delta g/g$ [10]. The existence of a small anisotropy in J is also supported by measurements of the differential susceptibility [11] and is certainly not in contradiction with the crystal structure of cupric nitrate.

The thermodynamical properties of a spin-pair model in which the anisotropy is treated by first order perturbation theory will be calculated in the present chapter. Because the theory with isotropic J is used as a starting point and because it shows the physical implications more clearly, it will be summarized in the next section.

Isotropic J

If the intrapair interaction J is assumed to be isotropic, the hamiltonian of an isolated spin pair is given by equation (1). Owing to the isotropy the direction of the magnetic field can be chosen arbitrarily. If the eigenstates of this hamiltonian (1) are used as a basis, the general state of a spin pair can be given by a vector in the four-dimensional Hilbert space. However, since all experiments reported in Chapter III are carried out at temperatures which are at least an order of magnitude smaller than the exchange energy J/k, it suffices to describe the system by the lower two energy levels only. Restriction of the problem to the subspace spanned by these two energy levels allows a description of each spin pair by one effective spin $S' = \frac{1}{2}$. In order to express the hamiltonian in terms of Pauli spin matrices σ_i, it is convenient to introduce the spin pair operators $\vec{S} = \vec{S}_1 + \vec{S}_2$ and $\vec{t} = \vec{S}_1 - \vec{S}_2$. These operators can be expressed as [5]

$$S_x = S_y = t_z = 0 \qquad S_z = \tfrac{1}{2}(1 + \sigma_z)$$

$$t_x = -\tfrac{1}{2}\sqrt{2}\sigma_x \qquad t_y = -\tfrac{1}{2}\sqrt{2}\sigma_y \tag{2}$$

while the projection of the hamiltonian (1) onto the two-dimensional subspace mentioned above results in

$$\mathcal{H} = (\tfrac{1}{4}J - \tfrac{1}{2}g\beta H)1 - \tfrac{1}{2}(J + g\beta H)\sigma_z \tag{3}$$

where 1 and σ_z represent the unit matrix and the Pauli spin matrix, respectively. The lowest triplet state has been given an effective spin

$\sigma_z = 1$ and the singlet ground state has $\sigma_z = -1$. Neglecting the spin-independent term, the hamiltonian (3) is identical to that for a spin $S = \frac{1}{2}$ in an external magnetic field

$$g\beta H_{\text{eff}} = J + g\beta H \tag{4}$$

The introduction of the two-dimensional subspace giving no new information about the isolated spin pairs, its main importance lies in the simplification of the description of the interpair interaction which will be discussed next. Because nothing is known about the interpair interaction but that it is much weaker than the intrapair interaction J, it is assumed to be isotropic. Then the interaction hamiltonian for the spinpairs i and j can be written without much loss of generality as

$$\mathcal{H}'_{ij} = -J'_{ij}\{\vec{S}_1^i\cdot\vec{S}_1^j + \vec{S}_2^i\cdot\vec{S}_2^j + \alpha_{ij}(\vec{S}_1^i\cdot\vec{S}_2^j + \vec{S}_2^i\cdot\vec{S}_1^j)\} \tag{5}$$

Here J'_{ij} represents the interaction between like members of neighbouring pairs and $\alpha_{ij}J'_{ij}$ is the interaction between unlike neighbours. Introduction of the pair operators $\vec{S}$ and $\vec{t}$ and projection onto the lower two energy levels transform equation (5) into

$$\mathcal{H}'_{ij} = -\frac{1}{8}J'_{ij}\{(1+\alpha_{ij})(1+\sigma_z^i)(1+\sigma_z^j) + 2(1-\alpha_{ij})(\sigma_x^i\sigma_x^j + \sigma_y^i\sigma_y^j)\} \tag{6}$$

When the entire hamiltonian for a lattice containing $N/2$ spin pairs is expressed as a sum

$$\mathcal{H} = \sum_i^{N/2}\mathcal{H}'_i + \tfrac{1}{2}g\beta H_{\text{eff}}\sum_i\sigma_z^i \tag{7}$$

the interaction hamiltonian for the i-th spin pair $\mathcal{H}'_i$ can be split up into contributions from nearest neighbours ($k = 1$), next nearest ones ($k = 2$) and so on:

$$\mathcal{H}'_i = \tfrac{1}{2}\sum_j \mathcal{H}'_{ij} = -\tfrac{1}{2}\sum_{k=1}^{\infty} \tfrac{1}{4} q_k J'_k (1 + \alpha_k)\sigma_z^i - \tag{8}$$
$$- \tfrac{1}{4}\sum_{k=1}^{\infty}\sum_{j=1}^{q_k} \{\tfrac{1}{4} J'_k (1 + \alpha_k)\sigma_z^i\sigma_z^j + \tfrac{1}{2} J'_k (1 - \alpha_k)(\sigma_x^i\sigma_x^j + \sigma_y^i\sigma_y^j)\}$$

Here q_k is the number of k-th nearest neighbours and J'_k is their interaction with the i-th spin pair. A spin-independent term has been omitted. The first term contains σ_z^i as the only spin variable and therefore it can be transported to the isolated-pair hamiltonian (3) of the i-th pair. There it contributes to the effective field

$$g\beta H_{\text{eff}} = J + \sum_{k=1}^{\infty} \tfrac{1}{4} q_k J'_k (1 + \alpha_k) + g\beta H \tag{9}$$

In contrast to the second term at the right-hand side of equation (8) this first term leads directly to an extra contribution to the effective field without further simplifications of the theory.

An important feature of the result (8) is that although J' was taken isotropic, the effective interaction turns out to be anisotropic with respect to the field direction. The k-th neighbour exchange constant in equation (8) for the spin components perpendicular to the field equals $\frac{1}{2}(1 - \alpha_k)J'_k$, while parallel to the field it amounts to $\frac{1}{4}(1 + \alpha_k)J'_k$.

If only nearest neighbours are taken into account the whole system can be described as if it were a system of spins $S = \frac{1}{2}$ in an external field

$$g\beta H_{\text{eff}} = J + \tfrac{1}{4} qJ'(1 + \alpha) + g\beta H \tag{10}$$

with an anisotropic exchange interaction

$$\mathcal{H}'_i = -\frac{1}{8} J' \sum_{j=1}^{q} \tfrac{1}{2}(1 + \alpha)\sigma_z^i\sigma_z^j + (1 - \alpha)(\sigma_x^i\sigma_x^j + \sigma_y^i\sigma_y^j) \tag{11}$$

Therefore in an external field such that $H_{\text{eff}} \approx 0$, it may be expected that the behaviour of the magnetic pair system in cupric nitrate will be similar to that of a paramagnet with anisotropic exchange in zero

magnetic field. This implicates the possibility of a phase transition when the temperature is low enough compared to $|J'|/k$.

Further development of the theory requires a distinct choice of the configuration of the spin pairs in cupric nitrate. From the many possible models two important examples are selected which will be discussed below.

A) In their first paper [5] Tachiki and Yamada chose $\alpha = 0$ in equation (11) and introduced the molecular field theory by replacing the σ^j by their expectation values $\langle\sigma^j\rangle$ in the hamiltonian. In a later publication [12] they discussed the implications of the assumption $\alpha \neq 0$ within the same framework. This led to the prediction of a phase transition which was indeed detected [6], as has already been mentioned in the introduction.

B) Quite another situation originates from taking the number of nearest neighbours q equal to two. In this case the spin-dependent part of the hamiltonian is similar to that of a linear chain of coupled spins $S = \frac{1}{2}$ in an external field H_{eff}. In the linear chain model no phase transition occurs and the thermodynamical quantities are governed by the short-range order which developes gradually with decreasing temperature.

Since the experiments reported in Chapter III indicate a large amount of short-range order above the transition temperature T_c, the linear-chain model B may provide a successful description of cupric nitrate at temperatures above T_c. In both models A and B the thermodynamical quantities can be obtained from the partition function in the usual way. In model B the formalism of the linear chain as developed by Katsura and Inawashiro [12, 14, 15] can be used. This formalism leads to an exact solution of the partition function and to closed expressions for all thermodynamical quantities, if the coupling of the spins within the chain is of the Ising type or of the XY type [13]. In other cases approximative methods must be used [14, 15].

From equation (11) follows that the exchange constant for the x and y components of the interaction between the effective spins is larger than that for the z component when α is small or negative. Therefore Tachiki *et al.* [9] proposed the XY model (vanishing z inter-

action *i.e.* $\alpha = -1$) as most appropriate for cupric nitrate. In this model the specific heat, the entropy and the magnetization are expressed as

$$C_H/R = \frac{1}{\pi}\int_0^{\pi} \frac{p^2}{\cosh^2(p)}\, d\omega \; ; \quad S/R = \frac{1}{\pi}\int_0^{\pi} \log 2 \cosh(p)\, d\omega \; ;$$

$$M/Ng\beta = \tfrac{1}{2} + \frac{1}{2\pi}\int_0^{\pi} \tanh(p)\, d\omega \qquad (12)$$

in which p stands for the expression

$$p(\omega) = (g\beta H_{eff} - J'\cos\omega)/2kT \qquad (13)$$

All these quantities are even functions of the effective field H_{eff}. It must be stressed, however, that this property is not dependent on the model chosen for the interpair interaction, but that it is a necessary consequence of the assumption that the intrapair exchange J is isotropic. In the next section it will be shown that an anisotropic J leads to expressions for the specific heat and the entropy which are asymmetric with respect to $H_{eff} = 0$.

Anisotropic J

When the intrapair interaction tensor J in equation (1) is assumed to be anisotropic, it is convenient to express the hamiltonian for the isolated spin pair in the reference frame in which J has been reduced to its principal values J_x, J_y and J_z

$$\mathcal{H} = -J_x S_{1x} S_{2x} - J_y S_{1y} S_{2y} - J_z S_{1z} S_{2z} - g\beta\vec{H}\cdot(\vec{S}_1 + \vec{S}_2) \qquad (14)$$

From now on the direction of the magnetic field will be defined by the spherical coordinates θ and φ, which are related to the xyz frame in the usual way. Instead of J_x, J_y and J_z the quantities J, δ and ε will be used, defined as

$$J = \frac{1}{3}(J_x + J_y + J_z) \qquad \delta = 1 - J_z/J \qquad \varepsilon = (J_x - J_y)/J \qquad (15)$$

Analogous to the case of isotropic J it is sufficient to describe the system in terms of the lower two energy levels only, if the temperature is low compared to the exchange energy $|J|/k$. However, before this projection the hamiltonian (14) must be diagonalized. The deviations from isotropy δ and ε are assumed to be small compared to 1, so that a perturbation method can be used for this calculation. Up to the second order the energy levels are calculated as

$$E_4 = -(1 - \delta)J/4 + g\beta H(1 + 2E^2)$$

$$E_3 = -(1 + 2\delta)J/4$$

$$E_2 = -(1 - \delta)J/4 - g\beta H(1 + 2E^2)$$

$$E_1 = +3J/4 \qquad (16)$$

in which the quantity E is given by $E = \varepsilon J/8g\beta H$. Fig. 2 shows these energy levels as a function of the external field with arbitrarily

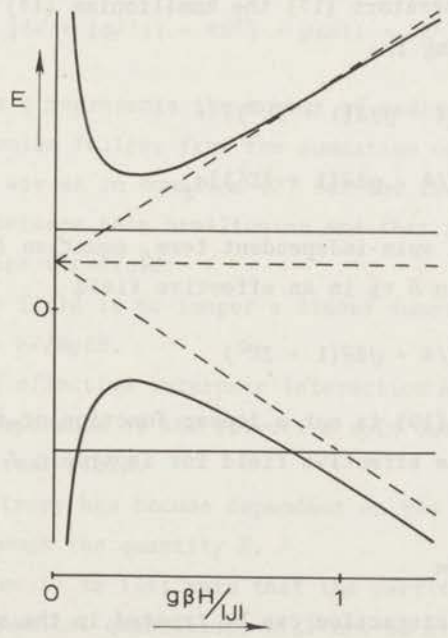

Fig. 2. Energy-level scheme of the pair model with anisotropic J. The values for δ and ε are chosen arbitrarily.

chosen values for δ and ε. For comparison the isotropic-J energy levels are also shown as dashed lines. From equations (16) and Fig. 2 it is clear that this approximation can be used in the vicinity of the "crossing point" $g\beta H = |J|$ but loses its validity when the external field approaches zero.

Again the spin pair operators $\vec{S} = \vec{S}_1 + \vec{S}_2$ and $\vec{t} = \vec{S}_1 - \vec{S}_2$ are introduced. After projection of the system on the subspace spanned by the energy levels E_1 and E_2 (a rather lengthy calculation which will be omitted here) the operators $\vec{S}$ and $\vec{t}$ are given by

$$S_x = \tfrac{1}{2} \tan\theta \cos\varphi (1 + E)(1 + \sigma_z) \qquad t_x = (-1 + E)\tfrac{1}{2}\sqrt{2}\sigma_x$$

$$S_y = \tfrac{1}{2} \tan\theta \sin\varphi (1 - E)(1 + \sigma_z) \qquad t_y = (-1 - E)\tfrac{1}{2}\sqrt{2}\sigma_y \tag{17}$$

$$S_z = \tfrac{1}{2}(1 - \tfrac{1}{2}\tan^2\theta - 2E^2)(1 + \sigma_z) \qquad t_z = \tan\theta \, \tfrac{1}{2}\sqrt{2}(\sigma_x \cos\varphi + \sigma_y \sin\varphi)$$

in which the σ_i are the Pauli spin matrices and 1 represents the unit matrix. Using the operators (17) the hamiltonian (14) is projected on E_1 and E_2 resulting in:

$$\mathcal{H} = \tfrac{1}{2}\{J/2 + \delta J/4 - g\beta H(1 + 2E^2)\} +$$

$$+ \tfrac{1}{2}\{-J + \delta J/4 - g\beta H(1 + 2E^2)\}\sigma_z \tag{18}$$

Apart from the first spin-independent term, equation (18) equals the hamiltonian of a spin $S = \frac{1}{2}$ in an effective field

$$g\beta H_{\text{eff}} = J - \delta J/4 + g\beta H(1 + 2E^2) \tag{19}$$

The effective field (19) is not a linear function of the external field H, in contrast to the effective field for isotropic J given in equation (4).

Interpair interaction

The interpair interaction can be treated in the same way as in the case of isotropic J. As an example the interpair interaction hamiltonian as given in equation (5) is treated with the parameters α_{ij} equal to

zero. This means that the interpair interaction J' is taken to be isotropic and that the "left" spins of each pair interact only with the "left" spins of the surrounding spin pairs, while the "right" spins interact only with the "right" neighbour spins.

Restriction of the interpair interaction to nearest neighbours and projection of the interaction hamiltonian (5) onto the lower two energy levels proceed in the same way as for isotropic J, but with the use of the spin operators (17). This results in an interaction hamiltonian which is the analogon of equation (11):

$$\mathcal{H}'_i = -\frac{1}{8}J' \sum_{j=1}^{q} \tfrac{1}{2}(1 - 4E^2)\sigma_z^i\sigma_z^j + \{(1 - E)^2 + \tan^2\theta \cos^2\varphi\}\sigma_x^i\sigma_x^j +$$

$$+ \{(1 + E)^2 + \tan^2\theta \sin^2\varphi\}\sigma_y^i\sigma_y^j +$$

$$+ \tfrac{1}{2}\tan^2\theta \sin^2\varphi(\sigma_x^i\sigma_y^j + \sigma_x^j\sigma_y^i) \qquad (20)$$

while the effective field becomes

$$g\beta H_{\text{eff}} = J - \tfrac{1}{4}\delta J + \tfrac{1}{4}qJ'(1 - 4E^2) + g\beta H(1 + 2E^2). \qquad (21)$$

In these equations q represents the number of nearest neighbours, while the entire hamiltonian follows from the summation over the $N/2$ spin pairs in the same way as in equation (7) for the isotropic case. The main differences between this hamiltonian and that for isotropic intrapair interaction are threefold:

i) The effective field is no longer a linear function of the external field H, since $E = \varepsilon J/8g\beta H$.

ii) The resulting effective interpair interaction $\mathcal{H}'_i$ is different for the x and y components of the effective spin due to the direction (θ, φ) of the external field.

iii) This xy anisotropy has become dependent on the magnitude of the external field through the quantity E.

The differences i) to iii) make that the partition function, and hence all thermodynamical quantities, will not be even functions of the effective field, in contrast to the isotropic case. Although this treatment has been given for the specific case of $\alpha_{ij} = 0$ the differ-

ences i) to iii) are fundamental consequences of the anisotropic intra-pair interaction J and appear also when the $\alpha_{ij} \neq 0$ though in a more complicated manner.

Comparison with experiment

As in the isotropic case, a distinct choice must be made about the configuration of the spin pairs in the cupric nitrate lattice, in order to calculate its thermodynamical properties. Because of its success in fitting the specific-heat curves (see Chapter III) the *XY* linear chain model was selected. Starting again from Katsura's [13] partition function the formulae for the specific heat capacity C_H, the entropy S and the magnetization M are obtained. Since the first aim of these calculations consists of a comparison with the experiments reported in Chapter III, the formulae for C_H, S and M can be simplified by assuming θ to be so small that those terms in the hamiltonian which contain $\tan^2\theta$ can be neglected. This assumption is justified because the angle between the magnetic field, which was parallel to the crystallographic b axis, and one of the principal axes of the J tensor, which may safely be assumed to coincide with the diagonals of the octahedron of oxygen atoms surrounding the Cu^{2+} ion, amounts to only 10 degrees. In that case the hamiltonian is simplified to

$$\mathcal{H} = -\frac{1}{8} J' \sum_{i=1}^{N/2} (1 - 2E)\sigma_x^i\sigma_x^{i+1} + (1 + 2E)\sigma_y^i\sigma_y^{i+1} - \tfrac{1}{2}g\beta H_{\text{eff}} \sum_{i=1}^{N/2} \sigma_z^i .$$

The partition function belonging to a system with this hamiltonian has been given by Katsura [13], the expressions for C_H, S and M being identical with those given in equation (12) except for the function p, which must now be expressed as

$$p(\omega) = \frac{1}{2kT} [(g\beta H_{\text{eff}} - J'\cos\omega)^2 + E^2]^{\frac{1}{2}} \qquad (22)$$

and for the effective field, for which equation (21) should be used instead of (10).

Numerical results

In all calculations the values J/k = - 5.2 K and g = 2.35, taken from ref. 3, are used. In Fig. 3 the specific heat *vs.* temperature curves with ε = 0.3 are compared for positive and negative effective fields on a reduced temperature scale. This figure clearly shows that the curves drawn for positive effective field (high external field) indicate a higher specific heat capacity in the temperature range

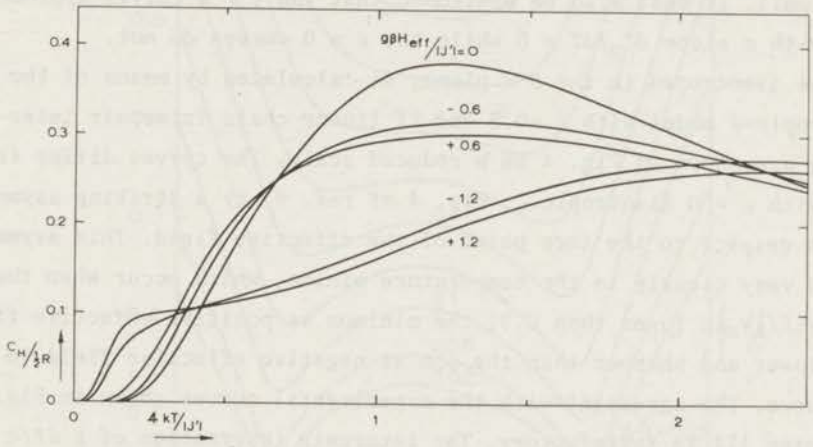

Fig. 3. Calculated curves for the specific heat in positive and negative effective fields, according to the *XY* linear-chain model with anisotropy parameter ε = 0.3.

$0.5 < 4kT/|J'| < 2$ than the curves with negative effective field. This difference is largest for effective fields comparable to the interpair exchange energy, *i.e.* for $|g\beta H_{eff}| \simeq |J'|$. According to Chapter III, a value of $\frac{1}{4}\ J'/k$ = - 0.22 K results in a good fit of the isotropic-*J XY* model with the experimental points. Adopting this same value for the anisotropic model, the largest influence of the anisotropy on the specific heat must be expected in the temperature range 0.1 K < T < 0.4 K at external fields around 30 kOe ($H_{eff} < 0$) and 41 kOe ($H_{eff} > 0$).

Owing to the influence of the anisotropy it is impossible to determine the zero point of the effective field more accurately than within 0.5 kOe. Consequently it is impossible to compare specific heat

data measured in effective fields which differ only in sign. However, a comparison of the Figures 10 and 11 of Chapter III reveals that at temperatures between 0.15 K and 0.4 K the curves obtained in negative fields are systematically lower than those in positive effective fields. In spite of the fact that the *XY* model may not be the best approximation and that the anisotropy in J has been accounted for only by first order perturbation theory, the experiments support the present theory rather well. It must also be mentioned that the $\varepsilon \neq 0$ curves approach $T = 0$ with a slope $dC_H/dT = 0$ while the $\varepsilon = 0$ curves do not.

The isentropes in the H–T plane, as calculated by means of the anisotropic-J model with $\varepsilon = 0.3$ and *XY* linear chain interpair interaction, are shown in Fig. 4 on a reduced scale. The curves differ from those with $\varepsilon = 0$ (isotropic J; Fig. 4 of ref. 9) by a striking asymmetry with respect to the zero point of the effective field. This asymmetry appears very clearly in the temperature minima, which occur when the entropy $S/\frac{1}{2}R$ is lower than 0.3, the minimum at positive effective field being lower and sharper than the one at negative effective field in the same curve. The agreement with the experimental curves shown in Fig. 14 of Chapter III is satisfactory. The interpair interaction of $\frac{1}{4} J'/k$ -0.33 K, which is slightly outside the range of best fits obtained from the specific-heat measurements given in Table II of the previous chapter, causes the calculated temperature minima to occur at the right external field values. This discrepancy between the J' values, obtained from specific heat measurements and isentropes, may very well be due to the neglect of the interaction between the z components of the effective spins, *i.e.* to the use of the *XY* model.

Effects on the magnetization and on the phase boundary

The anisotropic intrapair interaction should also influence the magnetization isotherms $M_T(H)$. However, there are three reasons why the experimental data will not be compared with calculations based on the theory discussed before. First, the *XY* linear chain model does not fit the experimental points in a very satisfactory way; secondly, the corrections for the demagnetizing effect due to the non-spherical shape of the sample are of the same order of magnitude as the expected

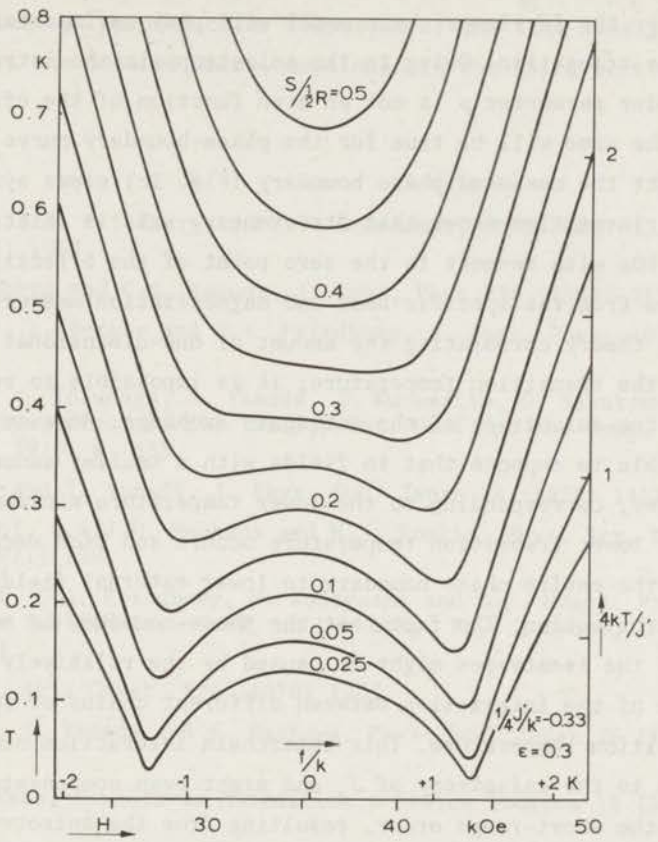

Fig. 4. Calculated isentropes for the *XY* linear-chain model with anisotropy paramater $\varepsilon = 0.3$.

asymmetry in the $M_T(H)$ curves, and thirdly, the calculation of these isotherms requires a detailed choice not only for ε and J' but also for the parameters δ, θ and φ. Therefore it is merely stated that a closer inspection of the experimental data represented in Fig. 3 of Chapter III reveals indeed a slight asymmetry around $H_{\text{eff}} = 0$ as one should expect from the theory.

Thus far, only calculations are reported concerning the *XY* linear chain model which is, owing to its one-dimensional nature, unable to account for the transition to the long-range ordered antiferromagnetic phase below 175 mK. However, the short-range order parameter $\rho = \partial F/\partial J'$

produced by the *XY* linear chain model will play an important part in this phase transition. Owing to the anisotropy in the intrapair exchange J, the order parameter ρ is not an even function of the effective field, so that the same will be true for the phase-boundary curve $T_c(H)$. At first sight the measured phase boundary (Fig. 1c) seems symmetric, but a careful inspection shows that its symmetry axis is shifted downwards over 0.5 kOe with respect to the zero point of the effective field as determined from the specific-heat and magnetization measurements. By lack of a theory correlating the amount of one-dimensional short-range order to the transition temperature, it is impossible to relate this shift to the anisotropy of the intrapair exchange. However, it is not unreasonable to suppose that in fields with a smaller amount of short-range order, corresponding to the lower temperature minimum in the isentropes, a lower transition temperature occurs and *vice versa*. Hence a shift of the entire phase boundary to lower external fields results in first approximation. The fact that the phase-boundary is not as asymmetric as the isentropes might be caused by the relatively important influence of the interaction between different chains of spin pairs on the transition temperature. This interchain interaction need not be as sensitive to the anisotropy of J, and might even compensate the differences in the short-range order, resulting from the anisotropy.

Conclusion

The conclusions which follow directly from the experimental results given at the end of Chapter III, can now be completed by the following statements:

i) The intrapair interaction J is slightly anisotropic, which can be characterized by an $\varepsilon = 0.3$.

ii) Owing to the anisotropy of J, the effective field describing the spin-pair system at low temperatures, is a non-linear function of the external magnetic field.

iii) The interactions J'_x and J'_y between the x and y components of the effective spins within the chains vary with the magnitude of the external field. This might cause the slight field dependence of the direction

$\vec{u}'$ of the spontaneous perpendicular component of the time-averaged magnetization in the ordered phase, mentioned in the third section of Chapter III.

References

1. L. Berger, S.A. Friedberg and J.T. Schriempf, Phys. Rev. 132 (1963) 1057.
2. S.A. Friedberg and C.A. Raquet, J. appl. Phys. 39 (1968) 1132.
3. B.E. Myers, L. Berger and S.A. Friedberg, J. appl. Phys. 40 (1969) 1149.
4. T. Haseda, Y. Tokunaga, R. Yamada, Y. Kuramitsu, S. Sakatsume and K. Amaya, Proc. of the Twelfth Int. Conf. on Low Temp. Phys., Kyoto 1970, p. 685.
5. M. Tachiki and T. Yamada, J. Phys. Soc. Japan 28 (1970) 1413.
6. M.W. van Tol, L.S.J.M. Henkens and N.J. Poulis, Phys. Rev. Lett. 27 (1971) 739.
7. J.C. Bonner, S.A. Friedberg, H. Kobayashi and B.E. Myers, Proc. of the Twelfth Int. Conf. on Low Temp. Phys., Kyoto, 1970, p. 691.
8. B. Morosin, Acta Cryst. B26 (1970) 1203.
9. M. Tachiki, T. Yamada and S. Maekawa, Phys. Soc. Japan 29 (1970) 663.
10. J.H. van Vleck, Revista de Matemática y Física Teórica 14 (1962) 189.
11. M.W. van Tol, H.M.C. Eijkelhof and A.J. van Duyneveldt, Physica 60 (1972) 223.
12. M. Tachiki and T. Yamada, Progr. Theor. Phys. Suppl. 46 (1970) 291.
13. S. Katsura, Phys. Rev. 127 (1962) 1508.
14. S. Katsura and S. Inawashiro, J. Math. Phys. 5 (1964) 1091.
15. S. Inawashiro and S. Katsura, Phys. Rev. 140 (1965) A892.

CHAPTER V
WEAKLY COUPLED LINEAR CHAINS

Introduction

The theory of the antiferromagnetic linear chain (a.l.c.) of atoms with spin $S = \frac{1}{2}$ is relatively simple compared to that of two and three-dimensional lattices. As with most antiferromagnetic insulators, the properties of the linear chain are often discussed on the basis of the Heisenberg model of exchange interactions between nearest neighbours. For this model it is convenient to introduce periodic boundary conditions, so that the hamiltonian

$$\mathcal{H} = -J \sum_{i=1}^{N} \vec{S}_i \cdot \vec{S}_{i+1} - g\beta H \sum_{i=1}^{N} S_i^z \qquad (1)$$

describes rings instead of chains. Here J is the exchange integral and H the external magnetic field, applied along the positive z axis.

The first attack to the eigenvalue problem was made by Bethe [1] as early as 1931, who showed that the solution of equation (1) could be reduced to that of a set of coupled transcendental algebraic equations. Using this procedure Hulthén [2] calculated the exact ground-state energy in the limit $N \to \infty$ for zero field $H = 0$. The development of fast electronic computers made exact calculations much easier on rings and chains with a finite, though relatively large number of spins [3, 4]. From these calculations reasonable extrapolations could be made concerning properties such as the susceptibility and the specific heat capacity. Encouraged by these results, Des Cloizeaux and Pearson [5] obtained the spin-wave spectrum of infinite linear chains. The central assumption in their calculations is that the ground state and the lowest excitations belong to a class "C" of unbound states in the Bethe [1] formalism. This assumption was then used by Griffiths [6] in the calculation of the zero-temperature magnetization isotherm. Quite another approach was used by Katsura and Inawashiro [7], who obtained the partition function of the a.l.c. in second order by means of cluster-expansion methods.

It may be concluded that the isolated Heisenberg a.l.c. is reasonably well understood. The experimental evidence on chain-type compounds agrees with the existing theoretical predictions [8, 9, 10]. However, up to now the models describing antiferromagnetic Heisenberg chains with weak interchain interaction have received little attention.

The two-dimensional lattice of spins, resulting from a weak coupling J' between antiferromagnetic linear chains of Ising spins can be described exactly [11] by means of a slight modification of the Onsager [12] solution. The three-dimensional lattice of Ising spins with a dominant interaction in one dimension has been discussed in the molecular-field approximation by Stout and Chrisholm [13]. Unfortunately, the Heisenberg character of the interaction in (1) provides complications which necessitate the use of approximative theories even for two-dimensional lattices. As indicated by Oguchi [14] some progress may be expected from Green-function theory, which produces a transition temperature T_c in zero field as a function of the ratio J'/J, but it is difficult to judge the validity of the approximations made in this way.

The main theme of this chapter will be to show that in the presence of an external magnetic field a system of weakly coupled antiferromagnetic Heisenberg chains exhibits a transition to a state in which the transverse components of the individual spins are long-range ordered. For that purpose a hybrid theory will be set up which treats the interaction within the chains J exactly, while the interchain coupling J' is treated within the frame of the molecular-field theory.

Since the interchain interaction J' is much weaker than J, appreciable effects will only occur at temperatures $T \ll |J/k|$. At these temperatures only the lowest energy levels of the chains will be populated. Therefore the states with minimum energy in a certain external field are of special interest in this study. The nature of the lowest energy levels in the presence of a field may be illustrated by Fig. 1 which represents the energy-level diagram of a ring of 8 spins with Heisenberg coupling. From this figure, which has been reproduced from Bonner and Fisher [15], it is clear that the expectation value for the total spin $m = \langle \Sigma_i S_i^z \rangle$ of the state with minimum energy increases with increasing magnetic field. It will be useful to define a class C^* which

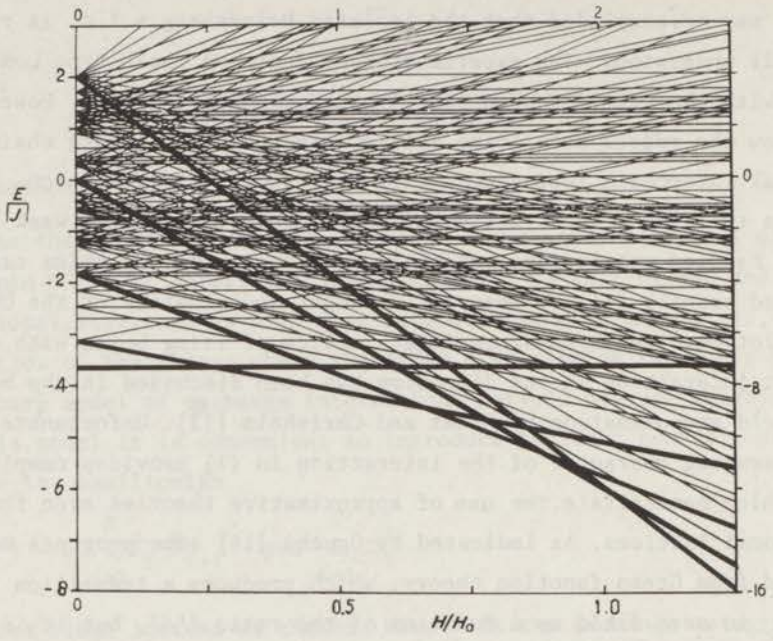

Fig. 1. Energy levels of a ring of eight spins $S = \frac{1}{2}$ with isotropic Heisenberg interaction. Heavy drawn lines indicate the levels corresponding to states in class C^*. The figure has been reproduced from Bonner and Fisher (ref. 15).

contains all these states. The energy levels corresponding to the states in class C^* are represented by heavy drawn lines in Fig. 1. Since all states in class C^* are non-degenerate, as has been proved by Lieb and Mattis [16], they can be denoted by the quantum number for the total spin in the z direction m only. An asterisk within the brackets will mark the membership of the state $|^*m\rangle$ of the class C^*. An important feature of the antiferromagnetic linear chains can now be expressed by the fact that when in a certain field the ground state is formed by $|^*m\rangle$, the first excited state is either $|^*m+1\rangle$ or $|^*m-1\rangle$.

Interchain interaction

The interchain interaction is introduced as a perturbation of the simplest possible form

$$\mathcal{H}' = -J' \sum_{\alpha} \sum_{i} \vec{S}_i \cdot \vec{S}_{i\alpha} \qquad (2)$$

where $S_{i\alpha}$ represents the i-th spin in the α-th neighbour chain. Since in any magnetic field the ground state as well as the first two excited states belong to the class C^*, the matrix elements of $\mathcal{H}'$ connecting the states in class C^* will play a very important part in the description of a lattice of weakly coupled linear chains. In order to get some insight in these matrix elements, the perturbation (2) is replaced by its molecular-field equivalent

$$\mathcal{H}' = - qJ' \sum_i \vec{S}_i \cdot \langle \vec{S}_{i\alpha} \rangle \tag{3}$$

where q represents the number of neighbouring chains and $\langle S_{i\alpha} \rangle$ is the mean magnetization of the spins S_i in these chains.

Because of the presence of the magnetic field H in the z direction, the terms $\langle S^z_{i\alpha} \rangle$ will contain a large part $\langle S^z_\alpha \rangle$ independent of the position of the spins in the neighbouring chains, which can easily be separated

$$\langle S^z_{i\alpha} \rangle = \langle S^z_\alpha \rangle + \langle \delta S^z_{i\alpha} \rangle \, . \tag{4}$$

That part of the perturbation (3) which contains $\langle S^z_\alpha \rangle$ commutes with the unperturbed hamiltonian (1), so that it does not alter the magnetic behaviour of the chain, provided the external field is replaced by an effective field

$$H_{\text{eff}} = H + \frac{qJ'}{g\beta} \langle S^z_\alpha \rangle \, . \tag{5}$$

Since $\langle S^z_\alpha \rangle = \langle S^z \rangle$ is equal for all chains in the crystal, the effective field (5) introduces only a simple transformation of axes in the $M = Ng\beta \langle S^z \rangle$ *vs.* H diagram. Hence it creates the possibility to obtain an estimate of the quantity qJ' of existing a.l.c. compounds by comparing experimental magnetization isotherms with calculated ones for isolated chains ($J' = 0$).

The remaining i-dependent part of the perturbation (3)

$$\mathcal{H}'_r = - qJ' \sum_i \{ S^x_i \langle S^x_{i\alpha} \rangle + S^y_i \langle S^y_{i\alpha} \rangle + S^z_i \langle \delta S^z_{i\alpha} \rangle \} \tag{6}$$

will be treated next. According to standard perturbation theory, the first order perturbation $|{}^*m_1\rangle$ of a ground state $|{}^*m\rangle$ is of the form

$$|{}^*m_1\rangle = \sum_{k\neq {}^*m} |k\rangle \frac{\langle k|\mathcal{H}'_r|{}^*m\rangle}{E_m - E_k} \tag{7}$$

so that the largest contributions to $|{}^*m_1\rangle$ originate in the states for which $E_m - E_k$ is small. As has been shown in the previous section, the first excited states are $|{}^*m \pm 1\rangle$ and belong to C^*. Now a very important property of the states in class C^* will be used. In the Appendix it will be proved that all states $|{}^*m\rangle$ behave under translation as

$$T|{}^*m\rangle = (-1)^m|{}^*m\rangle \tag{8}$$

where the operator T translates the whole chain (ring) over one lattice distance. Therefore, the only non-zero contributions to $\langle {}^*m|\mathcal{H}'_r|{}^*m \pm 1\rangle$ are those which behave as $(-1)^i$ under translation. The elements $\langle {}^*m|\Sigma S^z_i \langle \delta S^z_{i\alpha}\rangle|{}^*m \pm 1\rangle$ being zero, the largest contribution to $|{}^*m_1\rangle$ in equation (7) comes from the mixing of $|{}^*m\rangle$ and $|{}^*m \pm 1\rangle$ by the operators $-qJ'\langle S^{x,y}_\alpha\rangle \Sigma (-1)^i S^{x,y}_i$.

Without loss of generality it can be assumed that $\langle S^y_\alpha\rangle = 0$, so that after neglecting the states outside C^*

$$|{}^*m_1\rangle = \frac{qJ'}{J}\langle S^x_\alpha\rangle \{\frac{C^+_m}{N\Delta^+}|{}^*m+1\rangle + \frac{C^-_m}{N\Delta^-}|{}^*m-1\rangle\} \tag{9}$$

where $\Delta^\pm = (E_{m\pm1} - E_m)/NJ$ represents the difference in reduced energy per spin between the states $|{}^*m\rangle$ and $|{}^*m \pm 1\rangle$, while the coefficients $C^\pm_m$ stand for the matrix elements $C^\pm_m = \langle {}^*m|\Sigma_i (-1)^i S^x_i|{}^*m \pm 1\rangle$. The correction E'_m on the ground-state energy amounts to

$$E'_m/J = (\frac{qJ'}{J}\langle S^x_\alpha\rangle)^2 \{\frac{(C^+_m)^2}{N\Delta^+} + \frac{(C^-_m)^2}{N\Delta^-}\} \tag{10}$$

The internal consistency of the theory demands that $\langle S^x\rangle \neq 0$ for the ground state. This perpendicular component is calculated at $T = 0$ as

$$\langle S^x\rangle = \frac{1}{N}\langle \sum_{i=1}^{N} (-1)^i S^x_i\rangle = \frac{2qJ'}{J}\langle S^x_\alpha\rangle \{\frac{(C^+_m)^2}{N^2\Delta^+} + \frac{(C^-_m)^2}{N^2\Delta^-}\} \tag{11}$$

In the limit $N \to \infty$ the energy difference per spin $J\Delta_m^{\pm}$ approaches zero as N^{-2} while the coefficients $(C_m^{\pm})^2$ are proportional to N. Hence the perpendicular component $\langle S^x \rangle$ in equation (11) is certainly not zero when $N \to \infty$.

Therefore the conclusion from the preceding theory is that in a non-zero external field the ground state of a lattice of Heisenberg-type antiferromagnetic linear chains coupled by a weak isotropic Heisenberg interaction, consists of a canted spin arrangement. The canted arrangement does not occur in external (*e.q.* effective) fields larger than $H_0 = 2|J/g\beta|$, because above that value the energy difference Δ^- in equations (9), (10) and (11) increases rapidly. However, both the energy correction (10) and the perpendicular spin component (11) diverge when N approaches infinity, indicating that then the first order perturbation theory fails. This could be expected since the energy differences $J\Delta_m^{\pm}$ approach zero.

The phase transition

The previous section shows that at zero temperature the interacting chains possess a canted spin arrangement. It is further clear, that at temperatures $T >> |J'/k|$ the chains will be in the paramagnetic phase and the canting has disappeared. Somewhere between these two situations a temperature T_c must exist at which the system shows a transition to the ordered phase. However, apart from the molecular field approximation another simplification is necessary in order to obtain an explicit expression for the transition temperature $T_c(H)$. A very rough approach will leave out all energy levels of the chain except the lowest two.

In an external field H_m of such a magnitude that the total magnetization per chain $\langle \Sigma_i S_i^z \rangle$ equals $m + \frac{1}{2}$ at $T = 0$, only the energy levels $|*m\rangle$ and $|*m+1\rangle$ will be considered. Analogous to the spin-pair case described in Chapter IV, each chain will be represented by an effective spin S', this time with components

$$S'_x = \tfrac{1}{2}(C_m^+)^{-1} \sum_i (-1)^i S_i^x \qquad S'_y = \tfrac{1}{2}(C_m^+)^{-1} \sum_i (-1)^i S_i^y$$

$$S'_z = -(m + \tfrac{1}{2}) + \sum_i S_i^z \qquad (12)$$

When this effective spin is inserted, the hamiltonian (1) with perturbation (3) is replaced by

$$\mathcal{H} = - g\beta(H - H_m)S'_z + \eta[\langle S'_{\alpha x}\rangle S'_x + \langle S'_{\alpha y}\rangle S'_y] \tag{13}$$

in which $\eta = 4|qJ'|(C_m^+)^2/N$. This equation, in which the spin-independent term has been neglected, is formally equal to the hamiltonian of a spin $S' = \frac{1}{2}$ in a field with components

$$H_x = \eta\langle S'_{\alpha x}\rangle \; ; \qquad H_y = \eta\langle S'_{\alpha y}\rangle \; ; \qquad H_z = g\beta(H - H_m) \tag{14}$$

The eigenvalues of (13) are easily calculated as

$$E^{\pm} = \pm \tfrac{1}{2}\sqrt{g^2\beta^2(H - H_m)^2\langle S'_z\rangle^2 + \eta^2\langle S'_\perp\rangle^2} \tag{15}$$

in which $\langle S'_\perp\rangle = (\langle S'_x\rangle^2 + \langle S'_y\rangle^2)^{\frac{1}{2}}$ represents the perpendicular spincomponent. The partition function of the system becomes

$$Z = \exp\frac{-E^+}{kT} + \exp\frac{-E^-}{kT} \tag{16}$$

In deriving the free energy F for an assembly of N' effective spins S' from eq. (16), one must be aware of the fact that the interchain interaction is included twice in $-N'kT \ln Z$. Subtraction of this interaction energy finally produces

$$F = N'\{-kT \ln Z + \tfrac{1}{2}\eta\langle S'_\perp\rangle^2\} \tag{17}$$

The value of $\langle S'_\perp\rangle$ is determined by minimizing the free energy (17) *i.e.* by setting $\partial F/\partial\langle S'_\perp\rangle$ equal to zero. The result is given in implicite form as

$$\langle S'_\perp\rangle = \frac{\eta\langle S'_\perp\rangle}{4kTx}\tanh x \tag{18a}$$

$$x = \frac{1}{2kT}\{g^2\beta^2(H - H_m)^2\langle S'_z\rangle^2 + \eta^2\langle S'_\perp\rangle^2\}^{\frac{1}{2}} \tag{18b}$$

Equation (18) contains the two solutions

$$\langle S'_\perp\rangle = 0 \tag{19a}$$

$$\frac{\eta}{4kTx}\tanh x = 1 \tag{19b}$$

Above the temperature T_c, which will be determined below, no real solution of the type (19b) exists, so that (19a) represents the paramagnetic phase in which the perpendicular magnetization equals zero. Below T_c equation (19b) has three solutions, one of which is identical to (19a) and corresponds to a maximum in the free energy F. The other two solutions of (19b) have non-zero values for the perpendicular magnetization $\langle S_1' \rangle$. They can be obtained by solving equations (17), (18) and (19) simultaneously.

When the external field H is exactly equal to H_m, the formulae (17) and (18) become much simpler

$$F = N'\{- kT \ln(2 \cosh \frac{\eta \langle S_1' \rangle}{2kT}) + \tfrac{1}{2}\eta \langle S_1' \rangle^2\} \tag{17'}$$

$$\langle S_1' \rangle = \tfrac{1}{2} \tanh \frac{\eta \langle S_1' \rangle}{2kT} \tag{18'}$$

The transition temperature at H_m follows immediately from the coincidence of the three roots of equation (18')

$$kT_c = \eta/4 = |qJ'|(C_m^+)^2/N \tag{20}$$

The quantity $|qJ'|$ being known from magnetization measurements, the phase boundary $T_c(H)$ can be evaluated by calculation of the coefficients C_m^+. Although these coefficients have not yet been obtained for infinite ($N \to \infty$) chains, a first approximation is provided by their values for finite rings. In the Appendix the wave functions for rings of 6, 8, 10 and 12 spins are calculated as far as they belong to the class C^* defined in the previous section. From the wave functions a straightforward calculation yields the values for the C_m^+. The values of $(C_m^+)^2/N$ for rings with 6, 8, 10 and 12 spins are plotted in Fig. 2 against the appropriate values of H_m.

This figure indicates that in this approximation the transition temperature T_c increases slightly with increasing external field up to $H \approx \frac{3}{4} H_0$. At higher fields T_c decreases and finally drops sharply at $H = 2|J/g\beta|$. It must be stressed that the approximation given above, which is already very rough, is certainly not valid at zero field be-

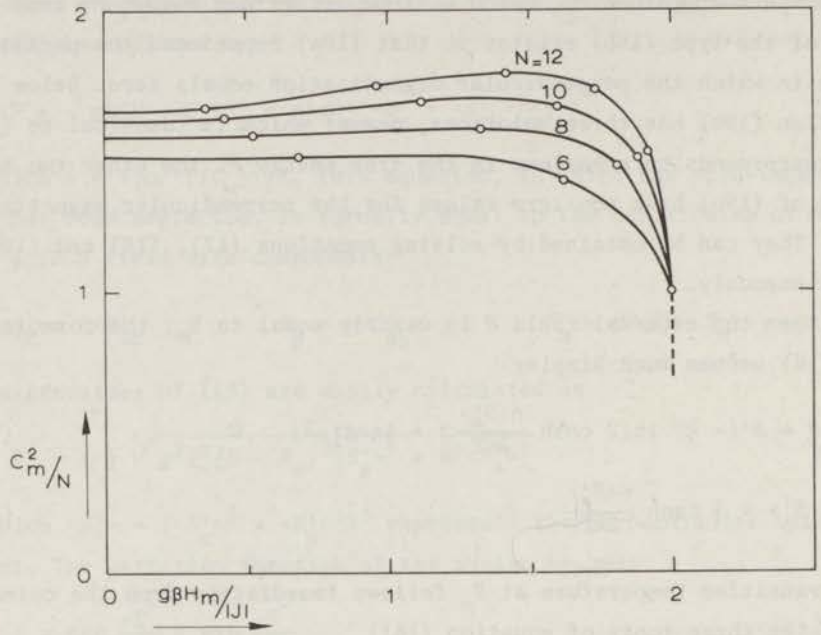

Fig. 2. Values of the coefficients $(C_m^+)^2/N$ *versus* H_m as calculated for rings of 6, 8, 10 and 12 spins.

cause then the first excited state is a triplet, of which one component does not belong to the class C^*.

Although the continuum-like energy spectrum in the limit $N \to \infty$ would suggest an approximation by classical spins S', exact calculations will become complicated because also wave functions outside C^* enter, while it is not even certain whether states outside class C [1, 6] play an important role. However, the dominant contribution of the states $|{}^*m \pm 1\rangle$ to the first order approximation $|{}^*m_1\rangle$ suggest the importance of the coefficients $C_m^{\pm}$. Therefore we believe that the transition temperature calculated according to equation (20) provides a reasonable estimate of the phase boundary.

The argumentation given above must be considered as a first attempt to solve the problem of weakly coupled Heisenberg chains. One of the striking results is that in the presence of an external field, an ordered state occurs in which the individual spins are canted, without the

introduction of an interaction of the type described by Moriya and Dzialozhinsky [17, 18].

Experiments

This section describes the experimental evidence for a transition to an ordered state in the two linear-chain compounds $CuSO_4 \cdot 5H_2O$ and the isomorphic $CuSeO_4 \cdot 5H_2O$. These crystals are triclinic and contain two cupric ions at inequivalent positions in the unit cell. The experiments of Miedema, Van Kempen, Haseda and Huiskamp [19] indicated the existence of two independent magnetic systems originating from the two inequivalent Cu^{2+} ions. One system was supposed to have relatively strong exchange interactions in one dimension, leading to short-range order in linear chains at about 1 K and causing the maxima in the specific-heat capacity at T = 1.4 K and 0.8 K for the sulphate and selenate, respectively. The other system had much weaker interactions, for both salts leading to a transition of the whole crystal to the ferromagnetic state below 80 mK in zero field. The susceptibility of the ions in the latter system follows a Curie-Weiss law with a small θ value (+ 0.02 K) down to below 0.1 K [19]. At the transition temperature in H = 0 a sharp λ-peak occurs in the specific heat, as reported by Giauque *et al.* [20].

The n.m.r. experiments of Wittekoek, Poulis and Miedema [21] confirmed the hypothesis of Miedema *et al.* [19] and proved that the ions at (0,0,0) constitute the a.l.c. system while the paramagnetic system is formed by the $(\frac{1}{2},\frac{1}{2},0)$ ions. From the small temperature dependence of the Curie-Weiss θ value of the paramagnetic system, Wittekoek *et al.* [21] also obtained an estimate for the interaction J_{12} between the two dissimilar cupric ions. The small discrepancies between their very accurate measurements of the susceptibility $\chi_{(0,0,0)}$ of the a.l.c. ions and the theoretical curve of Bonner and Fisher [22] were ascribed to small deviations from isotropy of the interaction J within the chains.

The value of J and the Curie-Weiss constant θ_p of the paramagnetic system as obtained by Wittekoek [21] and Miedema [19], together with the unit-cell dimensions determined by Bacon and Curry [23] are given in Table I.

It is impossible to derive an estimate for the interchain interaction J' from the existing susceptibility and specific-heat data, be-

Table I

	a	b	c	α	β	γ	$-J/k$	θ_p	J_{12}/k
$CuSO_4 \cdot 5H_2O$	6.14	10.74	5.99	82°3	107°4	102°7	3.0	0.02	0.1
$CuSeO_4 \cdot 5H_2O$	6.23	10.87	6.08	82°2	107°1	102°8	1.7	0.05	0.07

cause the influence of J' cannot be separated from that of a slight anisotropy in the main interaction J. According to equation (5) in the preceding section, measurement of the magnetization isotherms provides the solution.

The magnetization isotherms of a linear chain compound exhibit their typical character most clearly at temperatures $T << |J/k|$ as illustrated in Fig. 3*. According to Griffiths [6] the zero-temperature isotherm represents a nearly linear relation between the magnetization

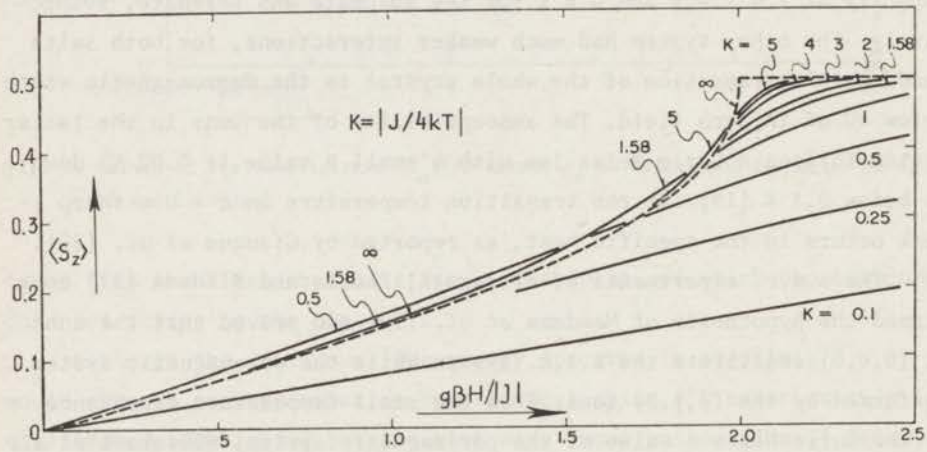

Fig. 3. Magnetization *versus* external magnetic field for isolated antiferromagnetic linear chains. The figure has been reproduced from the paper by Katsura and Inawashiro (ref. 7).

M and the external field H for small H values. With increasing field, the derivative dM/dH gradually increases until it reaches infinity at $H_0 = 2|J/g\beta|$. Above this field the magnetization remains constant at its saturation value $\frac{1}{2} Ng\beta$. The calculations of Katsura and Inawashiro [7] show that at temperatures which are low compared to $|J/k|$ the isotherms follow the zero-temperature isotherm closely, except in the near vicinity of H_0, where the sharp edge is rounded off. With increasing

* The Figure has been copied from Katsura and Inawashiro (Phys. Rev. 140 (1965) A 892).

temperature $T > |J/k|$, the curves resemble more and more the familiar Brillouin function for spin $S = \frac{1}{2}$.

According to the molecular field treatment given in the previous sections, the influence of J' consists of a transformation of axes as expressed by the "effective field" in equation (5). The effects will be most pronounced in the vicinity of H_0 at $T << |J/k|$. Therefore the first aim of this research project was the determination of the a.l.c. magnetization in cupric sulphate in high magnetic fields at the lowest temperatures possible.

In order to obtain the magnetization of the linear chain system separately, proton magnetic resonance was used to discriminate between the contributions of the paramagnetic and the a.l.c. system. In low external fields this discrimination is a complicated procedure, since the internal fields at a proton site produced by the two magnetic systems are in general not parallel to the external field while the resonance frequency of the proton is proportional to the vector sum of the external field and the internal fields. As indicated by Wittekoek [21] the discrimination between the two contributions can be simplified by the selection of a special orientation of the crystal with respect to the external field and by studying the resonance line (line 3) which is the most sensitive to the magnetization of the a.l.c. system in the selected orientation.

According to the discussion in the second section of Chapter III, the application of high magnetic fields provides a substantial simplification. In high fields the shift Δ of the resonance line is almost proportional to the projection of the internal fields on the direction of the external field, as long as the crystal to be studied remains in the paramagnetic state (compare equation (7) of Chapter III). In this case the study of the shifts of only two resonance lines allows discrimination between the two magnetic systems present in cupric sulphate.

Further simplification is obtained by lowering the temperature to a value at which the paramagnetic ions have reached their maximum magnetization in external fields of, for instance, 5 kOe. In fields above this "saturation value" it suffices to subtract the constant contribution of the paramagnetic system from the lineshift Δ, in order to ob-

tain a frequency difference which is proportional to the magnetization of the linear-chain system. Although in this way the a.l.c. magnetization can be obtained from any resonance line, the study of line 3 in the special orientation in which its shift is maximal produces the most accurate results.

This may be illustrated by Fig. 4 where the positions of all ten proton resonance lines relative to the free proton resonance frequency are plotted as a function of the external magnetic field at a temperature of 0.11 K. The "initial" shifts occurring at field values below 3 kOe are mainly due to the magnetization of the paramagnetic system,

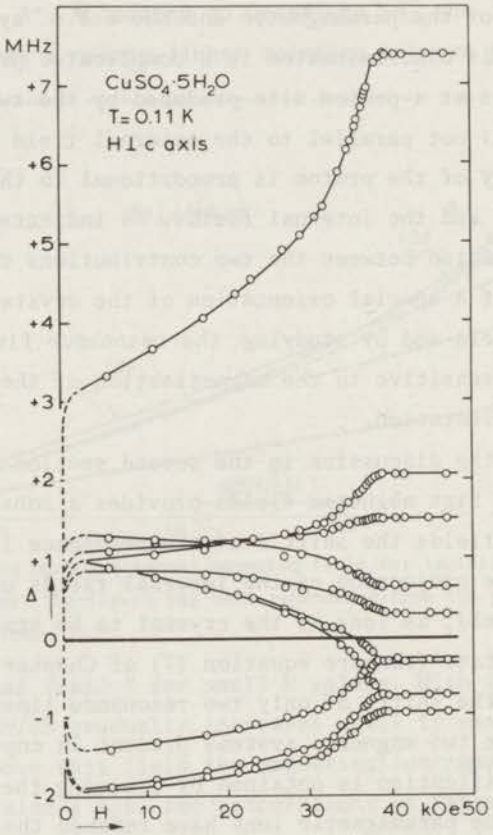

Fig. 4. Lineshifts $\Delta^{(i)}$ for the ten proton resonance lines in cupric sulphate *versus* external field at 0.11 K.

while at higher fields the changes in the shifts Δ are entirely due to the influence of the linear chains.

The magnetization of the a.l.c. system obtained in this way is shown on a reduced scale in Fig. 5 for temperatures of 0.11 K and 0.27 K. The drawn lines in this figure represent Griffiths' [6] curve for $T = 0$ and the isotherms for $T = 0.11$ K and 0.27 K according to Katsura and Inawashiro [7], corrected for interchain interaction.

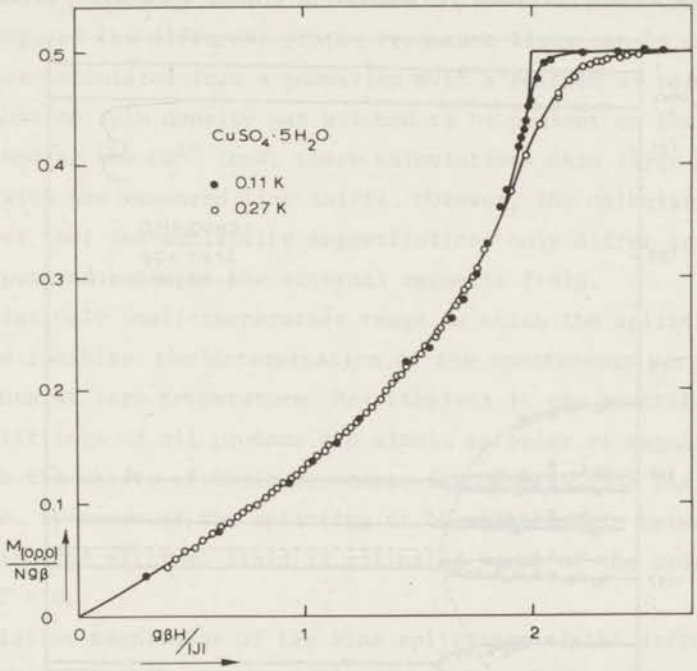

Fig. 5. Magnetization of the linear chain system in cupric sulphate *versus* field at 0.11 K and 0.27 K. Drawn lines represent the theoretical curves according to refs. 6 and 7, corrected for interchain interaction.

The value of $|qJ'/k|$ from the fitting of the theoretical curves to the experimental data amounts to 0.14 (± 0.03 K). This result together with the existing information about cupric sulphate gathered in Table I ascertains that the (0,0,0) ions in that compound are a very good example of a lattice of weakly coupled antiferromagnetic linear chains. According to equation (20), a transition to the "canted"

state can be expected at $T_c \simeq 0.2$ K. In order to exclude possible influences originating in the paramagnetic system, the transition was searched for in external fields of such a magnitude that the magnetization of the $(\frac{1}{2},\frac{1}{2},0)$ ions was perfectly saturated.

Therefore a systematic exploration of the temperature region below 0.3 K was carried out by n.m.r. experiments in high fields. An example of these measurements is given in Fig. 6, where the resonance frequencies of the various protons in the unit cell are plotted against

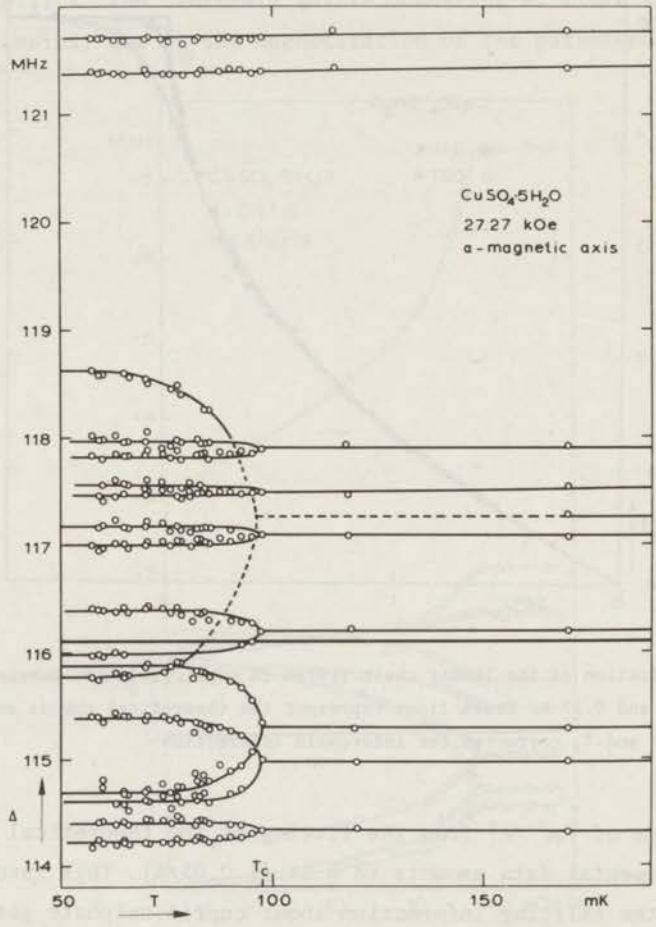

Fig. 6. Resonance frequencies $\nu^{(i)}$ for the ten proton lines in cupric sulphate as a function of temperature. The external field is directed parallel to the a-magnetic axis.

temperature in a field of 27 kOe. Above 98 mK the resonance frequencies are independent of the temperature, as can be expected from the experimental magnetization isotherms given in Fig. 5. Below this temperature the resonance lines split and the frequency difference of each pair of "components" shows the characteristic temperature dependence of a spontaneous magnetization. As has been argued in Chapter III, the splitting $\nu^+ - \nu^-$ is a direct measure of the difference in the two sublattice magnetizations. Analogous to the procedure followed in that chapter, the splittings of the different proton resonance lines can be compared to the values calculated from a summation over a lattice of point dipoles. Because no spin density was assumed to be present on the oxygen atoms surrounding the Cu^{2+} ions, these calculations show large discrepancies with the measured line shifts. However, the calculations still suggest that the sublattice magnetizations only differ in their components perpendicular to the external magnetic field.

The relatively small temperature range in which the splittings are measured inhibits the determination of the spontaneous perpendicular magnetizations at zero temperature. Nevertheless it can be stated that the line splittings of all protons are almost an order of magnitude smaller than the shifts of their resonance frequencies from the free proton value. By means of the splitting at 60 mK the angle between the spin direction and external field is estimated to be of the order of 0.1 rad at $T = 0$.

The relative magnitudes of the line splittings of the different protons in the unit cell prove unambiguously that the canting occurs in the antiferromagnetic linear chain system only. In the next section the interaction between the paramagnetic system and the antiferromagnetic linear chain system will be discussed. It will appear that when the magnetization of the paramagnetic system is not entirely saturated, the canted a.l.c. spins induce also a canting of the paramagnetic spins.

The heat capacity C_H of cupric sulphate will contain contributions of both the paramagnetic and the antiferromagnetic chain system. When the paramagnetic ions are regarded as free spins, the energy-level

separation of $g\beta H$ induced by the external magnetic field H will cause a contribution to the specific heat of the Schottky type. The maximum of 0.22 R of this contribution occurs at a temperature $T_{max} = 0.42\ g\beta H/k$. The expression for T_{max} shows that at temperatures of the order of the transition temperature T_c the paramagnetic system will appreciably contribute to the specific heat in relatively low external fields only. The slight deviations of the C_H *vs.* T curve from the pure Schottky shape, due to the interactions within the paramagnetic system and to the "cross-interaction" J_{12} between the two magnetic systems will not be discussed here, because of their relative unimportance.

At temperatures of the order of T_c the contribution of the antiferromagnetic linear chains to the specific heat is expected to be small in external fields up to H_0, since most of the entropy of the chains has already been removed above 1 K. So an anomaly in the specific heat capacity at the transition temperature T_c should be very small, if it occurs at all.

At first sight one might be inclined to calculate the entropy variation associated with the specific heat anomaly by means of the model given previously in which each chain is represented by one effective spin $S' = \frac{1}{2}$. In that case the entropy involved in the transition amounts only to

$$S_c = N^{2/3}\, k \ln 2 \qquad (21)$$

where N is the total number of Cu^{2+} ions in the a.l.c. system and $N^{1/3}$ is the number of cupric ions per chain. The number N being of the order of 10^{21} for a sample of 1 gram, the entropy S_c and the specific heat C_H should be entirely negligible compared to the contribution of the rest of the crystal. However, it must be stressed that the approximation given in the previous sections is very rough and that especially the specific heat capacity is very sensitive to the presence of excited energy levels other than those corresponding to the $S' = \frac{1}{2}$ picture. Therefore it is not unreasonable to expect that the phase transition is accompanied by an anomaly in the specific heat which, although small, might be well observable.

Because the maximum of the specific heat of the paramagnetic system shifts to lower temperatures with decreasing external field, the anomaly caused by the a.l.c. system at T_c will be superposed on the well-known Schottky curve in low fields. An example of this situation is given in Fig. 7, which shows the specific heat of $CuSO_4 \cdot 5H_2O$ in a

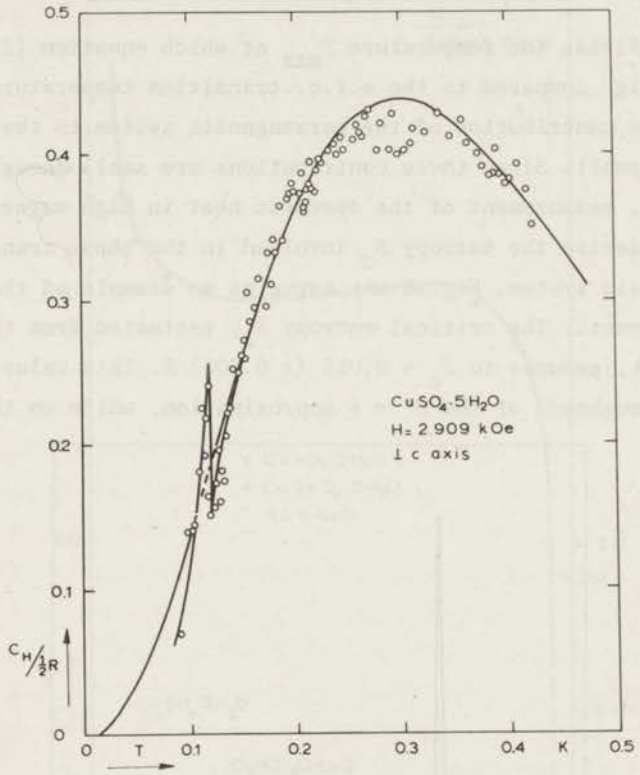

Fig. 7. Specific heat *vs.* temperature of cupric sulphate in a field of 2.9 kOe. The drawn curve represents the calculated Schottky anomaly originating in the paramagnetic system.

field of 3 kOe. A sharp peak is clearly visible although it is small compared to the contribution of the paramagnetic system. The drawn curve represents the specific heat of a two-level system calculated by

$$C_H/\tfrac{1}{2}R = \left(\frac{\Delta}{2kT}\right)^2 \cosh^{-2}\left(\frac{\Delta}{2kT}\right) \qquad (22)$$

with $\Delta = g\beta H$. At fields lower than 3 kOe the large maximum of the

Schottky curve (32) shifts to still lower temperatures, thereby inhibiting the detection of the small linear-chain peak. In zero field only the anomaly at 30 mK, reported by Giauque *et al.* [20] remains. According to their analysis this temperature indicates the transition of the whole crystal from the paramagnetic state to the ferromagnetic state.

At high fields the temperature T_{max} at which equation (22) is maximal, is high compared to the a.l.c. transition temperature T_c, so that at T_c the contribution of the paramagnetic system to the specific heat will be small. Since these contributions are small enough to be corrected for, measurement of the specific heat in high magnetic fields is useful to derive the entropy S_c involved in the phase transition of the linear chain system. Fig. 8 may serve as an example of these high-field measurements. The critical entropy S_c, estimated from the area under the peak, amounts to $S_c = 0.015\ (\pm\ 0.005)\ R$. This value gives an idea of the roughness of the $S' = \frac{1}{2}$ approximation, while on the other

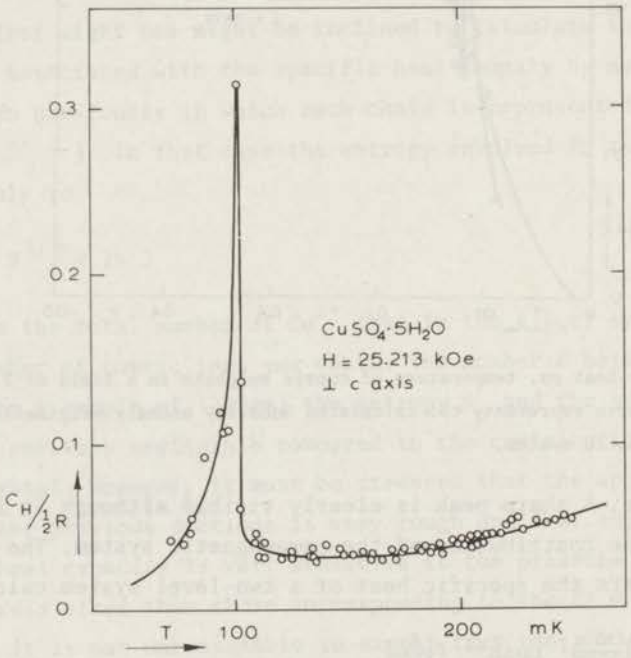

Fig. 8. Specific heat of cupric sulphate in a field of 25 kOe. The drawn curve is for visual aid only.

hand it can be used to obtain an estimate for the "real" effective spin which has to represent each linear chain at the transition temperature.

A careful study by n.m.r. and specific-heat experiments finally led to the phase diagram shown in Fig. 9. During these experiments, the

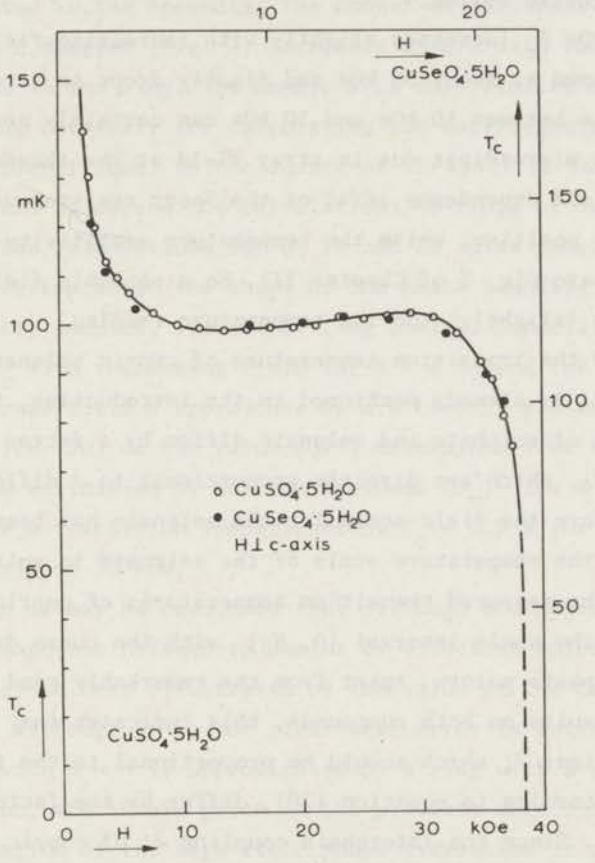

Fig. 9. Phase-boundary curve $T_c(H)$ for cupric sulphate. Black dots indicate the transition temperature of cupric selenate and refer to the upper and right scales.

external magnetic field has the same direction perpendicular to the c-axis as applied in the magnetization measurements represented in the Figures 4 and 5. Analogous to the treatment of the specific heat capacity given above, the phase-boundary curve $T_c(H)$ will be discussed separately for low ($H < 5$ kOe) and high ($H > 5$ kOe) magnetic fields.

Again, at high fields the specific heat is entirely due to the antiferromagnetic linear-chain system, while with decreasing field the influence of the paramagnetic system will gain in importance. In the next section it will be shown that the rise of T_c below 5 kOe originates in the paramagnetic system.

Above 5 kOe T_c increases slightly with increasing field, until it reaches a maximum at about 30 kOe and finally drops to zero at 38.4 kOe. The slight rise between 10 kOe and 30 kOe can certainly not be ascribed to temperature misreadings due to stray field at the thermometer site. The (small) field dependence $\partial R/\partial H$ of the Speer resistor used has been measured to be positive, while the temperature sensitivity $\partial R/\partial T$ is negative (compare Fig. 5 of Chapter II). So a possible field effect can only produce a (slightly) too low temperature reading.

In Fig. 9 the transition temperature of cupric selenate has also been indicated. As already mentioned in the introduction, the intrachain interactions J of sulphate and selenate differ by a factor 1.73. The field values H_0, which are directly proportional to J differ by the same factor. Therefore the field scale for the selenate has been multiplied by 1.73. When the temperature scale of the selenate is multiplied by a factor 0.83, the measured transition temperatures of cupric selenate coincide over the whole interval $[0, H_0]$ with the curve drawn through the cupric sulphate points. Apart from the remarkably good agreement between the results on both compounds, this indicates that the interchain interactions J', which should be proportional to the transition temperature according to equation (20), differ by the factor 0.83 for both compounds. Since the interchain coupling J' of cupric sulphate is determined from the magnetization measurements in Fig. 5 as $|qJ'/k| = 0.14\ (\pm\ 0.03)$ K, a value of $|qJ'/k| = 0.17\ (\pm\ 0.04)$K results for the selenate.

In the third section of this chapter the phase-boundary curve has been derived as

$$kT_c = |qJ'|\,(C_m^+)^2/N \qquad (20)$$

in a field H_m in which the magnetization equals $M/\frac{1}{2}Ng\beta = (m + \frac{1}{2})/N$.

According to this equation the field dependence of T_c depends entirely on the coefficients C_m^+ . Because the values of these coefficients are unknown for infinitely long antiferromagnetic linear chains, we have calculated them for rings with 6, 8, 10 and 12 spins following the method indicated in the Appendix. The number of different points in the $(C_m^+)^2$ *vs.* H diagram (Fig. 2) increases as $N/2$ with increasing number N of spins in the ring. The number N is only limited by the amount of machine time necessary for calculating the coefficients C_m^+. Since this time is proportional to the square of $N!/(\frac{1}{2}N)!$ it has been judged senseless to extend the calculations to rings of over 12 spins. Fortunately, the calculations for 8, 10 and 12 spins provide already a definite suggestion about the shape of the phase boundary $T_c(H)$ for a system of weakly coupled, infinitely long chains. Especially the slight increase of T_c with increasing field for $H < \frac{3}{4} H_0$ and the sharp decrease when the external field H approaches H_0 are clearly present. Substitution in equation (20) of the value $|qJ'|$ determined from the magnetization data, and estimation of the coefficients $(C_m^+)^2$ for $N \to \infty$ from Fig. 2 produce a transition temperature of $T_c = 0.2$ K for cupric sulphate in a field of 30 kOe.

Therefore it may be concluded that although the approximation of the antiferromagnetic Heisenberg chains by effective spins $S' = \frac{1}{2}$ is very rough, as has been illustrated by the value of the critical entropy S_c, and although it is not clear what error is introduced when a linear chain with $N \to \infty$ is approximated by a ring with a relatively low number of spins, the theory given in the previous sections produces a useful explanation of the high-field phase transition in cupric sulphate and selenate.

As a last experiment the adiabatic magnetization curves $T_s(H)$ were measured. Since the heat inleak of 10^{-7} W caused a continuous change in the entropy which gave serious errors because of the small heat capacity of cupric sulphate, the experimental "isentropes" in Fig. 10 are to be regarded qualitatively. However, the sharp temperature minimum at $H = 0$ due to demagnetization of the paramagnetic system is clearly visible. At higher fields the lowest isentrope follows more or less the phase-boundary curve $T_c(H)$ and reaches a second minimum at $H = H_0$. The higher

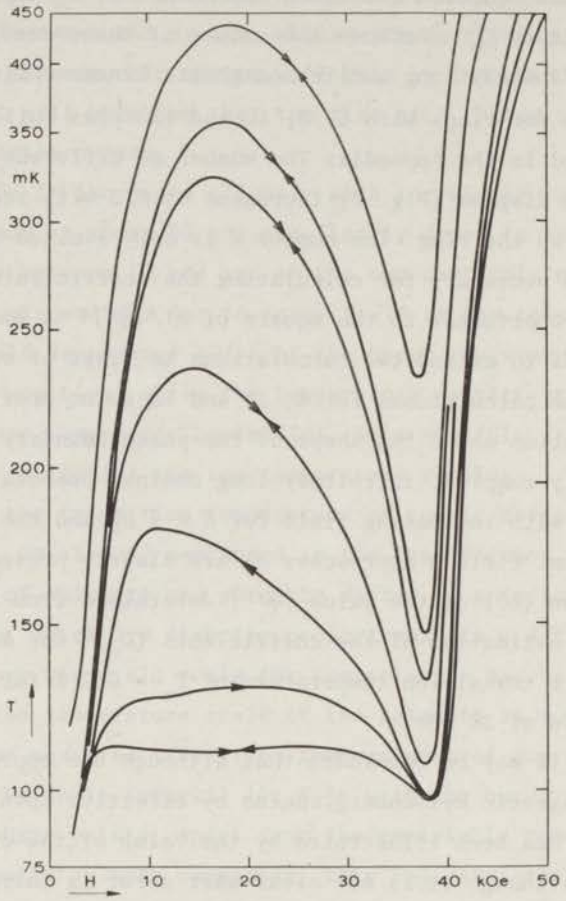

Fig. 10. Experimental isentropes of cupric sulphate in the H–T diagram. Arrows indicate whether the field was varied up or downwards.

isentropes reflect the presence of the "paramagnetic" Schottky anomaly in the specific heat, especially the shift of its maximum to higher temperatures with increasing field.

Influence of the paramagnetic system

The interaction J_{12} between the paramagnetic Cu^{2+} ions at $(\frac{1}{2},\frac{1}{2},0)$ and the antiferromagnetic linear-chain system has been determined by Wittekoek [21] in magnetic fields below 10 kOe. Since the paramagnetic

ions lie exactly half way between the chains, it is evident that the interaction J_{12} will contribute to the interchain interaction J' as long as the magnetization of the $(\frac{1}{2},\frac{1}{2},0)$ ions differs from its saturation value. Moreover, in the ordered state the canting of the spins in in the a.l.c. system will influence the direction of the paramagnetic spins via the interaction J_{12}. By means of a very simple theory it will be shown that the spins of the paramagnetic ions are also canted and that, in sufficiently low external fields, this canting can be even larger than the "original" canting of the spins in the antiferromagnetic linear chain system.

In Figure 11 the unit cell of cupric sulphate pentahydrate has been sketched schematically. The Cu^{2+} ions at (0,0,0) are coupled by the intrachain interaction J, most probably along the a axis as indicated by n.m.r. [24] and heat-conduction [25] experiments. In that case the chains interact via J' along the b and c axes. The shortest connection between the (0,0,0) ion and the paramagnetic ion at $(\frac{1}{2},\frac{1}{2},0)$ has been assumed to be the most probable path for the interaction J_{12}.

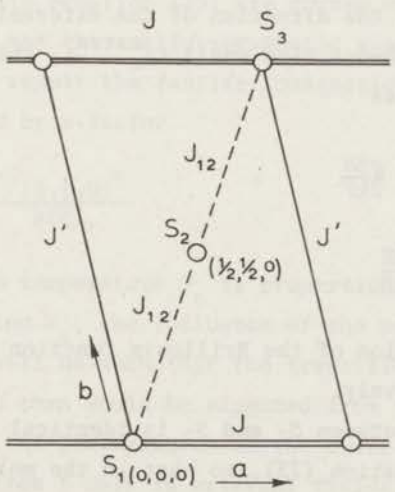

Fig. 11. Sketch of the unit cell of cupric sulphate pentahydrate. Detailed information about the structure can be found in ref. 23.

The interaction between the spins S_1 and S_2 in Fig. 11, given by the hamiltonian

$$\mathcal{H}_{12} = - J_{12} \vec{S}_1 \cdot \vec{S}_2 \tag{23}$$

can be regarded as the action of a molecular field at the position of the paramagnetic spin S_2

$$\mathcal{H}_{12} = - g\beta \vec{H}_m \cdot \vec{S}_2 \qquad \text{with} \qquad \vec{H}_m = J_{12} \langle \vec{S}_1 \rangle / g\beta \tag{24}$$

The field $\vec{H}_m$, added to the external field $\vec{H}$, will polarize the paramagnetic ion. When H_m is assumed to be small compared to H, the extra polarization of S_2 induced by H_m may be represented as

$$\begin{aligned} \langle S_{2//}^{\text{extra}} \rangle &= \chi_{p,//} H_{m,//} \\ \langle S_{2\perp}^{\text{extra}} \rangle &= \chi_{p,\perp} H_{m,\perp} \end{aligned} \tag{25}$$

Here χ_p represents the (field and temperature-dependent) susceptibility of the paramagnetic ions, while the indices $\perp$ and $//$ are to be interpreted with respect to the direction of the external field $\vec{H}$. In the limit of small H_m and hence also small $\langle S_2^{\text{extra}} \rangle$, the components $\chi_{p,//}$ and $\chi_{p,\perp}$ are obtained as

$$\begin{aligned} \chi_{p,//} &= \frac{g\beta}{4kT} \cosh^{-2} \frac{g\beta H}{2kT} \\ \chi_{p,\perp} &= \frac{1}{2H} \tanh \frac{g\beta H}{2kT} \end{aligned} \tag{26}$$

by simple differentiation of the Brillouin function for spin $S = \frac{1}{2}$ to $H_{m//}$ and $H_{m\perp}$, respectively.

The interaction between S_2 and S_3 is identical to that between S_1 and S_2 given in equation (23), so that in the molecular-field approximation

$$\mathcal{H}_{23} = - J_{12} \langle \vec{S}_2 \rangle \cdot \vec{S}_3 \tag{27}$$

results. Elimination of $\langle \vec{S}_2 \rangle$ from equations (24) and (27) gives the in-

teraction of the spins S_1 and S_3 via the paramagnetic spin S_2

$$\mathcal{H}_{13} = \frac{J_{12}^2}{g\beta} \{\chi_{p,//} \langle S_{1,//} \rangle S_{3,//} + \chi_{p,\perp} \langle S_{1,\perp} \rangle S_{3,\perp}\} \tag{28}$$

which is exactly the molecular-field equivalent of an anisotropic exchange interaction. However, the presence of the paramagnetic susceptibilities in this equation introduces a strong dependence of the effective exchange energy on the temperature and the external magnetic field. From equation (26) immediately follows that - while at $H = 0$ both components of the susceptibility χ_p are equal to $g\beta/4kT$ - with increasing field the parallel susceptibility $\chi_{p,//}$ decreases much more rapidly than the perpendicular one $\chi_{p,\perp}$. Therefore in non-zero external fields and at temperatures of the order of 0.1 K a first estimate of the total interchain interaction J_t' is obtained by adding the perpendicular part of equation (28) to the original interchain interaction J'

$$-J_t' = -J' + \frac{J_{12}^2}{g\beta} \chi_{p,\perp}(H,T) \tag{29}$$

The different signs in equation (29) are caused by the different paths of the interactions and the antiferromagnetic sign of the intrachain interaction J. As a result the (antiferromagnetic) interaction J' is effectively enlarged by a factor

$$\kappa = 1 - \frac{J_{12}^2}{J'} \cdot \frac{\langle S_{(\frac{1}{2},\frac{1}{2},0)} \rangle}{g\beta H} \tag{30}$$

Since the transition temperature T_c is proportional to the total interchain interaction J_t', the influence of the paramagnetic system on the phase boundary will be such that the transition temperature T_c, is larger by a factor κ than would be expected from the weakly coupled a.l.c. system alone. At temperatures of the order of 0.1 K, κ will differ appreciably from 1 only in external fields lower than about 5 kOe. With decreasing field κ increases as H^{-1} until it reaches its maximum value for $H = 0$

$$\kappa_{max} = 1 - \frac{J_{12}^2}{J'} \chi_p\ (0,T) \tag{31}$$

which still depends on temperature. Although the argument given above is very simple, it accounts at least qualitatively for the field dependence of T_c in low external fields observed in Fig. 9.

The angle φ between the paramagnetic spins and the direction of the external field results immediately from equations (24) and (25)

$$\tan \varphi = \langle S_{2\perp}^{\text{extra}} \rangle / \langle S_{2//} \rangle = \frac{\chi_{p\perp} J_{12} \langle S_{1\perp} \rangle}{\langle S_{2//} \rangle} \tag{32}$$

Substitution of equation (26) leads to

$$\tan \varphi = \frac{J_{12}}{H} \langle S_{(0,0,0)\perp} \rangle \tag{33}$$

so that φ is proportional to the spontaneous perpendicular magnetization of the a.l.c. system $\langle S_{1\perp} \rangle$ and inversely proportional to the external magnetic field H.

This "induced" canting in the paramagnetic system might provide an explanation for the anomalous doublet structure of the proton resonance lines below 0.6 K as observed by Wittekoek and Poulis [26]. They reported that this splitting was due to a canted arrangement of the spins of the ions at the $(\frac{1}{2},\frac{1}{2},0)$ positions and gave an empirical equation for the canting angle

$$\varphi \sim \frac{\langle S_{(\frac{1}{2},\frac{1}{2},0)} \rangle}{H} \tag{34}$$

The similar field dependence in equations (33) and (34) already indicates a relation between the experimentally determined values of φ and the ordered state of the a.l.c. system. The most important indication, however, is that the canting measured by Wittekoek *et al.* [26] is not related to the crystal axes, but only to the direction of the magnetic field. In low fields H the canting φ in the paramagnetic system can certainly become larger than that in the antiferromagnetic chain system as can be deduced from equation (33). So it is not surprising that Wittekoek *et al.* [26] regarded the paramagnetic system as the origin of the canting.

The temperature dependence of φ represented by equation (33) is very complicated, because the temperature dependence of the perpendicular magnetization $\langle S_{(0,0,0)\perp} \rangle$ of the a.l.c. ions depends strongly on the factor κ in equation (30), which is based on quite a number of approximations and assumptions about J_{12}. Hence a quantitative explanation of Wittekoek's [26] splittings requires a much more refined theory than the one given above and also a more detailed knowledge of the various interactions present in cupric sulphate pentahydrate.

Appendix

In the first part of the Appendix the Bethe formalism will be presented in the same representation as used in the paper by Griffiths [6]. After this short introduction the translation property (8) will be proved and finally the matrix elements C_m^+ are calculated for rings of 6, 8, 10 and 12 spins.

Since the exchange part and the Zeeman part of the hamiltonian (1) commute with each other, we will start with the exchange part only

$$\mathcal{H} = -J \sum_{i=1}^{N} \vec{S}_i \cdot \vec{S}_{i+1} \; ; \qquad \vec{S}_{N+1} \equiv \vec{S}_1 \tag{A1}$$

The smallest eigenvalue of (A1) has been calculated by Hulthén [2] in the limit $N \to \infty$

$$\lim_{N\to\infty} E_0/N = J(-\tfrac{1}{4} + \ln 2) \tag{A2}$$

For a state with energy E the "normalized" energy ε will be defined by

$$\varepsilon = (\tfrac{1}{4} NJ + E)/NJ \tag{A3}$$

With "up" and "down" defined with respect to the positive z axis, let $|n_1,n_2,\ldots,n_r\rangle$ be the state for which the spins $n_1,n_2,\ldots,n_r$ are down and all other spins are up. Any eigenstate $|\Psi_r\rangle$ of (A1) with a z component of the spin $\langle \Sigma_i S_i^z \rangle = \frac{1}{2} N - r$ may then be written as a linear combination of such states

$$|\Psi_r\rangle = \sum_{n_1 n_2 \ldots n_r} a(n_1,n_2,\ldots,n_r) |n_1,n_2,\ldots,n_r\rangle \tag{A4}$$

where the summation extends over all sets of r distinct indices n_j. Bethe [1] derived the coefficients of the eigenfunctions (A4) to be

$$a(n_1,n_2,\ldots,n_r) = \sum_{P=1}^{r!} \exp i\Big(\sum_{j=1}^{r} k_{Pj}n_j + \tfrac{1}{2}\sum_{j<l} \Phi_{PjPl}\Big) \qquad \text{(A5)}$$

Here the summation extends over all permutations of the integers 1, 2, $\ldots,r$ and Pj is the image of j under the P-th permutation. The wave vectors k_j and the phase factors Φ_{jl} satisfy the coupled equations

$$Nk_j = 2\pi\lambda_j + \sum_{l\neq j} \Phi_{jl}\,; \qquad j = 1,2,\ldots,r \qquad \text{(A6)}$$

$$2\cot \tfrac{1}{2}\Phi_{jl} = \cot \tfrac{1}{2} k_j - \cot \tfrac{1}{2} k_l\,; \quad -\pi < \Phi_{jl} < \pi \qquad \text{(A7)}$$

where the λ_j are integers between 0 and N. The energy of the state corresponding to the coefficients a in (A5) is equal to

$$\varepsilon = N^{-1} \sum_{j=1}^{r} (1 - \cos k_j) \qquad \text{(A8)}$$

The order of the λ's associated with (A5) is unimportant. Also a state with some λ's equal to zero has the same total spin and energy as the corresponding state in which the zero's are eliminated. Hence without loss of generality it may be assumed that

$$0 < \lambda_1 < \lambda_2 < \ldots < \lambda_r < N \qquad \text{(A9)}$$

The class "C" defined by Griffiths [6] denotes the sets $\{\lambda_j\}$ satisfying, in addition to (A9), the restriction

$$\lambda_{j+1} \geq \lambda_j + 2 \qquad \text{(A10)}$$

as well as the eigenstates defined by (A5) corresponding to these sets. The importance of class C comes from the following properties.

i) Each set $\{\lambda_j\}$ in C leads to a solution of (A6) and (A7) for which all k_j are real and distinct.

ii) For a given total spin $\frac{1}{2}N - r$, the state $|\Psi_{r,\min}\rangle$ with the lowest energy belongs to C.

The first property has been proved rigorously in the paper by Griffiths [6]. The second property, although it has not yet been proved, is very plausible on the basis of arguments by Des Cloizeaux and Pearson [5] and calculations on finite rings [4].

The energy E of an a.l.c. ($J < 0$) is mimimal when ε is largest. From equation (A8) it is easy to deduce that ε is maximal when the k_j cluster around π. To realize this, the λ_j must cluster around the centre of the interval $[0,N]$, still under the constraint (A10). Hence, for a given total spin $S = \frac{1}{2}N - r$, the state of minimum energy in class C will correspond to

$$\lambda_1 = \tfrac{1}{2}N - r + 1,\ \lambda_2 = \lambda_1 + 2,\ \lambda_3 = \lambda_2 + 2,\ \ldots,$$
$$\lambda_r = \tfrac{1}{2}N + r - 1 \qquad \text{(A11)}$$

It is tacitly assumed that N is even; minor modifications are necessary when N is odd. The minimum-energy states corresponding to (A11) clearly form a subclass C^* of C. Because they are non-degenerate, the wave functions belonging to C^* can be denoted by $|{}^*m\rangle$, m being equal to the total spin value $\langle \Sigma_i S_i^z \rangle = \frac{1}{2}N - r$ of the state.

Let T be the operator which translates the whole chain (ring) over one lattice distance. The effect of T on an eigenstate (A5) in class C^* of the hamiltonian (A1) can be expressed as

$$T|{}^*\tfrac{1}{2}N - r\rangle = \sum_{n_1..n_r} a(n_1,n_2,\ldots,n_r)\,|n_1 + 1,\ n_2 + 1,\ldots,n_r + 1\rangle \qquad \text{(A12)}$$

Since the summation extends over all distinct indices n_j, (A12) can also be written as

$$T|{}^*\tfrac{1}{2}N - r\rangle = \sum_{n_1..n_r} a(n_1 - 1,\ n_2 - 1,\ldots,n_r - 1)\,|n_1,n_2,\ldots,n_r\rangle \qquad \text{(A13)}$$

The coefficients a in (A13) are then expressed as

$$a(n_1 - 1,\ldots,n_r - 1) = \sum_{P=1}^{r!} \exp i\Big\{\sum_{j=1}^{r} k_{Pj}(n_j - 1) + \tfrac{1}{2}\sum_{j<l} \Phi_{jl}\Big\}$$
$$= (\exp - i\sum_{j=1}^{r} k_j)\ a(n_1,n_2,\ldots,n_r) \qquad \text{(A14)}$$

By means of (A6) and (A7) the sum over all vectors k_j becomes

$$\sum_{j=1}^{r} k_j = 2\pi N^{-1} \sum_{j=1}^{r} \lambda_j + N^{-1} \sum_{j=1}^{r} \sum_{l \neq j} \Phi_{jl} = 2\pi N^{-1} \sum_{j=1}^{r} \lambda_j \tag{A15}$$

For states in C^* the special choice of the set $\{\lambda_j\}$ given in (A11) finally leads to:

$$\sum_{j=1}^{r} k_j = r\pi \tag{A16}$$

so that

$$T|{}^*\tfrac{1}{2}N - r\rangle = \exp - ir\pi\, |{}^*\tfrac{1}{2}N - r\rangle \tag{A17}$$

which equals the required translation property (8) of states in class C^*.

The calculation of the coefficients C_m^+ for finite rings of N spins, as necessary in equation (2), proceeds straightforward. First the wave vectors corresponding to the state $|{}^*m\rangle$ are calculated from the simultaneous equations (A6) and (A7), using the λ's given in equation (A11). Equation (A6) is solved by an iteration procedure which uses the $k_j = 2\pi N^{-1}\lambda_j$ as starting values; the Φ_{jl} from (A7) give a better approximation of the k_j, new Φ_{jl} are calculated *etc.* Then the coefficients $a(n_1 \ldots n_{\frac{1}{2}N-m})$ are calculated according to equation (A5). The same is done for the state $|{}^*m+1\rangle$ and finally the matrix elements

$$C_m^+ = \langle {}^*m | \sum_i (-1)^i S_i^x | {}^*m + 1\rangle \tag{A18}$$

are obtained. In practice the states $\langle {}^*m|$ and $\Sigma_i (-1)^i S_i^x |{}^*m + 1\rangle$ can be calculated simultaneously from equation (A5) if the wave vectors are properly chosen, *i.e.* if a wave vector $k = \pi$ is added to the existing set $\{k_j\}$ for the state $|{}^*m + 1\rangle$.

Since the exchange part (A1) of the hamiltonian commutes with the Zeeman energy $g\beta H \Sigma_i S_i^z$, the energy eigenvalue of the total hamiltonian (1) belonging to the state $|{}^*m\rangle$ is given by

$$E_m = NJ(\varepsilon_m - \tfrac{1}{4}) - g\beta mH \tag{A19}$$

The field H_m for which this energy equals the energy E_{m+1} of the neigh-

bouring state $|*m + 1\rangle$ becomes

$$H_m = NJ(\varepsilon_{m+1} - \varepsilon_m)/g\beta \qquad \text{(A20)}$$

The results of the calculations of C_m^+ and H_m for rings of 6, 8, 10 and 12 spins are gathered in Table II, while the quantity $(C_m^+)^2/N$, which should be proportional to the transition temperature T_c according to equation (20) is represented graphically in Fig. 2.

Table II

The calculated matrix elements C_m^+ for rings with 6, 8, 10 and 12 spins.

N	m	$-g\beta H_m/J$	C_m^+	$(C_m^+)^2/N$
6	0	0.68474	+2.97359	1.47371
	1	1.61803	-2.89443	1.39629
	2	2.00000	+2.44949	1.00000
8	0	0.52267	-3.52828	1.55609
	1	1.32648	+3.54705	1.57270
	2	1.80194	-3.39711	1.44255
	3	2.00000	+2.82843	1.00000
10	0	0.42324	+4.01632	1.61308
	1	1.11628	-4.08686	1.67024
	2	1.59655	+4.06717	1.65419
	3	1.87939	-3.83918	1.47393
	4	2.00000	+3.16228	1.00000
12	0	0.35584	-4.45817	1.65628
	1	0.96101	+4.55940	1.73234
	2	1.41879	-4.61230	1.77277
	3	1.73275	+4.53635	1.71487
	4	1.91899	-4.23724	1.49619
	5	2.00000	+3.46410	1.00000

References

1. H.A. Bethe, Z. Physik 71 (1931) 205.
2. L. Hulthén, Arkiv Mat. Astron. Physik 26A (1938) 11.
3. J.C. Bonner and M.E. Fisher, Phys. Rev. 135 (1964) A640.
4. R. Orbach, Phys. Rev. 112 (1958) 309.
5. J. Des Cloizeaux and J.J. Pearson, Phys. Rev. 128 (1962) 2131.
6. R.B. Griffiths, Phys. Rev. 133 (1964) A768.
7. S. Katsura and S. Inawashiro, J. math. Phys. 5 (1964) 1091.
8. S. Kadota, I. Yamada, S. Yonezawa and K. Hirakawa, J. Phys. Soc. Japan 23 (1967) 751.
9. T. Haseda and A.R. Miedema, Physica 27 (1961) 1102.
10. K. Takeda, M. Matsuura, S. Matsukawa, Y. Ajiro and T. Haseda, J. Phys. Soc. Japan, to be published.
11. see also: C.Y. Weng, R.B. Griffiths and M.E. Fisher, Phys. Rev. 162 (1967) 475;
    M.E. Fisher, Phys. Rev. 162 (1967) 480.
12. L. Onsager, Phys. Rev. 65 (1944) 117.
13. J.W. Stout and R.C. Chrisholm, J. chem. Phys. 36 (1962) 979.
14. T. Oguchi, Phys. Rev. 133 (1964) A1098.
15. J.C. Bonner and M.E. Fisher, Proc. Phys. Soc. 80 (1962) 508.
16. E. Lieb and D. Mattis in "Mathematical Physics in One Dimension" p. 481.
17. T. Moriya, Phys. Rev. 120 (1960) 91.
18. I. Dzyaloshinski, Soviet Physics JETP 6 (1968) 1130.
    J. Phys. Chem. Solids 4 (1958) 241.
19. A.R. Miedema, H. van Kempen, T. Haseda and W.J. Huiskamp, Physica 28 (1962) 119.
20. W.F. Giauque, R.A. Fisher, E.W. Hornung and G.E. Brodale, J. chem. Phys. 53 (1970) 3733.
21. S. Wittekoek, N.J. Poulis and A.R. Miedema, Physica 30 (1964) 1051.
22. J.C. Bonner and M.E. Fisher, Phys. Rev. 135 (1964) A640.
23. G.E. Bacon and N.E. Curry, Proc. Roy. Soc. A266 (1962) 95.
24. S. Wittekoek, Thesis Leiden (1967).
25. J.N. Haasbroek, private communication.
26. S. Wittekoek and N.J. Poulis, Physica 32 (1966) 2051.

SAMENVATTING

Dit proefschrift beschrijft overgangen in magnetische systemen van een ongeordende (paramagnetische) fase naar een geordende fase, in het bijzonder naar een geordende fase die niet voorkomt wanneer geen uitwendig magnetisch veld aanwezig is. Deze overgangen kunnen voorkomen in systemen, die opgebouwd zijn uit magnetische ionen met heeltallige spin, clusters van magnetische ionen of lineaire ketens van magnetische ionen. De drie soorten samenstellende eenheden hebben een niet-ontaarde grondtoestand gemeen. In aanwezigheid van een uitwendig veld van voldoende sterkte kan een van de hogere energietoestanden van zo'n ion, cluster of keten de grondtoestand kruisen. Als bovendien een relatief zwakke wisselwerking tussen de ionen, clusters of ketens aanwezig is kan, bij voldoende lage temperatuur, een overgang naar een geordende toestand plaatsvinden. Fase overgangen van dit type zijn waargenomen in kopernitraat "trihydraat", $Cu(NO_3)_2 \cdot 2\frac{1}{2}H_2O$ en in kopersulfaat pentahydraat, $CuSO_4 \cdot 5H_2O$. Hoofdstuk I geeft een algemene inleiding in het verschijnsel van fase overgangen in hoge magnetische velden, terwijl hoofdstuk II de apparatuur beschrijft waarmee de experimenten zijn uitgevoerd.

Het eerstgenoemde zout, kopernitraat, is van het cluster type: het bevat paren van exchange gekoppelde Cu^{2+} ionen met een relatief zwakke koppeling tussen de paren onderling. In een veld van ongeveer 36 kOe kruist een van de hogere energie niveaus van zo'n paar de grondtoestand, zodat formeel een paar koperionen in 36 kOe op dezelfde wijze beschreven kan worden als een ion met spin $S = \frac{1}{2}$ in nulveld.

De zwakke koppeling tussen de paren veroorzaakt een fase overgang bij 175 mK in 36 kOe naar een toestand waarin de spincomponenten loodrecht op het uitwendige veld geordend zijn. Het geordende gebied strekt zich uit van 29 kOe tot 42 kOe (hoofdstuk III). De overgang naar deze geordende fase wordt gekenmerkt door het optreden van lijnsplitsingen in de n.m.r. spectra van de protonen uit het kristalwater en door het voorkomen van de typische λ-anomalie in de soortelijke warmte. De overgangstemperatuur is gemeten als functie van het magne-

tische veld, evenals het verloop van de soortelijke warmte en de spontane component van de magnetisatie met de temperatuur.

Het verschillende gedrag van kopernitraat in velden boven en beneden 36 kOe wordt in hoofdstuk IV verklaard door aan te nemen dat de wisselwerking tussen de koper-ionen binnen het paar niet isotroop is.

In hoofdstuk V wordt een eenvoudige beschrijving ontwikkeld van zwak gekoppelde antiferromagnetische lineaire ketens met Heisenberg wisselwerking. Met behulp van deze theorie wordt aangetoond dat in een uitwendig magnetisch veld de grondtoestand van dergelijke ketens gekenmerkt wordt door het feit dat de magnetische momenten van de ionen niet parallel zijn aan het uitwendig veld, maar een spontane component vertonen loodrecht daarop. Deze grondtoestand treedt op zolang het veld kleiner is dan het equivalent van tweemaal de wisselwerking binnen de ketens. Verdere vereenvoudiging van het gebruikte model leidt tot de berekening van de overgangstemperatuur als functie van het uitwendige veld.

Experimenteel is een dergelijke fase-overgang gevonden bij 0.1 K in kopersulfaat pentahydraat en in het isomorfe koperselenaat, stoffen waarin de helft der Cu^{2+} ionen gekoppeld is in lineaire ketens. De overgangstemperatuur is bepaald m.b.v. zowel n.m.r. als soortelijke-warmte experimenten. De gevonden fasegrens stemt kwalitatief goed overeen met de ontwikkelde theorie, mits in aanmerking wordt genomen dat de helft der koperionen in kopersulfaat en -selenaat *niet* in lineaire ketens zijn gekoppeld, maar zich gedragen als min of meer vrije spins. De invloed van dit "paramagnetische systeem" wordt kort besproken.

NAWOORD

De inhoud van dit proefschrift is niet het resultaat van de inspanningen van de auteur alleen. In werkelijkheid hebben velen aan het tot stand komen van deze dissertatie en het eraan ten grondslag liggende onderzoek meegewerkt.

De veelvuldige discussies met mijn promotor, Prof. Dr. N.J. Poulis en met de andere leden van de werkgroep Magnetische Resonantie hebben mijn inzicht in de fase-overgangen in sterke magnetische velden verdiept. Tijdens het onderzoek heb ik veel steun gehad van de heer J. Heijn, vooral bij de ontwikkeling en de opbouw van de opstelling, en van Drs. L.S.J.M. Henkens en de heer K.M. Diederix bij de experimenten. Dr. Matsuura ben ik dankbaar voor het feit dat hij de spinpaarverbinding kopernitraat onder mijn aandacht heeft gebracht. Zijn belangstelling in de experimenten was een belangrijke stimulans in het beginstadium van het onderzoek.

Dat het onderzoek zo voorspoedig is verlopen, is te danken aan de technische en administratieve faciliteiten van het Kamerlingh Onnes laboratorium, waarvoor een groot aantal personen zorg dragen. In het bijzonder wil ik de heren J. Hoogwerf, W.F. Elbers en D. de Jong noemen, die een groot aandeel hadden in de constructie van de gebruikte apparatuur, en de heren C.J. van Klink en L. van As, die de opeenvolgende versies van het glaswerk hebben vervaardigd zonder ooit hun goede humeur te verliezen. De bijzonder stabiele stroombronnen voor de supergeleidende magneten zijn gebouwd door de heer H.P.J.M. van Amersfoort. Voor de benodigde hoeveelheden vloeibaar helium werd nooit een vergeefs beroep gedaan op de heer J.D. Sprong.

De heren J.A.J.M. Disselhorst en W.F. Tegelaar zijn zo vriendelijk geweest de tekeningen voor dit proefschrift te verzorgen, terwijl

mejuffrouw S.M.J. Ginjaar een deel van het typewerk voor haar rekening nam. Voorts ben ik mejuffrouw S.C. de Vroe erkentelijk voor het corrigeren van de engelse tekst van het manuscript.

Mijn belangstelling voor natuurkunde is reeds in een vroeg stadium gewekt en gestimuleerd door mijn vader, Ir. M. van Tol en door mijn natuurkundeleraren Ir. P.J. ten Have en Dr. B. Groeneveld, waarvoor mijn oprechte dank hier op zijn plaats is.

Ten slotte zijn het de jarenlange toewijding en belangstelling van mijn echtgenote geweest die de verwezenlijking van dit proefschrift en het eraan ten grondslag liggende onderzoek over de moeilijke perioden hebben heengeholpen en tot een plezierige bezigheid hebben gemaakt.

Maurits W. van Tol was born in Eindhoven in 1945. He attended the *Lorentz Lyceum* in the same town and took up the study of physics, mathematics and chemistry at the Leiden University in 1962. In 1966 he entered the Kamerlingh Onnes Laboratory. The first principles of experimental physics were taught him by Dr. W.Th. Wenckebach on a project of low-temperature hypersonics. From 1968 he worked on high-field nuclear magnetic resonance under supervision of Prof.Dr. N.J. Poulis. After his final exam in physics and mathematics in 1969, he joined Philips' Research Laboratories in Eindhoven, from which he was detached in order to complete the research project described in this thesis. During his stay in Leiden he was an assistant in the physics practicals from 1968 - 1969, and a teaching assistant from 1969 to 1972.

The present work is part of the research program of the *Stichting voor Fundamenteel Onderzoek der Materie*, which is financially supported by the *Stichting voor Zuiver Wetenschappelijk Onderzoek*.